AEON
AFRICA EARTH OBSERVATORY NETWORK
EARTH STEWARDSHIP THROUGH SCIENCE

Nelson Mandela Metropolitan University
for tomorrow

Evaluation for harnessing low-enthalpy geothermal energy in South Africa based on a model pilot plant in the Limpopo Mobile Belt

T Dhansay

2012

IIASA International Institute for Applied Systems Analysis

Council for Geoscience

Evaluation for harnessing low-enthalpy geothermal energy in South Africa based on a model pilot plant in the Limpopo Mobile Belt

By

Taufeeq Dhansay[1,2]

Submitted in fulfilment of the requirements for the degree of Masters in Geology at the Nelson Mandela Metropolitan University

December 2012

Supervisor:
Professor Maarten de Wit[1]

1 Nelson Mandela Metropolitan University, Port Elizabeth, South Africa
2 Council for Geoscience, Limpopo Regional Unit, Polokwane, South Africa

Declaration

I, Taufeeq Dhansay (S211276863), hereby declare that the thesis for students qualification to be awarded is my own work and that it has not previously been submitted for assessment of completion of any postgraduate qualification to another University of for another qualification.

Taufeeq Dhansay

Official use:

In accordance with Rule G4.6.3,

4.6.3 A treatise/dissertation/thesis must be accompanied by a written declaration on the part of the candidate to the effect that it is his/her own work and that it has not previously been submitted for assessment to another University or for another qualification. However, material from publication by the candidate may be embodied in a treatise/dissertation/thesis.

Abstract

South Africa generates more than 90 % of its total energy capacity through non-renewable sources. With coal forming the predominant energy source, South Africa became the leading carbon emissive nation in Africa, emitting 450 million tonnes of CO_2 in 2011. In an international effort to restrict global average temperature rise to 2° C above the average prior the industrial revolution, the Kyoto Protocol has been extended for another 8-year commitment period. This is complementary to an expected resolution of a new legally binding climate change policy in 2015. This policy will aim to introduce financial penalties for nations failing to meet ascribed GHG emission targets by 2020. In an attempt to meet these climate change resolutions South Africa will research and develop cleaner, alternative forms of energy, including hydro, wind, and biomass forms of renewable energy, in addition to designating stringent building regulations for the incorporation of solar energy. These measures form part of an Integrated Development Plan that aims to generate a target of 10,000 GWh of renewable energy in 2013. South Africa is also investigating the possibilities of extracting its shale gas reserves and implementing it as a major energy source. This energy mix has given little attention to geothermal energy. The reasons for this omission appears to be the lack of active volcanism and previous research that suggests South Africa, largely underlain by the Kaapvaal Craton, has a relatively low heat flow profile, deemed insufficient for harnessing geothermal energy.

Despite the available knowledge illustrating South Africa's poor potential for geothermal energy, anomalously higher heat flow regions could potentially be successful in harnessing low-enthalpy geothermal energy. This study investigates the possibility of harnessing low-enthalpy geothermal energy from one of these anomalous areas, namely, the Limpopo Mobile Belt, north east of South Africa. This is accomplished by considering a 75 MW hypothetical Enhanced Geothermal System (EGS) plant, sustainable over a 30-year period. The plant would theoretically yield energy from a minimum of three producing wells, from a reservoir with a minimum volume of 1,000 m^3.

All parameters associated with the total cost and total potential energy yield of this hypothetical plant are inculcated within a Levelised Cost of Electricity (LCOE) model. These parameters include: 1. The available heat flow data, which estimate basal reservoir temperature at a specific depth. 2. Engineering and geological parameters, which calculate the potential energy yield and sustainability of the plant. 3. Hydrogeological parameters, which ascertain the impact on the regional water supply. 4. Economic and business development

factors, which estimate the economic viability of the plant. 5. Financial factors associated with construction to operation and maintenance. The aforementioned parameters function toward the calculation of a single unit cost of electricity generated from low-enthalpy EGS at this site in South Africa. This aims to better ascertain its viability and potential impact toward South Africa's mitigation of climate change and future energy security.

The LCOE model for a hypothetical EGS plant within the Limpopo Mobile Belt estimates the unit cost of electricity as 14 $c/KWh. This generation avoids adverse effects on the groundwater quality and supply, and has the potential of mitigating CO_2 emissions by 1.5 gCO_2/KWh. The model also estimates a maximum basal reservoir temperature drawdown of 10-15° C over the 30-year period, which could potentially result in an overall capacity decrease of 1 MWh.

The results of this study indicates that EGS in South Africa would be at least 7 $c/KWh more expensive than the current coal-generated forms of energy in addition to having a much lower energy capacity. However, with an added, globally comparable, $25/MWh renewable energy production incentive, the LCOE decreases to 12 $c/KWh. Making it comparable with other forms of renewable energy, including concentrated solar power. With the 2015 Conference of the Parties 18^{th} meeting climate change resolution deadline looming, further research and development toward cleaner and alternative forms of energy is an important feature for South Africa's GHG emissions reduction and energy development. Low-enthalpy geothermal energy development could potentially form another alternative energy option in South African climate change adaption and broad energy security.

List of Acronyms

CFB	Cape Fold Belt
COP	Conference of the Parties
CSP	Concentrated Solar Power
DWA	Department of Water Affairs
EAR	East African Rift
EGS	Enhanced Geothermal Systems
Ga	Billion years
GHG	Greenhouse Gas
GRIP	Groundwater Research Information Project
GWh	Giga watts per hour
IDP	Integrated Development Programme
IEA	International Energy Agency
IGA	International Geothermal Association
IIASA	International Institute for Applied Systems Analysis
KC	Kaapvaal Craton
KRISP	Kenya Rift International Seismic Project
KWh	Kilo watts per hour
LMB	Limpopo Mobile Belt
LCOE	Levelised Cost of Electricity
Ma	Million years
MPa	Mega Pascal
MWh	Mega watts per hour
mWm^{-2}	Mega watt per square metre
NEI	Nuclear Energy Institute
NERSA	National Energy Regulator of South Africa
NNMB	Namaqua Natal Mobile Belt
OM	Operation and Maintenance
ppm	Parts per million
PTC	Production Tax Credit
PV	Photovoltaic
REFIT	Renewable Energy Feed-in Tariff
SAMTEX	Southern African Magneto Telluric Experiment
TDEM	Time Dependant Electromagnetism
TWh	Terra watts per hour
UNFCCC	United Nations Framework Convention of Climate Change
WB	Witwatersrand Basin
YSSP	Young Scientists Summer Programme
ZC	Zimbabwe Craton

List of Figures

List of Tables

List of Equations

List of Definitions

Annual Inflation	Increase in costs related to the expenses of operating the EGS plant
Capacity	Total amount of energy producible from the EGS plant
Conference of the Parties	The governing body for the Convention of Climate Change responsible for overseeing implementation and defining of new legislation
Discount factor	Factor for estimating the future value of the EGS plant and future energy generated
Downtime factor	Future value related to lack of operation due to planned maintenance and/or breakdown
EGS	"Enhanced/Engineered Geothermal Systems" a method of generating energy from an artificially generated geothermal well using hydraulic fracturing and exploiting a naturally high heat flow
Flow rate	Rate that fluid is pumped into and/or out of the geothermal reservoir
Geothermal loss rate	Estimated factor related to fluid loss in an open geothermal reservoir
Grid parity	Cost associated with feeding surplus energy back into the National Energy Grid
Heat Productivity	Radiogenic elements contained within plutonic rocks that through natural decay emit heat
Hydraulic stimulation	Mechanism of opening the spaces within a deep-seated fracture network through pumping a fluid and propping agent to maintain spaces generated

LCOE	“Levelised Cost Of Energy”: a method of ascertaining the viability of a specific energy source through weighing up all cost factors against the potential energy output
Mantle keel	An extension of the lithosphere below Archean cratons into the subcontinental lithospheric mantle
Nameplate plant size	Estimated energy production of the EGS plant
O&M	“Operation and Maintenance”: costs relating to the upkeep and running of the EGS plant
Primary geotherm	Geothermal gradient of insulating sedimentary cover rocks
Primary thickness	Thickness of insulating sedimentary cover rocks
PTC	“Production Tax Credit”: tax credit for reduction of carbon emissions
REFIT	“Renewable Energy Feed-In Tariff”: an incentive for renewable energy projects generating an energy surplus feeding into the national energy grid
Secondary geotherm	Geothermal gradient of targeted plutonic rocks
Secondary thickness	Depth of geothermal reservoir within targeted plutonic rocks
Thermal drawdown	Factor related to the heat loss from the geothermal reservoir to the surface
Utilisation	Factor relating to the actual energy output of the EGS plant compared against the theoretical energy yield

Contents

Chapter 1: Introduction and scope of this thesis

1.1 South African climate change mitigation and adaption scenarios

Becoming the leading carbon emissive nation in Africa, South Africa joined several other developing nations aiming to decrease their overall Greenhouse gas (GHG) emissions (Figure 1). Previously, it was only developed nations owning stringent environmental policies toward decreasing their GHG emissions, however the rate of GHG emissions from developing nations are predicted to increase beyond that of developed nations by 2020 (Reid and Goldemberg, 1998). This shift in the rate of increase of developing nations can be related to previous climate combatting legislation, like the Kyoto Protocol[1] that only proposed the allotment of financial tax penalties to the developed nations, while developing nations were exempted from these penalties. However, under continuous global development newer international environmental legislation is expected to hold developing nations accountable for failing to meet millennium GHG reduction targets. This decree was agreed upon under the Bali Action Plan during which key mitigation scenarios were outlined for developing nations. This occurred during the COP13 (Conference of the Parties)[2] climate change summit held in Bali, Indonesia, December 2007 (United Nations Framework Convention on Climate Change, 2007).

An IPCC (Intergovernmental Panel on Climate Change) report estimates that the sea level will continue to rise at a constant rate proportional to global warming (IPCC, 2007). This poses a huge threat to all coastal nations and especially small island states and developing nations most vulnerable to the effects of large fluctuations rainfall and soil moisture contents. These future impacts have forced the COP group to act more aggressively toward decreasing the level of GHG emissions and lower the rate of climate change.

---

[1] The Kyoto Protocol was a decree under the United Nations Framework Convention on climate change committing European countries and other industrialised nations to reduce their greenhouse gas emissions to 5 % of that in 1990. The protocol was decreed on 11 December 1997 in Japan and applied at the COP 7, Morocco. As of 2011, 189 countries have ratified the Kyoto Protocol, however the protocol expires in 2012.

[2] The Conference of the Parties is the governing body of the convention of climate change aimed to create legislation and act on implementation of various climate change policies.

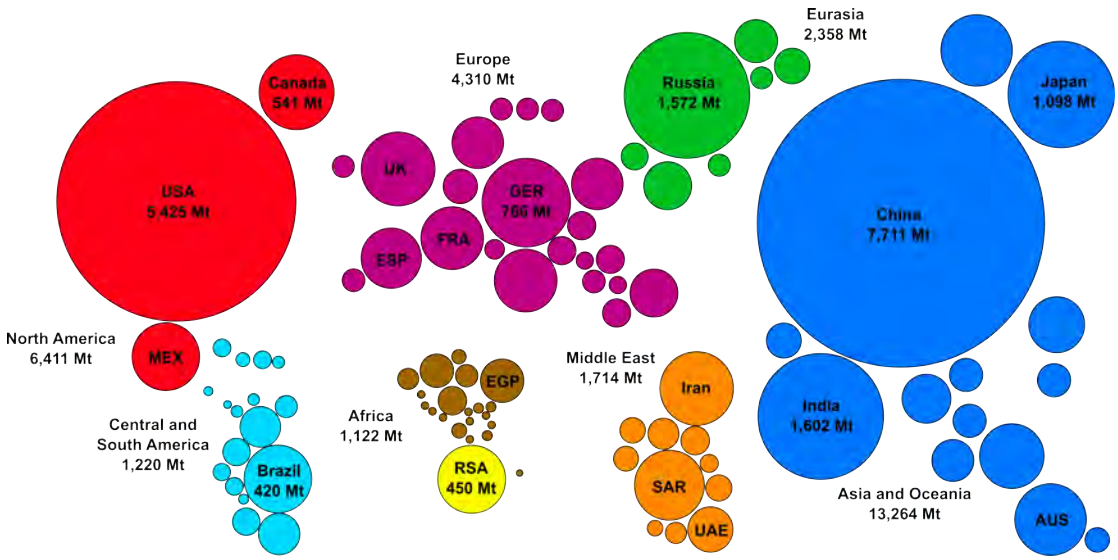

Figure 1: Graphic of the World's greenhouse gas emissions per capita in 2011, South Africa highlighted in yellow. Data from the US Energy Information Administration (www.eia.gov) and illustration produced by Mark McCormick and Paul Scruton. According to the EIA, South Africa had a decrease of 6.7 % over 2010/11. The Guardian (www.guardian.co.uk/news/datablog/2011)

Impacts of climate change-related critical events are not generally addressed in developing nations, like South Africa, because long-term mitigation and adaption studies in these nations are at a relatively immature stage. A common and very important aspect of adaption and mitigation considers the effect a continued global sea level rise would have on low-lying areas. An example would include smaller islands and coastal areas with mean height above sea level of only several metres. Many of these regions include some of the poorest countries in the world and are the most vulnerable to the effects of climate change. These include the small Pacific islands such as Vanuatu, Tuvalu and the Solomon Islands. These nations are typically referred to as the least developed countries (LDC) (Tisdell, 2002; Huq et al., 2004). Gornitz, (1991) considered the effect that continued global sea level rise would have on various parts of North and South America. Her findings suggest that not only will those populations living along the coast be adversely affected by flood damage to their homes, but also through saltwater contamination of their shallow fresh groundwater supply. Furthermore, she notes a considerable lack of adequate hazard analyses and appropriate mitigation scenarios related to various effects of possible future climate change. Nicholls and Hoozemans, (1996) considered a similar scenario for countries along the Mediterranean coastline. The authors deduce that a global sea level rise at a metre-scale growth rate would have adverse economic and financial effects exponentially proportional to the growth of sea level. They continue and conclude that adaption and mitigation methods are easily implemented and simply require early consideration within any coastal management and development planning and/or reviewing phase.

In a South African context, an example of an area susceptible to global sea level rise is the Cape Flats region, within the Western Cape. This area only reaches a mere 5 m above sea level and has a large percentage of its population living in a low to very low-income bracket (Census, 2011)[3]. A vast majority of this population relies on the national government for social and housing allowances (Oldfield, 2000). It is clear that if Nicholls and Hoozemans, (1996) research can be applied to the Cape Flats, and in the event of accelerated global sea level rise, a national disaster could be eminent in Cape Town. While the IPCC report estimates that the sea level will rise at a constant rate proportional to global warming (IPCC, 2007), Tol et al., (2008) considered the possible collapse of the West Antarctic ice sheet, and estimate a sudden global sea level rise of up to 6 m. A sea level rise on this magnitude would be highly detrimental to the Cape Flats region and highlights an important need for proper adaption and mitigation research and implementation.

Livingstone, (1975) was the first to actually conceive the effects of global sea level rise in an African context, extended to the Cape Peninsula. He acknowledged the threat posed by global sea level rise, while recognising the lack of adequate disaster management. His research was simplified by Mukheibir and Ziervogel, (2007) who concluded that while there are very simplistic mitigation scenarios on a national level, there are none instigated on a smaller municipal level. Especially the more susceptible communities like those residing in the Cape Flats. In 2008, the City of Cape Town Environmental Resource Management Department hired *LaquaR Consultants CC*[4] to perform a sea-level rise risk assessment of Cape Town. They constructed a model that considered different scenarios for global sea level rise and associated increased in storm swells that could potentially affect the coastline around the Cape Peninsula. Their predictions considered the effect posed to the population and tourism industry and they estimated a total potential cost of up to R 50 billion in damages (Cartwright, 2008). Despite this potential devastation, mitigation of climate change and sea level rise has not been the significant factor driving South Africa's response to climate change. It does however remain an ever-present factor supporting adaption and mitigation scenario research globally (i.e. Barth and Titus, 1984; Warrick and Oerlemans, 1990; Douglas, 1991; Church and White, 2006). The most prominent mitigation factor is, and will remain preventing further climate change through the reduction of atmospheric CO_2 and other GHG emissions. The burning of fossil fuels for energy development is the leading

[3] More information, and Census 2011 results available from: www.statssa.gov.za.
[4] A private consulting company based in Cape Town, South Africa, contracted by the City of Cape Town to perform a sea level rise risk assessment for the Cape Peninsula.

cause of GHG emissions, especially in South Africa. Not surprisingly, this is the leading theme in the combat against climate change with a global shift toward the research, development and implementation of alternative sources of energy in most countries around the world.

Having ratified the Kyoto Protocol, the South African Government affirmed its commitment to combat climate change, furthered with the introduction of the Environment Act, 1998 (South African Government Gazette, 1998) and the White Paper on Renewable Energy, 2003; 2012 (United Nations Framework Convention on Climate Change, 2003). These policy documents aim to reduce the overall GHG emissions by 40% on, or before 2050 through the development and implementation of various forms of renewable energy. A preliminary goal was set to reach this target by installing a capacity of 10,000 GWh by 2013 (Edkins et al., 2010). This was planned with the development of new wind, hydro bio and an extensive solar project. The solar project targeted all low-cost housing projects with the addition of a solar water-heating system. It was envisioned that through this system at least 23 % of the renewable energy target would be met. With added pressure on the South African Energy Grid from the industrial and social sectors for an uninterrupted electricity supply, heightened after a prolonged period of rolling blackouts, especially throughout 2008, the development of two large-scale coal-fired power plants were commissioned.

These are the Medupi station in the Limpopo Province and Kusile station in the Mpumalanga Province. These power stations are the latest in coal-fired energy technology that uses supercritical steam generators capable of producing up to 5,000 MW. These are also retrofitted with flue gas desulphurisation filters capable of reducing the total sulphur emissions by up to 90 %. However, they remain relatively energy inefficient, since they are limited to using less than 40 % of the total burnt coal for energy production, while the rest is emitted into the atmosphere. In addition, this new development commenced despite the fact that South Africa became the leading carbon emissive nation in Africa, emitting a total of 450 million tonnes of CO_2 in 2011, 258 million tonnes more than second placed Egypt. These values far exceed Wheeler, (2008) predictions that South Africa would reach 450 million tonnes only by 2025. The planned coal-fired power station development is further compounded with an expected coal shortage, forecasted by 2017 (Eskom Annual Report, 2008). Presently, South Africa being is the 7th largest coal mining country in the world. All the above factors underscores the need for renewable energy, however clearly defines the current strain being placed on the South African Energy Grid and the nations need for large-scale energy generation.

1.2 Present and future of climate change mitigation and adaption

Adaption and mitigation against climate change intensified during the previous COP17 climate change summit, hosted by South Africa. Herein, the majority of nations participating in the COP agreed upon a climate change pact. This pact aims to introduce legally binding taxation on nations who do not have stringent climate change policies in place by 2015 (Jacobs, 2012). These climate change policies fall within the Durban Platform aiming to reduce GHG emissions to levels as originally agreed as defined in the Kyoto Protocol, while providing a level of insurance for energy-intensive industry and still maintaining a commitment toward the Green Climate Fund that supports developing nations in their climate change combat. This follows one of the main resolutions from the COP16 summit in Cancun, Mexico that defined a need to restrict global temperature rise to an average of 2° C before the industrial revolution[5]. The precise legal implementations of these climate change policies were largely undecided during previous COP meetings, however were addressed at the recent COP18 meeting[6].

One of the largest factors delaying any decree of new legally binding climate change documents is equating economic development to GHG emission rates. As climate change documentation largely considers current and more recent GHG emissions, many developing nations note that the now developed nations had similarly high, and higher emissive rates during their individual periods of economic and industrial growth. These rates would eventually lead to the development of the Kyoto Protocol. This creates a consensus among developing nations that any new climate change pact should consider past GHG emissions to ensure a fair ruling. An example may consider China, which currently needs 50 % more energy than the USA for every USD 1 billion of GDP, and still relies predominately on fossil fuels as its major energy source (Leggett, 2011)[7]. Being a developing nation, China can avoid stringent climate change resolutions, while the USA would face financial penalties. This provides a conundrum for both developing and developed nations: should developing nations be allowed to emit

[5] The 16th Conference of the Parties Meeting was held in Cancun, Mexico from November 29 to December 10, 2010. More information available on the conference website: http://www.cc2010.mx/en/.

[6] The 18th Conference of the Parties Meeting was held in Doha, Qatar from November 26 to December 7. More information available on the conference website: http://www.cop18.qa/news/singlestory.aspx?id=297.

[7] Report by the U.S. Congressional Research Service on China's Greenhouse Gas Emissions and mitigation policies, available from: http://www.fas.org/sgp/crs/row/R41919.pdf.

large concentrations of GHG, while developed nations face stringent penalties, or should past GHG emissions be factored less and we look globally toward sustainable development?

Upon finalisation, the COP18 summit had several key points that included: the extension of the Kyoto Protocol from 2013 for a further 8-year commitment period. This occurred because the Kyoto Protocol was the only legally binding document ensuring that countries are responsible for their GHG emissions. The amended document will require nations to have active policies in place by 2014 for reviewing their GHG emission targets and implementing necessary reduction protocols. In addition, there will be a renewing of various funding programmes, namely, the Clean Development Mechanism (CDM), Joint Implementation (JI) and the International Emissions Trading (IETA). These programmes largely relate to creating funding platforms for developing nations to attain future sustainable energy development.

Despite being the only legally binding climate change resolution, the Kyoto Protocol was not ratified by all major nations, including high GHG emitting nations. Therefore another resolution decided during the COP18 was the need for a broader climate change policy encompassing all nations. This resolution aims to have a global climate change resolution implemented by 2020, and have nations in agreement by 2015. The UN secretary general, Ban Ki-moon, has agreed to address all nations in 2014 to ensure global adherence in unison to this policy.

Another important decision made was that the Green Climate Fund would be launched and hosted in South Korea. This fund aims to ensure development of infrastructure and makes significant financial contributions to ensure global efforts toward climate change are met. This fund is predominantly directed at developing countries and those most vulnerable to the effects of climate change, such as the Least Developed Nations (LDN). To ensure climate change mitigation targets are met, a sum total of USD 100 billion is needed by 2020. Germany, France, UK, Denmark, Sweden and the EU commission have already agreed to this and have pledged USD 6 billion by 2015.

Global attention will now shift to Warsaw, Poland for the next Conference of the Parties' 19th meeting in December 2013. This meeting will form an important platform for ascertaining the success of implementation of the various policies highlighted during the COP18 and ultimately the progress of the global combat against climate change.

1.3 Renewable energy sources and environmental solutions

1.3.1 Current alternative energy sources in South Africa

The target for generating renewable energy in South Africa is planned with the implementation of hydro-, wind-, solar- and bio-energy projects. Present renewable projects include wind farming at the Cookhouse Wind Facility in the Eastern Cape that is expected to produce up to 135 MW and pump-storage hydroelectricity that includes the Drakensburg (1000 MW) and Palmiet (400 MW) plants. There are also plans to build a large-scale concentrated solar power farm near Upington, expected to generate more than 100 MW of renewable energy. In addition, solar framing is expected to become attractive to a large privatised sector allowing companies to benefit from carbon reduction tax credits. Solar is now implemented as a legislation with the inclusion of solar PV panels on all new building construction, as amendment to the National Building Regulation and Building Standards Act, effective in 2011. These forms of renewable energy are expected generate the target of 10,000 GWh by 2013. This would include renewable energy sources that operate at least 50 % of the time and this target will account for 20 % of South Africa's total energy needs. However, they will not alleviate South Africa's position as the leading GHG emitter on the African continent. In order to reach millennium targets and reach a sustainable green energy future, South Africa will have to expand research and development toward longer-term renewable energy solutions and also consider other possible alternative energy sources.

1.3.2 Possibilities of shale gas toward future energy security

Another factor of the energy scenario in South Africa is a growing interest in shale gas exploration and exploitation. This interest rapidly grew following a report by the US Energy Information Administration (US EIA) that estimated shale gas reserves in the Karoo Basin of up to 485 trillion cubic feet (tcf)[8]. Subsequently, a report by a private economy firm, *Econometrix*[9], predicted reserves up to 50 tcf (Econometrix, 2012). Despite being considerably lower than initial estimates by the US EIA, *Shell* reports that even on the latter scale, the shale gas reserves will have the potential to supply half of the total energy requirements of South Africa. In addition to having the potential to provide

[8] Full report available from: www.eia.gov/cabs/South_Africa.pdf.pdf.

[9] *Econometrix* is one of South Africa's largest macro-economic and privately owned consulting firms applying business forecasting strategies linked to global markets.

South Africa with energy security, estimates from the *Econometrix* report suggest that the Karoo shale gas has the potential the generate an economic and financial investment influx of up R 200 billion. Having an energy and economic potential on such a high level makes the prospect of shale gas highly likely to be developed or at least tested for South Africa's future energy supply. However, large environmental and public outcry on the methods of hydraulic fracturing needed to extract this unconventional gas and its adverse effects on groundwater sources will yield further progress until it is deemed safe by an independent panel assigned by the Department of Mineral Resources, South Africa[10]. However, more recently the minister of mineral resources of South Africa lifted a moratorium on fracking in the Karoo, opening the way for further research. This will include detailed geological exploration with mapping, seismic studies, hydrogeological investigations and core drilling. It was agreed that hydraulic fracturing would be reframed from until all the preliminary geological investigations are completed.

1.3.3 Exclusion of EGS in South Africa

At least one of the reasons why geothermal energy is excluded as a potential renewable energy source in South Africa is because South Africa overlies the Kaapvaal Craton, which has a thick underlying lithospheric mantle keel (Bullard, 1939; Pearson et al., 1995; Shirey et al., 2002; Niu et al., 2004; Michaut, 2009). The keel provides the country with a relatively cold lithosphere and a resulting low heat flow signature (Ballard and Pollack, 1987; Jones, 1987). In addition, lacking of any active volcanism and tectonism it is understandable that geothermal energy has not been considered as a viable long-term renewable energy alternative. The lack of research in geothermal energy is largely based on a classical belief that areas devoid of active volcanism and having thicker crustal signatures are not ideal locations for geothermal exploitation. However, even these areas may still have the potential for sustainable low-enthalpy geothermal energy extraction. Low-enthalpy geothermal resources are not extracted on a large international scale since it is believed to only be viable for small direct-usage purposes. However, technological advancement made in drilling and heat exchange mechanisms are better developing this technology for much broader usage. Some successful low-enthalpy geothermal projects include Alaska, Austria and Germany (Chandrasekharam and Bundschuh, 2008). These projects have shown success in generating sustainable energy from relatively low temperatures 100-200° C at a depth ranging from 2-3 km (Axelsson, 2008).

[10] File available from: www.info.gov.za/view/DownloadFileAction?id=174015.

1.4 Enhanced Geothermal Systems as a possible intermediary solution

The Kaapvaal Craton exhibits relatively cold crust and mantle heat flow signatures (i.e. Fouch et al., 2003). However, anomalously high heat flow zones are evident along mobile belts flanking the craton (Jones, 1987; 1992; 1992). These occur most notably along the Cape Fold Belt (CFB), Namaqua-Natal Mobile Belt (NNMB) and Limpopo Mobile Belts (LMB) and are evident through the development of numerous hot springs (Nyabeze et al., 2010; Olivier, 2011; Tekere, 2011). These heat flow signatures are attributed to major continent collisional events, which resulted in crustal thickening and several associated phases of granitic emplacement (i.e. Belcher and Kisters, 2006; Harris and Vogeli, 2010). The granites were generally rich in heat producing elements such as U, Th and K, all capable of generating large amounts of heat during their natural radiogenic decay processes. With their higher heat flow signatures, these zones might potentially represent ideal locations for harnessing low-enthalpy geothermal energy through Enhanced Geothermal Systems (EGS).

EGS uses increased heat flow in fractured crystalline plutonic rocks to generate energy. Energy generation is possible with the development of a deep hydraulically generated fracture network that connects a well system. The well system comprises of an influx well and as many producing wells as is sustainable. A cold working fluid is pumped through the influx well and into the fracture reservoir. The fluid then circulates throughout the fracture reservoir constantly being heated through conduction with the surrounding rock. Thereafter, the energised hot fluid exits the reservoir through the numerous production wells before entering a binary generation system. Within this system, it invokes a heat-exchange process with a secondary organic-based fluid. The organic fluid has a much lower boiling temperature and flashes to steam after exposure to the high temperature primary working fluid. The process of flashing conveys the rapid phase change from liquid to gas. The steam then runs a generator that produces energy. The working and organic fluids are kept separated throughout the process. After the cycle, the now cold working fluid circulates back through the well system while the condensed organic fluid circulates back to the start of the binary system, and the cycle is repeated (also see Figure 2 and Figure 3).

A successful EGS plant will have the capacity to produce energy and feed it into the energy grid, while simultaneously sustaining the pumping energy required. In addition, there is no GHG emitted: this is therefore an ideal green energy system. Kohl and Speck, (2004) investigated the variation in the chemical composition of binary fluids. They found that it is possible to create an

economically viable EGS plant from a temperature source as low as 100° C by using a carefully composed organic fluid, thus making EGS a possibility in any of the anomalous heat flow areas of South Africa.

1.5 Economics of possible Enhanced Geothermal Energy in South Africa

This study considers the LMB as a possible target site for EGS, by characterising a relatively high heat flow zone surrounding the Siloam hot spring, Limpopo Province, South Africa. This spring displays the highest surface temperature in South Africa, measuring up to 70° C (Nyabeze et al., 2010; Olivier, 2011; Tekere, 2011). This study models the development of a 75 MW EGS plant over a period of 30 years. It includes the development of a preliminary 1 MW pilot plant allowing for initial flow and capacity testing to aid in model precision. The report is structured with an introduction to EGS development and special attention given to hydraulic fracturing. To attain an accurate assessment of the viability and sustainability, a Levelised Cost of Electricity (LCOE) model is developed. Such a model calculates the economic and financial constraints of developing an EGS plant within South Africa. The model also calculates the possible energy output based on various geological and engineering parameters. These factors are equated together to estimate the overall viability of the hypothesized plant. Another important factor considered within the model includes a calculated groundwater sustainability profile. Considering that EGS uses a large volume of water to operate, the model estimates the effect this will have on the present and future surrounding population and their water security. The economic model is based on similar alternative energy models as developed by Credit Suisse with comparative data from other international EGS projects. These include projects in Australia, France and Germany. The model is factored with South African economic and financial parameters and available geological data.

The results of this research aims to generate recommendations for the implementation of EGS as another alternative energy technology in South Africa's shift to long-term renewable energy production. It also aims to highlight the benefits associated EGS and finally, assess the current and required level of research toward possible future implementation.

Chapter 2: Introduction to Enhanced Geothermal Systems (EGS)

Geothermal energy is common and successfully employed in areas with active volcanism. This is related to their favourable geographic position near active plate boundaries or mantle hot spots. These geothermal locations usually overlie regions with relatively thin continental lithosphere, where groundwater within its natural flow path undergoes convective heating to reach boiling point and emanate at the surface as supercritical steam (Lund et al., 2005). An example of this method is commonly employed in Iceland. Here the mid oceanic ridge is exposed close to surface and provides an area of extremely high heat flow. Geothermal systems developed in these environments are referred to as volcanic geothermal systems. Conversely, geothermal systems can also be present surrounding a dormant volcano or an anonymously high heat flow region that attains high crustal temperatures and results in natural steam generation. This is typically referred to as hydrothermal systems and many experimental plants have been tested in these environments (Lovelock et al., 1982; Doi et al., 1990; Kiryukhin, 1993; Muraoka, 1993).

The East African Rift (EAR) system has both the volcanic and hydrothermal geothermal systems available, but many are not exploited. The EAR forms the present most active continental rift system, with the presence of an underlying mantle plume. The rift comprises of three distinctive rift branches (Chorowicz, 2005). These include the two dominant eastern and western rifts and the less prominent southern rift, in the Mozambique Channel. The eastern rift begins in the Afar triangle, where oceanic spreading ridge is revealed at the surface, and continues through Ethiopia and Tanzania. The western rift incorporates the African great lakes and dissipates into southern Africa. According to Hochstein, (2005) there are at least 54 potential geothermal target sites along the eastern rift with available information on 14 of those sites. From these known sites there is approximately 4000 MW of potential geothermal energy. In addition, there are 7 known targets along the western rift that amount to approximately 300 MW of potential energy. Furthermore, a large portion of the western rift is covered by the great lakes, and their inclusion would increase this value significantly, however requiring the addition of a water-based geothermal harnessing system. A common system employed is a lake-loop system. Herein a system of pipes containing a heat sensitive working fluid, commonly organic brine, undergoes heat transfer within the lake. The heated fluid is then used to power a generator and produce energy in a similar generation system as is employed in EGS.

Despite many countries being situated on ideal locations for harnessing geothermal, only 11 countries were actively investigating this technology in 2010 (Holm et al., 2010). According to the International Energy Agency, the number of countries has since increased to 14 at the end of 2011. However, many of these countries focus only on the exploitation of shallow hydrothermal reserves, and not on EGS. Within an African context, Kenya is the leading geothermal developing nation, with their investigation and implementation having started as early as 1960. Currently, they have an installed capacity of just less than 500 MW. The Kenyan Government has since targeted geothermal for further expansion and aims production to peak at 4000 MW over the next 20 years (Simiyu, 2008; Holm et al., 2010).

Unlike volcanic and hydrothermal geothermal energy systems, EGS employs a system of exploiting latent heat encapsulated in deep plutonic rocks. This heat is produced as a result of the natural decay of heat producing elements within these plutonic rocks. These heat-producing elements include U, Th and K and all are commonly found in plutonic minerals (Chamberlain and Sonder, 1990). Neumann et al., (2000) related a region of higher heat flow in southern Australia (see Figure 11) to an area of Proterozoic granite with anomalously high U, Th and K signatures, with Th/U values between 3-5. An EGS system is implemented where a working fluid is allowed to interact with the surrounding hot rocks and heat up substantially. The heated fluid is then pumped back to the surface and used in a binary generation system. The binary system has a second organic-based fluid with a much lower boiling point and upon exposure to the heated geothermal fluid, flashes to steam. The organic steam is then used to run a generator and produce energy (Vogt et al., 2012).

The original theory and applications to harness geothermal energy from a deep-seated plutonic reservoir was investigated and developed in 1970 under the Fenton Hill research project within the Los Alamos Scientific laboratory, USA. Here a pilot plant was set up at the base of Valles caldera in the Rio Grande Graben, New Mexico in an investigation of harnessing energy from what was originally known as “Hot Dry Rocks” (West, 1974). Initially, funded through the United States Government, the project would eventually receive further international attention and support from the International Energy Agency (IEA), France, Great Britain, Germany and Japan. Following the success of this project, EGS technology investigations started in the Europe, Japan and Australia. France (Hooijkaas et al., 2006; Schlagermann and Kolbel, 2011) and Australia (Chopra and Wynborn, 2003) were the first to investigate EGS in geological terrains devoid of any active volcanism. EGS in the USA is regarded as a major potential future alternative energy source, with further research and development

focussed toward a target of 100 GW of EGS installed capacity by 2050 (Idaho National Laboratory, 2006; Chamorro et al., 2011).

EGS is also being proposed as a mechanism for simultaneous CO_2 sequestration. This is thought to be possible by incorporating CO_2 into the working fluid pumped into the geothermal reservoir. The CO_2 would theoretically be trapped and stored in the reservoir before the working fluid returns up the production wells (Damiani et al., 2011). This process is similar to the application of using hydraulic fracturing as a mechanism to create a storage facility for spent nuclear fuel.

A schematic illustration of the modelled EGS system considered within this study is shown in (Figure 2), based on a simplified geologic basement underlying the Makuleni target area. The lower target Limpopo TTG plutonic basement rocks underlying the Soutpansberg volcano-sedimentary sequence. The Soutpansberg sequence furthermore acts as an insulating surface layer, capturing heat developed from the underlying basement rocks. The model illustrates the EGS system with one influx well and two production wells down to a depth of 5 km, attaining an estimated basal reservoir temperature of just below 200° C. Some of the various data sources implemented to construct this model are illustrated. The generation of energy occurs through a binary generation plant that functions through a heat-exchange system, as shown in Figure 3. Summaries of previous pilot EGS plants are provided in the following section below.

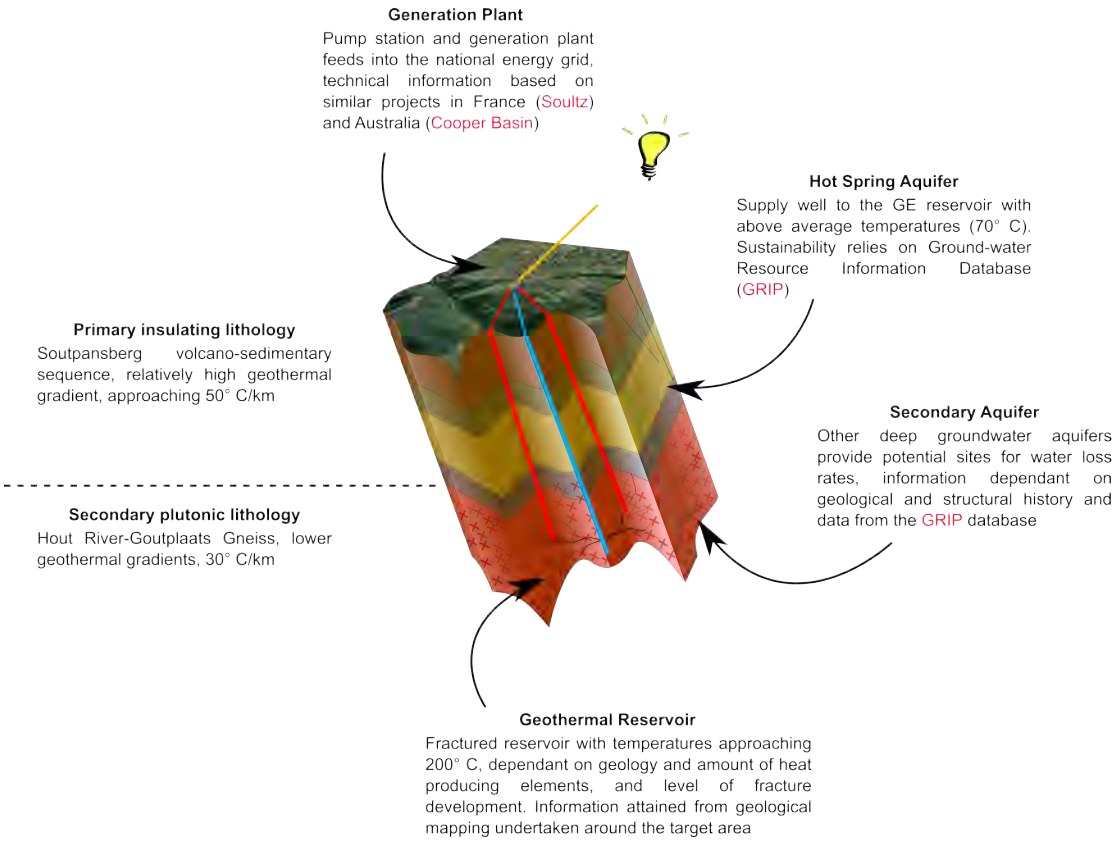

Figure 2: Schematic EGS illustration with the blue line representing the influx well and the red lines representing the production wells

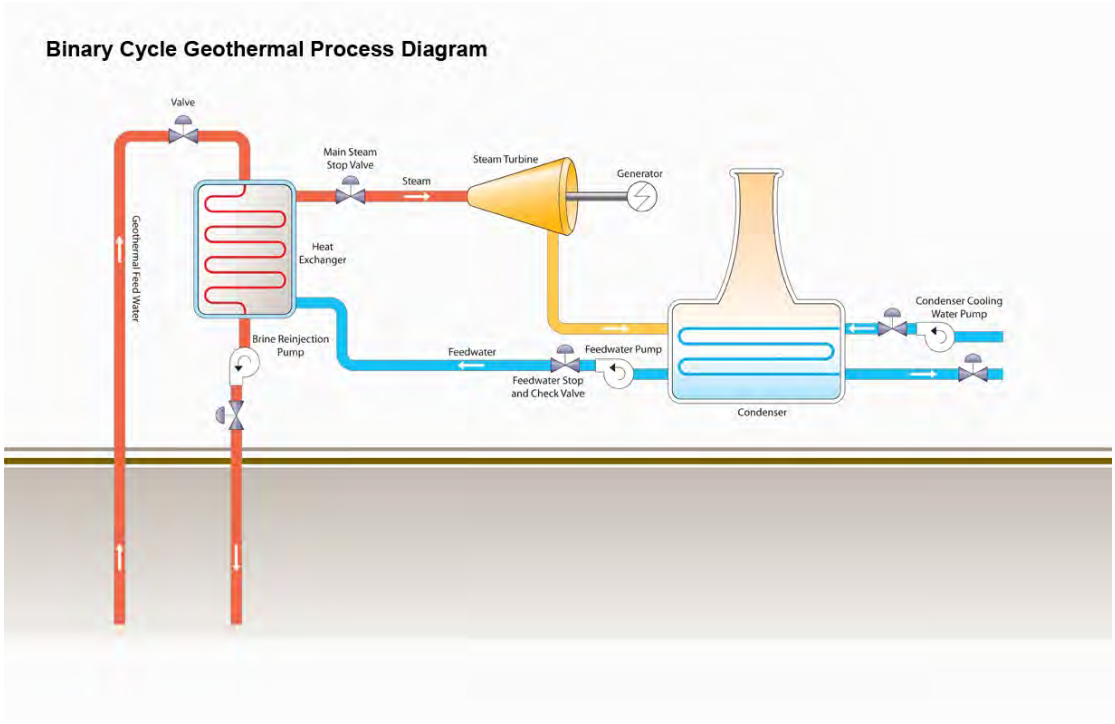

Figure 3: Overview of the binary system within the proposed EGS plant, Flowserve Corporation (www.flowserve.com/Industries/Power-generation/Geothermal

Chapter 3: Enhanced Geothermal Systems development outline

3.1 Background investigation

3.1.1 Heat flow and heat productivity

The first step in developing an EGS power plant is to identify a target site that exhibits a high heat flow. This high heat flow should ideally emanate from a plutonic unit that is both high in heat producing elements, and as has an extensive fracture network. The heat producing elements include U, Th and K that during their natural decay release heat, and provide the high heat flow signatures observed (Bickle, 1978; Lee et at, 1987; McLaren et al., 1999; Ting, 2011). The plutonic unit needs to attain an adequate depth and thickness, depending on the level of heat flow. Lower concentrations of heat producing elements will have a shallower geothermal gradient, requiring a deeper geothermal reservoir. The plutonic rocks should also have a composition and mineralogy as homogenous as possible. Large variation in mineralogy and composition within the plutonic rocks can lead to the formation of convective loops (Baria et al., 2006). Convective loops illustrate a variation in the concentration and type of heat producing elements in the targeted rock. These convective loops were first observed at the Soultz EGS project, France, and resulted in large fluctuation in the heat flow along the length of the well system.

Complimentary to the heat producing plutonic rocks, another unit is required to ensure adequate heat retention. Ideally, the pluton should be insulated by a thick overlying sequence of sedimentary and/or volcanic rocks. The thickness of the insulating layer depends on the level of heat flow observed. A high heat producing pluton requires only a thin insulating layer. In addition, an insulating unit thicker than 3 km can become detrimental for the EGS plant, as deeper drilling is required to reach the target plutonic unit.

3.1.2 Fracture network and stress regime

Hydraulic fracturing is essential for the success of the EGS plant. Fracturing ensures the development of a well connected and adequately porous fracture network. The fracture network serves as the geothermal reservoir responsible for heat exchange between the hot rocks and geothermal fluid. Since the geothermal reservoir is one of the main parameters controlling the efficiency of the plant, accurate and controlled hydraulic fracturing is a necessity. The

fracture network must be continuously monitored until it attains the desired size and orientation. This is done by numerous geophysical and imaging techniques (Valley et al., 2007).

The success of hydraulic fracturing relies on an accurate assessment of the overall stress regime and its effects on the target plutonic rocks. Understanding the regional to local stress regime and existing fracture orientation allows hydraulic fracturing to be orientated in a direction gaining maximum efficiency. Fracturing widens the spacing between fracture sets and results in the growth of the geothermal reservoir. Miscalculations of the stress regime can result in the reservoir expanding in an undesirable direction and possible failure of the project, evident from the Rosemanowes EGS project, U.K. Hubbert and Willis, (1957) were some of the first who investigated the propagation of fractures. They discovered that fractures were created through tensile failure in the rock and propagated perpendicular to the principle minimum stress regime.

The depth of drilling required depends on the result of heat flow calculations and estimation of basal reservoir temperatures. EGS is possible from temperature resources as low as 100° C, however is more effective between 200-300° C. The drilling depth needed for attaining the desired temperatures can vary from 1-5 km. Drilling and hydraulic fracturing contributes a large percentage of the overall EGS expenditure with the cost of drilling increasing exponentially with depth. The development of new laser drilling technology promises to decrease the price of future drilling projects substantially and could play a vital role in determining the viability of EGS. With drilling and hydraulic fracturing capable of determining the economic viability of the plant and subsequently the future of any planned EGS venture, the required depth of drilling and fracturing needs to be determined with a very high level of accuracy.

3.2 Exploration and pilot plant development

3.2.1 Generating an adequate fracture connectivity

An EGS system will require at least one influx well and several production wells. Depending on the results of the fracture modelling and stress regime, reservoirs of various sizes can be generated. Each production well will need to be adequately connected with its influx well(s). Hydraulic fracturing is used to generate the required connectivity between the various wells and to control the size of each geothermal reservoir (Rose et al., 2006). Similarly, uncontrolled hydraulic fracturing can result in the development of shorter preferred

pathways that may be irreversible and cause irreparable damage to the plant. A geothermal reservoir of 1000 m^3 is typically considered to be the minimum required volume for production. Depending on the heat flow and basal reservoir temperature an adequate residence time is needed to ensure that the geothermal fluid reach their maximum possible temperature.

3.2.2 Hindering mineral precipitates

Fractures are often sealed with mineral precipitates such as carbonates and sulphates. In this case a water-based fracturing fluid will be hindered by these mineral precipitates, and fail to create the desired porous network. In order to overcome this problem certain chemical-based fracturing fluids can be used, with a composition dependant on the types of mineral precipitates. Ledésert et al., (2009); Hébert et al., (2010); Hébert et al., (2011) investigated the relationship between the fluid flow pathways and the development of mineral precipitation in EGS reservoirs. These authors found that in some geothermal systems, precipitation was evident and formed proportional to the direction of fluid flow. They also found that maintaining a high fluid flow rate and pumping pressure resulted in less mineral precipitation. They also found that lower flow rates and pumping pressure decreased the size of fractures, while increasing the system impedance. These conditions appeared to be ideal for mineral precipitation, the composition of which depends on the surrounding geology. The addition of chemical stimulation requires the incorporation of calcimetry techniques to determine the rock and mineral chemistry and determine the ideal composition of fracturing fluid. These chemical stimulation processes typically require various acids capable of breaking down organic clays. These acids include hydrochloric acid and other high temperature clay acids.

3.2.3 Induced seismicity

Induced seismicity is a common consequence to hydraulic fracturing and numerous examples have been recorded. Majer and Peterson, (2007) measured seismicity at the Geysers EGS in California, U.S. and Cuenot et al., (2010) measured the induced seismicity associated with the long-term test at the Soultz EGS plant. Over a 6-month period, Cuenot et al., (2010) recorded more than 600 seismic events, these events did however rarely exceeded a magnitude of 2. Subsequently, they ran an experiment over a 3-year period where they varied the pumping pressure and flow rate. They concluded after the third year that seismic events were predominantly triggered by large fluctuations in the

pumping pressures and flow rates and by stabilising these factors, they decreased the number of seismic events to 53.

An active seismic monitoring system must be employed during hydraulic fracturing and flow testing of any prospective EGS plant. With this system in place, and by avoiding large fluctuation of pumping pressure and flow rate, induced seismicity can be kept minimal.

3.2.4 Pumps and well systems

The well system incorporated within an EGS plant typically focuses around a singular injection well and any number, and any layout of production wells. Areas with higher heat flow could use a system with fewer production wells, however to maximise energy production and depending on the size of the target pluton and reservoir size, a large number of wells can be employed. Typical 75 MW EGS plants surrounding a region with a heat flow of between 60-150 mWm^{-2} use up to 10 production wells linked to a singular injection well. Chopra and Wyborn, (2003) proposed that the Cooper Basin EGS project would possibly reach up to 37 production wells to reach commercial viability.

The use of groundwater often leads to the precipitation of various minerals within the well system (Adams et al., 2005). These mineral precipitates can have corrosive properties that are detrimental to the wells. Baticci et al., (2010) investigated scaling and corrosion on the wells associated to mineral precipitations. They used various types steel alloys, commonly used for the development of wells and wellheads, and exposed them to the various fluid compositions expected during EGS operation. These representative fluids commonly have high salinities and low pH. During their experiments they detected the precipitation of sulphates overlying corrosive iron oxides. These precipitates led to the development of pits in the well surface, which accelerated corrosion of the well. Muller et al., (2010) continued the work on the corrosion and scaling on the wellhead, by investigating the rates of corrosion experienced against different types of steel alloys and the effect of various anti-corrosive Teflon coatings. They found that without a protective coating, the wells corroded at 2 mm/year at a working temperature of 200° C. However, with the addition of Teflon coating mineral precipitation became minimal and the wellhead showed no deterioration over the same experimental period.

The injection well uses a surface pump with pumping pressure and flow rate dependent on the critical pressure of the fracture network. The critical pressure of the fracture network defines the pressure required to maintain fracture

spaces and keep the network adequately porous. In addition, the pump requires a wellhead pressure that prevents any degassing from the system and maintains a constant pressure. A loss of system pressure can result in the closure of fractures or well collapse. This was evident from the Fenton Hill EGS project where a well collapse was suffered after a loss in pressure through the influx well. A well collapse will result in the well needing to be closed and sealed with cement before being re-drilled.

Two types of pumps are commonly used in the production wells. This includes a line shaft pump, located close to the surface, or a submersible pump, located at any depth along the well. Both types of pump have similar efficiencies of up to 80 %. However, the submersible pump uses a smaller motor that runs at higher speeds and is generally prone to wear and tear. A submersible pump can however be used in deviated wells, while a line shaft pump is limited to a relatively straight well. Line shaft pumps have the capacity to operate at a much higher temperature and are less expensive than the submersible pumps. Varying geological and heat flow conditions will determine the type of well used, with a highly complex geological profile most likely requiring inclined wells and therefore submersible pump.

3.2.5 Binary generation system

The heated fluid exiting the production well(s) is used to generate energy after entering a binary generation system. A binary system uses an organic fluid to run the turbine that produces the energy. This fluid has a much lower boiling point and often a higher density than the geothermal fluid (Sauret and Rowlands, 2011). The binary system design allows the geothermal fluid to enter and remain separated from the organic fluid, however invoking a heat exchange between these fluids. Upon exposure to the heat, the organic fluid flashes to steam and consequently runs the generator. The cold geothermal fluid continues the cycle through the injection well, while the condensed organic steam is restricted and circulates within the binary system (Figure 3).

Within the Soultz project in France the common binary cycle used was an organic rankine cycle that employed the use of a low boiling point organic brine such as isobutane. Experiments were also performed using a Kalina Cycle, which employs a similar mechanism with an ammonia-water working fluid and results in a 50 % efficiency increase. The flashed working fluid enables the turbine and run a generator, typically at 1500 RPM, before exiting the turbine and entering a second stage condenser that condenses the working fluid, thereafter the cycle begins again.

3.2.6 Groundwater

Geothermal uses a substantially larger amount of water than all other renewable sources and the largest concern facing the use of geothermal remain the effect posed on the groundwater supply.

Clarke et al., (2012) investigated possible impacts, including those on the groundwater, of geothermal energy and its relation to those of other energy sources. This investigation included renewable and non-renewable sources and their findings showed that the construction time and cost of geothermal plants greatly exceeded those of other renewable sources. However, geothermal energy had the greatest affect with regard to GHG reduction. They also found that all alternative energy sources had a much lower impact on water resources than non-renewable source. Addressing these concerns, all EGS plants will have to undertake an extensive hydrogeological survey to ascertain a forecasted effect on the water supply (Chapter 7.4). In addition, analyses of the underlying reservoirs are required and are often performed using various magneto-telluric methods (Schill et al., 2010).

The largest parameter on the volume of water used within an EGS system is the water-loss rate. Water losses experienced throughout all previous EGS plants related to how well sealed the fracture reservoir was. The Hijiori EGS in Japan had water losses of more than 50 % due to an initial uncontrolled growth of the fracture network. Conversely, the Cooper Basin EGS managed to retain 95 % of all water pumped into the reservoir because the system remained closed. This again highlights the importance of accurate fracture modelling and controlled hydraulic fracturing.

Public concern regarding the effect of EGS on the groundwater quality and supply was recently addressed by the U.S. Department of Energy for the proposed *AltaRock* Newberry EGS plant. Their findings showed that the plant would have no notable detrimental effect on the groundwater supply. *AltaRock's* investigation was deemed appropriate and their investigations included a pump and tracer test on the proposed supply well. In addition, the injection and production wells were to be encased and sealed in cement to prevent any geothermal fluid being release into the surrounding country rock. This is for a scenario in which a chemical propping agent is included into the geothermal fluid. Other concerns from the public included induced seismicity, wildlife and scenic resource impact assessment. However based on the U.S. Department of

Energy, all these issues were adequately addressed and the project was cleared to continue[11].

3.3 Possibility of simultaneous carbon sequestration

Brown, (2000) considered the use of supercritical CO_2 as an alternative geothermal working fluid to water. He deduced that this would not only allow for possible sequestration of CO_2, but also render the system more efficient. An increase in the system efficiency is attributed to the fluid density variation between a cold injected supercritical CO_2 fluid and the hot supercritical fluid entering the binary system heat exchange. This would theoretically result in a pressure gradient double that of one created with a water-based geothermal fluid. The large pressure gradient would consequentially be capable of driving the binary system with a greater force and make the system more efficient. However, the mass heat capacity of a supercritical CO_2 fluid is much lower than that of water, making it thermally less efficient than a water-based geothermal fluid. CO_2 also has a much lower viscosity than water, which under EGS production conditions is expected to yield ca. 60 % greater thermal performance (Brown, 2000).

Additional tests with water as the main geothermal working fluid is limited to temperatures below the critical water level of 384° C and 22 MPa. Exceeding these conditions could result in the dissolution of calcites and silicates from the host rock resulting in large concentration of mineral precipitating in fractures (Rose et al., 2007). This would increase system impedance, deterioration of the wells and result in a drastic loss of efficiency. At these conditions CO_2 is less effective at dissolving these minerals and would lessen the formation of these mineral precipitates. However, EGS resources rarely exceed those temperatures.

Pruess, (2007) also investigated the use of supercritical CO_2 as a working fluid and found that CO_2 results in an increase in efficiency. He also deduced that it has the potential to provide better heat exchange by avoiding unwanted dissolution with the surrounding rock. He further concluded that additional interactions between the rock and supercritical CO_2 fluid requires more experimental work to better ascertain. Some of these fluid-rock interactions were made clear from the Hijiori EGS site during a long-term test run that ran over a 3-month period. Within this period 6 tons of CO_2 was injected into the system (Yanagisawa, 2010). High levels of scaling were observed together with calcite precipitation in

[11] The full Newberry report is available from: http://energy.gov/site/prod/files/EA-1897-FONSI-2012.pdf).

the shallower production wells (Yanagisawa et al., 2007). These events illustrate the sensitivity of fluid-rock interactions and how these are exemplified under fluctuating system conditions within an EGS system. Both water-based and CO_2-based geothermal fluids have their individual benefits; however, the composition of geothermal fluid will vary depending on a number of factors within the EGS system. Pistone et al., (2011) investigated the solubility of CO_2 during rock interactions to better ascertain its significance as a geothermal working fluid. In their experiments they consider the use of a 2-phase CO_2-H_2O system as an idealised geothermal fluid. They concluded that CO_2 remains soluble, while fluid-rock interactions occurred continuously throughout the experiment. Wan et al., (2011) complimented this work and further investigated the fluid-rock interactions associated with the incorporation of CO_2 into the geothermal fluid. They found that throughout the experiment, rock interaction resulted in the precipitation of carbonate minerals. These minerals aided in creating a trap for CO_2.

Pruess, (2006) developed a hypothetical model to test the variation between running a water and CO_2-based working fluid system in linear systems with one injection and one production well, and a five-spot system with one injection well and four production wells. The tests were run up to 200° C and a pumping pressure of 5 MPa and produced up to 50 % greater extraction temperatures with the supercritical CO_2 system than the water system. However, the difference between the water and CO_2 efficiencies decreased over the lifetime of the plant due to CO_2, causing a larger thermal depletion within the reservoir. In addition, the thermal extraction of the supercritical CO_2 fluid was notably higher in the five-spot system than in the linear system (Pruess and Azaroual, 2006). This was attributed to the variation in the viscosities between water and CO_2, with CO_2 having a greater thermal extraction coefficient than water.

In attempting to create a highly porous fracture reservoir, Pruess, (2007) proposed to accompany hydraulic fracturing with an additional step of CO_2 flushing. This would theoretically remove all water from the reservoir and create an anhydrous medium. He proposed to follow this by flushing the reservoir with H_2O, which would then create a 2-phase reservoir comprising of an inner and outer zone. Within this 2-phase reservoir fluid-rock interactions were not clear, and observations had to rely on natural geothermal systems with high concentrations of CO_2 (Ueda et al., 2005; Andre et al., 2007). Andre et al., (2007) complimented Pruess, (2007) and investigated the 2-phase reservoir system further. They discovered that the 2-phase reservoir had greater system impedance, which they could attribute to an increase in the concentration of mineral precipitates. They attributed the increase in mineral precipitations to

the presence of CO2, conveying similar results as Yanagisawa, (2010) who attributed increased system impedance to mineral precipitation at the Hijiori EGS site.

Pruess, (2007) further investigated the heat and energy capable of being harnessed from an EGS system employing supercritical CO_2-based fluid. He deduced that while CO_2 has a much smaller specific heat capacity than water, it does prove to be more mobile and also has the ability to flow at much higher mass rates. Therefore, it should be capable of generating at a much larger heat extraction rate than a water-based geothermal working fluid. However, considering research regarding the fluid-rock interaction and reservoir conditions, attaining a better energy generation from CO_2 over H_2O will first depend on the mineral chemistry of the underlying geology.

Chapter 4: Overview of Hydraulic fracturing

4.1 Introduction and history of hydraulic fracturing

The heat contained in the lithosphere is estimated to have enough capacity to support the Worlds energy needs (i.e. Fridleifsson and Freeston, 1994; Björnsson et al., 1998). However, the yielding factor remains the availability of technology required to extract the heat and its conversion to energy. A novel solution is the system of hydraulic fracturing, also known as hydraulic stimulation or simply fracking. Hydraulic fracturing is the process in which a fluid, most commonly water, is used to open and increase the porosity of deep fractures. Different chemical solutions are occasionally used, depending on the extent of fracturing required and the lithology in question. Chemicals used will be specific to rock and mineral chemistry, and act toward reacting and breaking down these units. The end result of hydraulic fracturing is the opening and widening of natural fractures to allow for increased fluid circulation and flow between pore spaces. This process is currently being used in the natural gas industry where a fluid is pumped into gas bearing shale. The gas is captured in fractures within the shales and held between the grain boundaries, and the fluid is used to displace gas for extraction. In order to accomplish this and increase the porosity within a fractured zone, the fluid must be injected to overcome the lithostatic pressure holding the gas within the fractures. To maintain the increased spacing between the various fractures, a propping agent is typically mixed with the fluid and serves to prevent the fractures from healing naturally. This is needed as the amount of gas being liberated decreases as the porosity within the fractures decreases, and therefore it is more viable to maintain adequate porosity throughout the extraction process. Propping agents vary according the lithology, however sand and various ceramic agents are the more commonly used.

According to Montgomery and Smith, (2010) hydraulic fracturing for exploration started in the late 1860's where it was used as a tool for exploiting oil and gas in the southern U.S. However, this was an illegal practice, because it relied on the use of volatile and hazardous chemicals and propping agents, including nitro-glycerine. Despite its legal status, this method was highly successful in stimulating fractures, fracturing the oil bearing lithologies and creating a porous conduit for oil and gas extraction. It would prove so successful that it was later legalised and applied in the early 1930's, however with the use of less volatile propping agents, like sand.

The fracturing fluids used in these early applications were all various acidic brines. These brines initiated chemical reactions with the rocks and led to maintaining of generated fracture spaces. Later, in an attempt to shift away from the use of the acidic chemicals, water was used in much larger volume and under higher pressure. However, water failed to maintain adequate fracture spaces and was subsequently paired with additional propping processes, like cementing. The cementing process used coarse sand and pebbles to prevent the fractures from completely sealing. This method did not however yield the same results as achieved by acidic brines, since acidic brines maintained a chemical reactive breakdown.

It was only in the 1940's that studies were conducted on hydraulic fracturing to ascertain the relationships between various fracturing fluids, propping agents and their interactions with the surrounding rock. This resulted in the first research-orientated hydraulic fracturing experiment performed in the Hugoton gas field, Kansas, U.S. This investigated the use of a gasoline-based fracturing fluid followed with an inorganic gel breaker propping agent (Montgomery et al., 2010). While this experiment failed to provide successful results, it initiated an industrial revolution toward early experimental hydraulic fracturing.

In 1949, the Halliburton Oil Well Cementing Company[12] was awarded a patent for hydraulic fracturing. Later that year, they ran experiments varying the composition of fracturing fluids until they attained their ideal composition. This composition included oil, gas and sand. Using this mixture as the main fracturing fluid, they attained a 75 % increase in tight gas extraction and as a result of these successful experiments, the number of hydraulic fracturing treatments performed throughout the U.S. increased exponentially. This also resulted in a large increase in the U.S. gas production. This early success spread throughout the world's gas producing nations, including Russia (then Soviet Union), and the North Shore of Europe. In 1968, Pan American Petroleum, now BP, performed the first large-scale commercial hydraulic fracturing in Oklahoma, U.S. a process that has now become common practice in the conventional natural gas and oil industry.

De Languna et al., (1968); Howard and Fast, (1970) considered the possibilities of using hydraulic fracturing to create a reservoir where medium-level spent nuclear fuel could be stored. They hypothesized that storing radioactive waste

[12] During the early 1930's the Halliburton Oil Well Cementing Company established a research lab for experimenting with varying mixtures of cement and acidizing solutions to break down rock and open fracture spaces, becoming the first laboratory of this kind in the world.

deep within the crust would allow for an adequate residence time for the relatively short-lived radioactive elements to decay, while simultaneously providing a permanent storage facility for the long-lived radioactive waste. These experiments were performed at a test well near the Oak Ridge National Laboratory, Tennessee, U.S. Similar to fracturing used in the gas industry it aimed to create a vast fractured network in targeted argillaceous shales. It then aimed to fill these fractures with a mixture of spent nuclear fuel and cement. Once the mixture was pumped into the fractures, it would harden and seal the fractures. Thereafter, the well would be capped with a thick layer of cement and the spent nuclear fuel would remain sealed for eternity, theoretically. The experiment commenced following the accurate determination of the fracture orientation and started with an experimental well being drilled to just over 300 m deep. This included a surface plant with a sophisticated nuclear waste monitoring system. After decades of monitoring, budgetary cuts forced the foreclosure of this plant and presently, the U.S. Department of Energy together with the Environmental Protection Agency are decommissioning many of the Oak Ridge nuclear facilities. The experimental nuclear waste storage wells will however remain[13].

While conventional hydraulic fracturing is now commonly used in the oil and gas industries, more unconventionally, its applications toward geothermal energy became apparent at the first EGS demonstration plant, Fenton Hill, New Mexico, U.S. Contrary to oil and gas exploration, hydraulic fracturing for geothermal application aims to create an extensive porous fracture network in plutonic rocks, and thereafter maintain a constant fluid circulation over a sustained period of time. In the gas industry fluid circulation is used only for the required period needed to extract all the gas and then fracture closure is allowed.

Figure 4 shows a schematic illustration of an EGS system employed in Germany (project operated in conjunction with the GFZ German Research Centre for Geosciences, Potsdam). The image shows the necessity for hydraulic fracturing in EGS exploration with a fracture system in the desired rocks existing between the injection and production wells. The generation of electricity relies on allowing a fluid to circulate between the injection and production wells, while giving the fluid adequate time to heat. The heating of the fluid occurs through interaction with the surrounding rock. Similar to the nuclear storage facility, the geothermal fracturing requires a detailed model of the underlying fractures to

[13] Media statement on the Yucca Mountain Project for nuclear waste disposal, available from: http://www.nirs.org/radwaste/yucca/yuccahome.htm).

allow for fracturing to occur in the most preferred orientations, and to generate a highly porous network, while maintaining a closed reservoir.

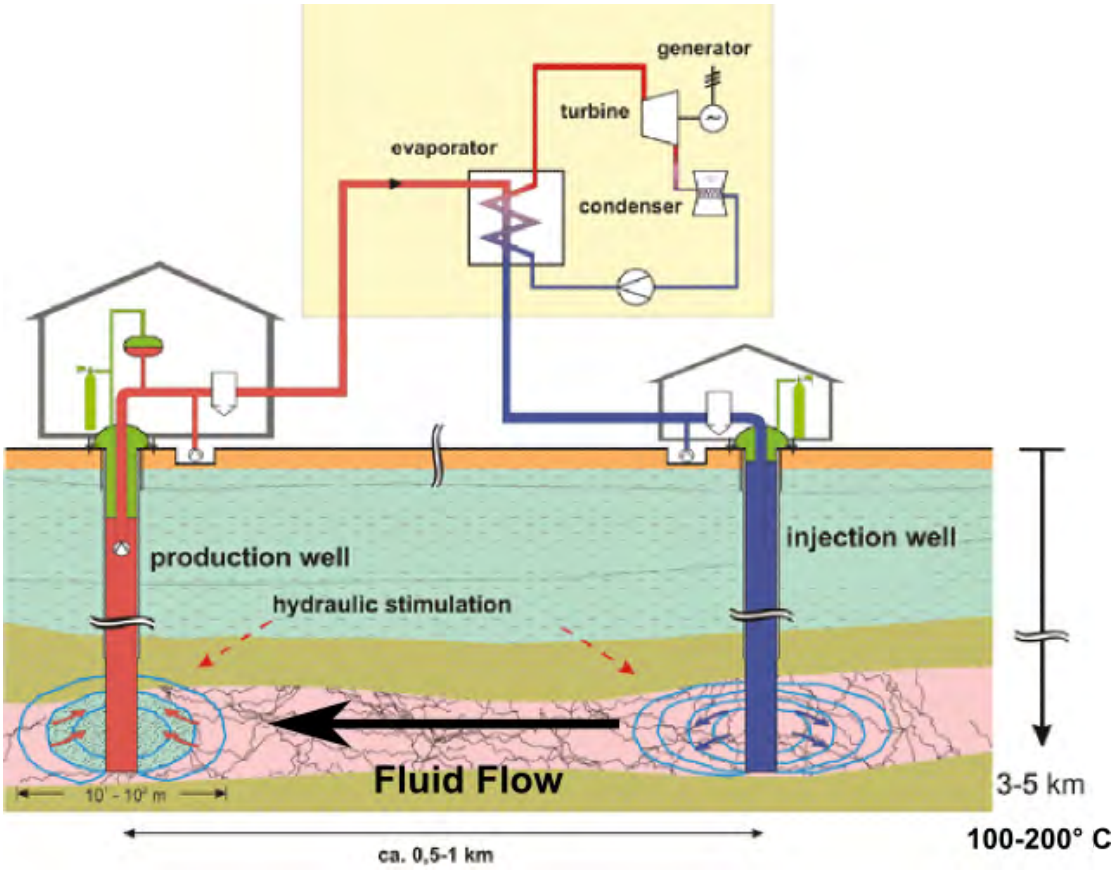

Figure 4: Illustration of an EGS system showing the importance of hydraulic stimulation to increase the porosity between the injection and production wells (www.renewables-made-in-germany.com)

4.2 An example of concerns about hydraulic fracturing

Following the increase in the application of hydraulic fracturing throughout the southern U.S. for oil and gas exploration, concerns grew in surrounding communities. Many of these concerns focused around the use of inorganic solvents within the fracturing fluids, and also in the apparent methane seepage into their water supplies. This was mostly associated with hydraulic fracturing related to the extraction of tightly contained gas. It culminated in the documentary *Gasland*[14]. This documented case studies of communities in the southern states of the U.S. and showed apparent methane inclusion in their water systems. This sparked further community outcry and resulted in the U.S. Energy Department scrutinising the use of hydraulic fracturing and calling for further investigations (Jones, 2011).

[14] Further information available from: http://www.gaslandthemovie.com.

Osborn et al., (2011) investigated possible methane contamination of drinking water associated with gas-well drilling and hydraulic fracturing. They discovered a significant increase in the methane concentration of drinking water near active gas extraction sites. Here they recorded values of up to 64 mg (CH_4)/l, which is considered an explosive hazard. They also measured the total dissolved methane in neighbouring non-extraction sites and attained lower values of 1.1 mg (CH_4)/l. They also measured the δ^{13} C-CH_4 and δ^{2} H-CH_4 concentration of the drinking water near the active gas-extraction sites. They found values consistent with a much deeper thermogenic methane source of the surrounding shale lithologies, while samples from non-extractive sites had signatures reflecting more biogenic to mixed biogenic/thermogenic methane sources. This suggests that the process of hydraulic fracturing released the deep-seated methane and led to contamination of the shallower drinking water supply. Davies; Schon (2011) suggests that there is little evidence to link the contamination to the process of hydraulic fracturing and they call for further investigation. However, a link between hydraulic fracturing and releasing deep-seated methane is clear and illustrates a need for additional research.

While these adverse effects of hydraulic fracturing were related to the oil and natural gas exploration, geothermal-related hydraulic fracturing has been subjected to similar scrutiny. Communities surrounding EGS plants in the U.S. and Europe frequently voiced concerns and fears (i.e. Newberry EGS development site, Newberry, USA). *AltaRock*[15] in charge of development ran active public meetings and reassured the surrounding communities that their fracturing fluids are highly diluted and pose no threat, and reaffirmed the use of an active seismic monitoring system (AltaRock Energy/Davenport Newberry, 2010; Cladouhos et al., 2012). The U.S. Departments of Energy endorsed the project monitoring system, and the project is currently continuing[16]. The project remains closely followed for any adverse effects.

Another concern surrounds induced seismicity associated to hydraulic fracturing. Hydraulic fracturing may cause a level of shearing and activation of microfaults in the underlying lithologies and subsequently causes microseismicity (Wesson and Nicholson, 1987). These seismic events generally attain low (<2.0) magnitudes, however mostly are never felt by the surrounding communities. Understandably, this causes great concern and subsequently EGS

[15] An American renewable energy company, focusing on the development of Enhanced Geothermal Systems in the USA.
[16]Bureau of Land Management report on the Newberry EGS project, available: http://www.blm.gov/or/districts/prineville/plans/files/NewberryEGS_FONSI.pdf).

projects in Landau, Germany and Basel, Switzerland were stopped due to the level and frequency of seismicity (Baisch et al., 2009), despite minimal damage to the villages surrounding the Landau site, damages in the Basel area amounted to more than $ 9 million (Giardini, 2009). With EGS commonly available along tectonically active regions, seismicity can possibly be induced through hydraulic fracturing. The Landau project was situated in the Upper Rhine Graben (Teza et al., 2011), a tectonically active region where natural seismic events can occur naturally. In 2006 the EGS investigative project in Basel, Switzerland was suspended following a 3.4 magnitude seismic event. This event occurred during hydraulic stimulation of a 5 km borehole and damage that included minor structural damage to the surrounding villages. The damaged homes and buildings had to be compensated by the project. Cypser and Davis, (1998) considered the legal implementations of induced seismicity in the USA and concluded that companies undertaking hydraulic fracturing can be held liable if their hydraulic fracturing processes result in any damage or injury. A later investigation in 2009 failed to prove that the hydraulic fracturing at the Basel EGS project was the cause of the seismic event and the project management were subsequently cleared of all the charges (IGA, 2009). This illustrates the need for an active monitoring programme and on going public participation when considering hydraulic fracturing, and also possible legal implications that can arise in the event of seismicity and damage to property.

Chapter 5: History of Enhanced Geothermal Systems

There are several current and previous EGS project from which a vast amount of knowledge and experience was gained. This accumulation of knowledge continued after each individual project and collectively resulted in substantial technological advancement of EGS development worldwide. Several key projects and their contributions are highlighted below:

5.1 The Fenton Hill Project, 1974

Figure 5: The Fenton Hill EGS site, Los Alamos, New Mexico U.S., left with a broad view with the site demarcated. The Valles Caldera on which the Fenton Hill plant is situated, near Los Alamos, shown on the right. Modified Google Map, (2012)

The base of the Valles Caldera (Figure 5) was deemed an ideal location for testing the theory of EGS. Recent localised volcanic activity provided a very high geothermal gradient with a heat flow of 112.5 mWm^{-2} (according to McLennan and Taylor, (1996) typical crustal heat flow falls between 18-48 mWm^{-2}). The initial project design was structured around a system with an influx well and a production well with a 100 m separation between them. The modelled plan was to drill the production well to a depth of 3 km, which would theoretically attain a basal temperature of ca. 200° C. The influx well was expected to attain a temperature of 300° C at a depth of 4.4 km.

Following a preliminary investigation and modelled calculations, the influx well was drilled to 2.93 km, where it attained a basal temperature of ca. 180° C (Duchane, 1993). The production well was drilled 100 m away from the influx

well and reached a depth of 3.06 km and similarly attained a ca. 180° C basal temperature.

The next phase was hydraulic fracturing to attain a porous fracture network between the influx and production wells. The initial phase of fracturing was however unsuccessful, because a connection between the influx and production wells could not be achieved. Failure in generating a fracture network between the two wells was attributed to an error in the initial modelled stress regime. It was discovered that the hydraulic fracturing caused the density of the fracture network between the wells to increase away from each other, rather than toward each other. After this discovery, it was announced that no further fracturing could rectify this error until additional stress modelling was undertaken. The additional modelling commenced, using the data acquired from the failed fracturing attempt, and subsequently a final phase of fracturing was initiated. This time fracturing was orientated at an acute angle, deviated from the orientation of the influx and production wells, and in 1977, it was declared a success and an adequately porous and connected fracture network between the influx and production wells was established (Tester and Albright, 1979). Five circulation tests were conducted over the preceding three years to test the system and within this period 5 MWh of renewable energy was generated through a 60 KW binary generation plant. This was the first renewable energy generated through the EGS system.

In 1979, deeper influx and production wells were drilled in an attempt to gain higher temperature and attain a larger energy capacity. The wells were separated by 380 m, with the influx well reaching a depth of 4.39 km and a basal reservoir temperature of ca. 327° C. At the start of hydraulic fracturing, the surrounding community reported seismicity. This subsequently led to the implementation of an active seismic monitoring system.

The hydraulic fracturing of the deeper wells encountered the same problem as the preceding wells, when an adequately connected fracture network was not attained. Again, this failure was attributed to an error in the modelled stress regime and the actual stress regime was later determined to be perpendicular to what was originally modelled. Similar to the previous solution, further hydraulic fracturing commenced via a well deviated at an acute angle to the original, and once again this proved successful. A deduction made from the second failure to model the stress regime accurately was the need for accurate seismic mapping. This would allow for a more precise assessment of the underlying stress regime and allow for hydraulic fracturing to be oriented in the most beneficial

orientation. In addition, this would avoid project delays and unforeseen expenditure.

An initial flow test was run at the plant for a period of 30 consecutive days. This served as a prerequisite before a long-term test could commence and it aims to ascertain the system stability and acquire final data prior long-term testing. This test also aims to better ascertain the strength of the wells at varying pumping pressures and flow rates, while getting a better understanding on the possible energy generation. During the initial test pumping pressures reached 30 MPa and flow rates were up to 19 l/s. The result was production temperatures of up to ca. 192° C with a fluid recovery of 86 %. This indicated that a large percentage of the system was closed, although not entirely sealed. The fractured reservoir was seismically mapped and determined to be 10 m^3. However, based on the results of the preliminary flow tests, this was three-orders of magnitude lower than the minimum reservoir size of 1,000 m^3 required for a large-scale economically viable EGS plant.

The initial test was successful and ran without any breakdown. After the test a venting process was initiated. During the venting process the system is cleared of fluid and steam. This does however also result in a large decrease in system pressure. The large pressure drop was underestimated and caused a partial well collapse of the influx well at 3.20 km. The influx well thereafter needed to be cemented and re-drilled from the point of collapse. Thereafter several further short-term flow tests were performed again, as preparation for more long-term testing.

These short-term tests showed that operating the system at pressures lower than the critical pressure needed for successful hydraulic fracturing resulted in a much lower fluid loss. This was due to the continued growth of the reservoir being inhibited and allowing the system to remain completely sealed, avoiding large water losses. Under these conditions the basal reservoir temperature remained constant, allowing for sustained energy generation (Duchane, 1993).

Long-term testing began in 1990, following the construction of the necessary infrastructure, including larger heat exchange and pumping systems. In 1992, long-term testing started and was kept at low pumping rates, not exceeding 15 l/s. This was to minimise the growth of the reservoir and decrease the overall fluid loss. However, these lower rates also resulted in a decrease of the overall surface temperature and consequentially a decrease of the plant efficiency.

The Fenton Hill site was decommissioned in 2000 after decrease in the overall project budget. The promising results did however pave the way forward for further projects.

5.2 The Rosemanowes Project, 1977

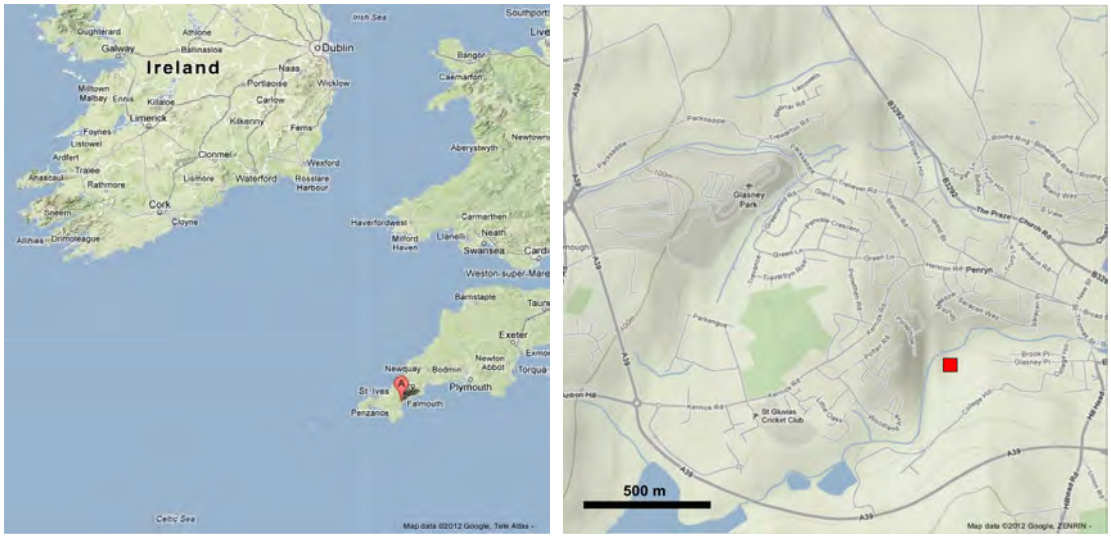

Figure 6: Relative position of the Rosemanowes EGS plant, Cornwall U.K, left, and proximity of the plant shown on the right, near Penryn. Google Maps, (2012)

The Camborne School of Mines began the Rosemanowes Project in 1977 (Figure 6) and focussed their research toward addressing the drilling and hydraulic fracturing problems encountered during the Fenton Hill Project. Therefore, the project was restricted to reaching a maximum basal temperature of ca. 100° C. This was meant to avoid increased system sensitivity and instrumental problems associated with operating at higher temperatures. Being orientated around understanding hydraulic fracturing, the project was planned toward the development of an adequately connected fractured reservoir (Batchelor, 1982). In addition, the project was meant to serve as a research plant to better improve and develop advanced drilling technology.

Previous tin mining activities surrounding the area provided detailed 3-D geological models to depths of up to 1 km. This included detailed analyses of the underlying fracture system and the overall controlling stress regime. The subsequent hydraulic fracturing was orientated based on this information, and was expected to avoid fracturing problems experienced at the Fenton Hill project.

The project targeted the Permian Carnmenellis granite massif of the Cornubian batholith. This granite has the highest heat flow in the UK, ca. 120 mWm^{-2} (Wheildon et al., 1977). This further resulted in a geothermal gradient of up to 40° C/km (Parker, 1991). The massif comprises porphyritic granite, reaching a depth of up to 9 km. There are also numerous hot springs throughout the granite, with the highest recorded surface temperature of 52° C (Edmunds et al., 1984). The project was structured as a 3-phase drilling programme over three decades, with the final drilling depth expected to reach 2 km.

Initially, two wells were drilled and attained a maximum basal temperature of ca. 80° C. Before hydraulic fracturing started, it was understood that there was a predominance of vertical fractures, formed within a dominantly horizontal stress regime. Considering these factors, it was predicted that during hydraulic fracturing, the fractures would propagate upwards as tensile fracturing. However, during hydraulic fracturing, seismic studies showed the dominant fracture propagation was in a shear plane, and not tensile as previously predicted. This miscalculation resulted in poor fracture connectivity between the wells (Batchelor et al., 1983; Pine and Batchelor, 1984; Baria and Green, 1989), effectively encountering the same problems as experienced at Fenton Hill.

Applying the new information on the stress regime, a third well was drilled into the fracture network and hydraulically fractured. This time the fracturing was orientated to allow fractures to propagate along the shear plane and it was later deemed successful as a sufficient network was established between the wells. Since the third well was drilled deeper than initially planned, it resulted in an increased overall basal temperature, which now reached ca. 100° C. Thereafter flow testing could commence and would continue for the next 4 years.

Following a period of short-term testing, the long-term flow test began in 1986. During this phase the pumping rate was varied between 5-24 l/s with pressures exceeding 10 MPa. A basal temperature drawdown to 70° C was observed and considered to be the result of shorter preferential flow path development between the injection and production wells. This limited the residence time for cold influx fluids to circulate and attain a equilibrium temperature before returning through the production wells (Batchelor, 1986). Problems were also compounded by an increase in the system impedance. This was attributed to the decreasing of the pumping pressures, which subsequently led to some fractures sealing, effectively slowing the flow of fluid throughout the system.

In an effort to overcome the increased system impedance, another phase of hydraulic fracturing commenced. However, this time with the addition of a sand-

based propping agent in the fracturing mixture. The sand was meant to inhibit closure of the fractures and therefore improve the overall flow throughout the network. However, this phase of hydraulic fracturing resulted in the shorter preferred flow path between the injection and production wells increase further, causing a larger decrease in the overall efficiency.

In a final attempt to solve all the project problems, the uppermost section of the fractured network was cemented. This essentially sealed the shorter preferred flow path and would theoretically force the fluid to find a longer flow path. However, this once again caused a drastic decrease in the system flow rate as the longer flow path was not adequately porous, and the result was an overall increase in system impedance. This warranted even more hydraulic fracturing. Unfortunately, the subsequent series of fracturing failed to create a porous network, but simply formed a shorter fracture system parallel to the previous, now cemented shorter path (Parker, 1989). This indicated that throughout the various attempts at finding solutions through further hydraulic stimulation, the problem was only compounded and the end result was an irreversible rock displacement effectively resulting in permanent closure of the fractured reservoir. The project would eventually be concluded in 1993.

5.3 The Hijiori, 1988 and Ogachi, 1982 Projects

Japan's placement on the Pacific Rim of fire has provided the country and surrounding islands with a very high level of continental heat flow. Japan also has a very unusual heat flow profile. This stems from a vast change in the heat flow on either side of the Japan Trench that separates the Pacific Plate and the Eurasian Plate. Figure 7 is an edited Google map illustrating the various tectonic boundaries surrounding Japan. The Red line indicates the inferred trend of the North American Plate. The abrupt change in the heat flow of Japan is evident from values on the Pacific Plate that ranges from 20-40 mWm^{-2}, while heat flow measurements on the Eurasian Plate range from 120-130 mWm^{-2}. Temperatures at a depth of 30 km are expected to vary from 100° C and 1000° C between the Eurasian and Pacific Plates (Nagao and Uyeda, 1989). This is clear when considering that the Pacific Plate is subducted under the Eurasian Plate effectively placing Japan on a volcanic island arc setting.

Japan started showing interest in geothermal energy during their support of the Fenton Hill project. This later paved the way for the first two EGS plants in Japan; these include the Hijiori and Ogachi EGS sites (Figure 7; Figure 8).

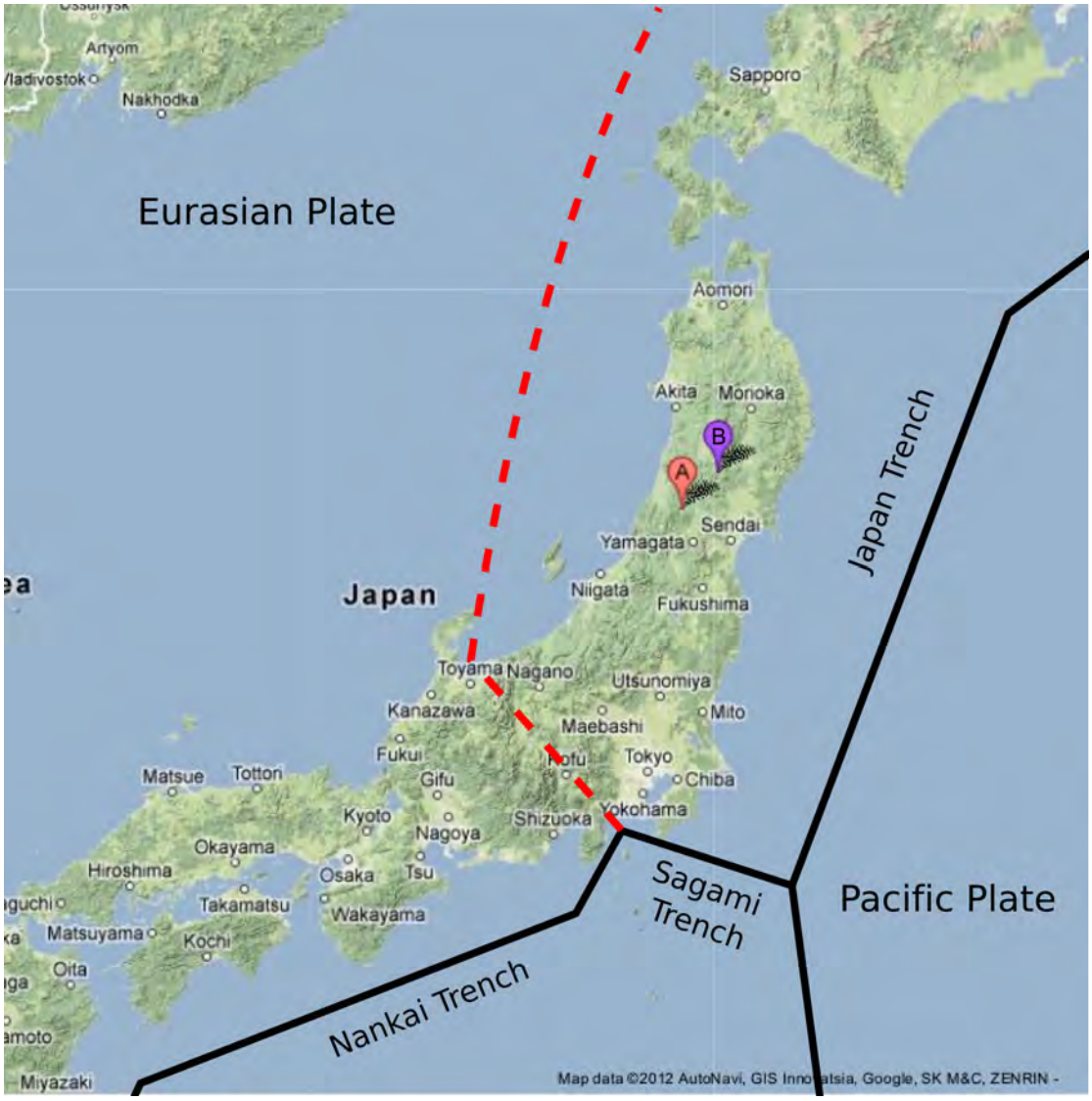

Figure 7: The Hijiori, A, and Ogachi, B, EGS plants. Located on the Honshu Island, Japan. Modified Google Map, (2012)

5.3.1 The Hijiori Project

The Hijiori EGS project aimed to produce geothermal energy from the Hijiori caldera on the Japanese island of Honshu. Since Japan has an active plate tectonic regime and recent volcanism, geothermal energy was considered as a highly viable alternative energy source. The Hijiori site was known to have a very high heat flow within highly fractured granitic rocks. However, it had a very complicated stress regime that needed to be understood for ensuring the most beneficial results from hydraulic fracturing.

In 1989 and 1992, the project commenced with four wells being drilled. This included a 2.15 km injection well and three production wells, varying up to a maximum depth of ca. 1.8 km (Swenson et al., 1999). Basal reservoir

temperatures from the production wells reached ca. 250° C. The well separation between the production wells was a mere 40, 80 and 130 m (Tenma et al., 2001). The shorter well separation distance illustrated the higher heat flow temperatures and lesser need for a longer circulation period. Hydraulic fracturing commenced in 1988 and thereafter short-term flow tests commenced. A total volume of 44,500 m^3 of water was injected into the system and produced a high concentration of steam. However, 70% of the influx water was lost within the system. These loses were attributed to the over-extensive fracture network paired with high pumping rates. These factors led to continuous reservoir growth and failure to maintain a closed system.

By 1995, two of the three production wells was deepened to 2.3 km and then hydraulically fractured. After a subsequent 25-day circulation flow test, the water loss was improved to 50 %. There however remained large fluctuations in the temperature and pressure of the system. In 1996, the influx and production wells were swapped around and were further fractured (Hori et al., 1999). This resulted in the development of two interconnected reservoirs, a shallow and a deep reservoir (Tenma et al., 2008).

From 2000 to 2002, long-term testing was initiated (Schoeder et al., 1998; Tenma et al., 2000; 2001) with an injection temperature of 36° C and steam production between 163° and 172° C. This resulted in an overall power production of 8 MW, capable of running a 130 MW binary power generator (Matsunga et al., 2000). However, it was noted that during the test, the injection pressure dropped from 9 MPa to 7 MPa with an associated overall water loss rate of 45 %. There was also a dramatic temperature drop from one of the production wells to 100° C (Yamaguchi et al., 2000). Like the Rosemanowes project, it was deduced that this drop in the temperature was due to the continued enlargement of the fractured reservoir resulting in the development a shorter preferred flow path that reduced the system efficiency. Yanagisawa, (2010) suggests that many of these fluctuations were not only due to the development of shorter preferential flow paths, but also associated with various mineral precipitation. These mineral precipitates were attributed to the addition of CO_2 into the working fluid, used to test sequestration. Presently, the Hijiori EGS project is not officially closed and remains an active EGS laboratory.

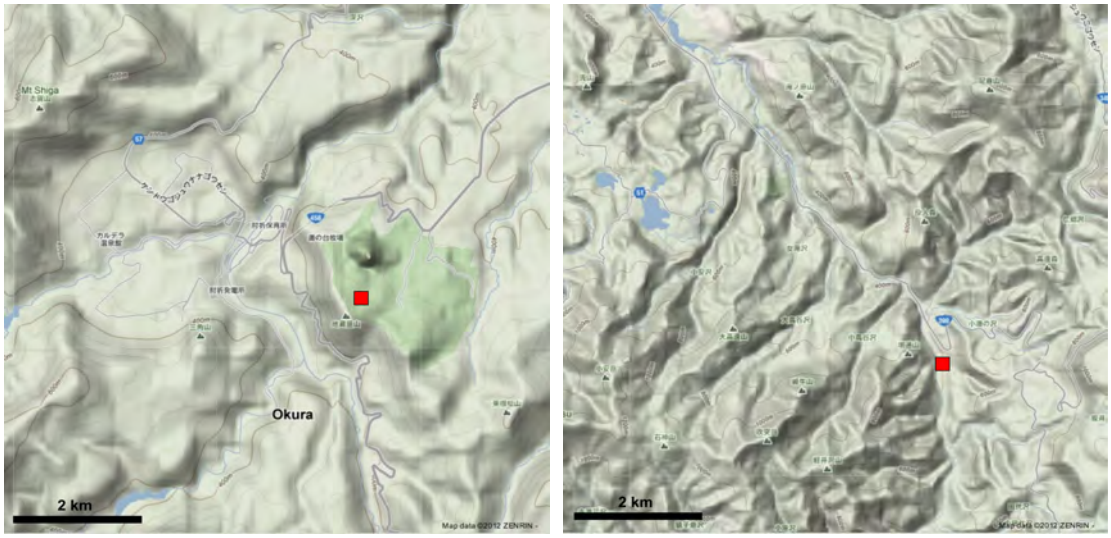

Figure 8: Hijiori EGS on the Hijiori Caldera, left. Ogachi EGS on Mt. Yamabushi, right. Modified Google map, (2012)

5.3.2 The Ogachi Project

The Ogachi project on the Mt. Yamabushi volcano, also on island of Honshu started concurrently with the Hijiori Project. An injection well was drilled to a depth of 1 km and attained a basal temperature of ca. 230° C (Hori, 1999). A production well was drilled 100 m away from the injection well to a depth of 1.1 km, and attained a temperature of ca. 240° C. During testing it was discovered that initial fracture connectivity between the injection and production wells was very poor and resulted in a mere 10 % fluid recover. Attempting to improve the connectivity, hydraulic fracturing was initiated in 1994 and again in 1995. However, this only improved the overall fluid recovery by a further 15 %. Subsequent investigations using down-hole cameras showed that the poor recovery was a result of the development of two separate reservoirs, similar to the Hijiori site. The additional reservoir formed below the planned one and also exhibited a different fracture orientation. The different fracture orientation of the lower reservoir resulted in the influx of water, but would without any outflow (Shin et al., 2000). Subsequently, additional hydraulic fracturing was carried out to connect the two reservoirs, but an economically sustainable connection was never attained. Similarly, the Ogachi EGS test site remains an active research laboratory for further investigation.

5.4 The Soultz-sous-Forêts Project, 1987

Figure 9: The relative position of the Soultz EGS indicated by the red marker and Rhine Graben delineated in blue, left. The relative position of the Soultz-sous-Forêts plant, right. Modified Google Map, (2012)

Following the drilling and hydraulic fracturing research at Rosemanowes, there were other similar projects in Germany and France. These also served as additional pilot EGS plants. However, the European Union and the United Kingdom decided to focus research and funding toward the most promising geothermal target site, aimed to develop of the first commercial EGS project in Europe. The selected target site was in Soultz-sous-Forêts, France, located in the upper Rhine Graben (Figure 9). Before the project began there was extensive geological and geophysical work available and this included a detailed heat flow analysis. While the average heat flow in the Rhine Graben is 80 mWm^{-2}, the Soultz site has a measured heat flow of 140 mWm^{-2} (Sanjuan et al., 2006).

The target lithology comprises of highly fractured and altered granitic rocks overlain by 1.4 km of Mesozoic and Tertiary sediments (Cocherie et al., 2004). The host granite was intruded by a later leucocratic, fine-grained amphibole granite that appears at a depth of 4.7 km (Hooijkaas et al., 2006). The host granite is porphyritic and has a large hydrothermal alteration aureole. This aureole appears highly altered and fractured below the sediments and fresher at greater depths. The altered zone comprises a pervasive vein alteration, due to water-rock interactions (Genter et al., 2002).

The first well was drilled to a depth of 2.02 km (Baria et al., 2005). Having initially been projected to attain a basal reservoir temperature of ca. 200° C, it only reached 140° C. This lower basal temperature was attributed to the

presence of alternating convective loops within the granite (Baria et al., 2006). These convective loops relate to heterogeneous distribution of the heat producing elements within the granite (i.e. Walton et al., 1985). These variations create a highly disjunctive heat flow profile making accurate geothermal modelling difficult.

A year later, it was decided to deepen the existing wells and penetrate further into the granite, and in 1992, a production well was drilled to a depth of 3.59 km and attained a basal temperature of 168° C. In 1995, a corresponding influx well was drilled to a depth of 3.88 km, separated from the production well by 450 m. Sustained hydraulic fracturing thereafter commenced and generated an appropriate fracture network connection (Baria et al., 1998). This culminated in a short-term circulation test with the use of an electric submersible pump and achieved a production flow rate of 21 l/s. The working fluid was injected at 40° C and produced at 136° C, resulting in a thermal power output of 9 MW. By 1997, the flow rate was increased to 25 l/s and produced 10 MW of energy.

Private corporations and utility companies took over the project in 1998. They decided to deepen the influx well to 5 km in an attempt to increase the economic viability of the plant. This required the replacing of all castings and additional inclusion of high-temperature cement. In 2000, hydraulic stimulation began on the influx well with a flow rate of 50 l/s and pressure of 14.5 MPa. This created in a fracture system 500 x 1500 x 1500 m without any recorded water loss.

In 2001, drilling of three production wells from the base of the previous wells started. The drilling was inclined in order to orientate with the principle horizontal stress regime, and was completed in 2004, reaching a depth of 5.11 km. During hydraulic fracturing significant seismicity was induced, felt by the surrounding public. However, no damage was recorded. The initial hydraulic fracturing failed to generate good connectivity and was attributed to the presence of an impenetrable low permeability layer. A heavy brine fracturing fluid was introduced to overcome the low permeability layer (Baria, 2006). Additional hydraulic fracturing was thereafter used to further improve the connectivity. While the project is believed to have generated a very well connected fracture network between the influx and three production wells, the project remains uneconomical due to the natural low permeability in the geothermal reservoir (Genter et al., 2010; Baillieux et al., 2011). Regardless of economical viability, the Soultz project remains the biggest contributor for scientific research into EGS. By October 2011, 235 scientific articles had been published and more then 40 PhD theses were completed from its research, which still continues.

5.5 The Cooper Basin Project, 2002

Figure 10: Cooper Basin EGS project location demarcated in pink, Southern Australia. Hunter Valley EGS plant demarcated in red, Southwest Australia, Cooper Basin marked in black. Modified Google Map, (2012)

In 2001, the Australian Federal Government launched their Mandatory Renewable Electricity Target (MRET) and Renewable Energy Demonstration Programme (RDEP) schemes. These schemes aimed to fuel research and the implementation of alternative forms of energy, toward achieving a set 9,500 GWh renewable energy target by 2010. With the implementation of this scheme, many private corporations began investigating the potential of renewable energy for economic gain (Chopra, 2005). In 1999, before outset of the MRET and RDEP schemes, Australia had already started investigating an EGS prospect at the Hunter Valley EGS site (Figure 10). This area displayed a strong gravity signature associated with a geothermal anomaly (Somerville et al., 1994). Figure 11 illustrates the 5 km temperature profile underlying Australia, together with images representing the data points and statistical confidence of each measurement. Similar to Japan, Australia displays a heat flow disparity. West Australia displays a cold temperature profile, which corresponds with the location of the Pilbara Craton. Similarly, these lower heat flow values, 40 mWm^{-2}

(Pollack and Chapman, 1977) correlate with those of the Kaapvaal Craton (i.e. Wingate, 1998; Nyblade, 1999). The area toward the east displays a much higher temperature profile and corresponds with the emplacement of Mesozoic-aged felsic granites. According to Neumann et al., (2000), who performed a regional study on the heat flow throughout Australia, the heat flow within this anonymously high region reaches up to 92 mWm^{-2}.

Following work at the Hunter Valley site and with the installation of the MRET and RDEP schemes, a private company, Geodynamics Limited began investigated the Cooper Basin (Figure 10). The exceptionally high, 92 mWm^{-2}, heat flow at the Cooper Basin was identified as an ideal target commercial EGS generation and this became the leading EGS research site in Australia (Figure 11).

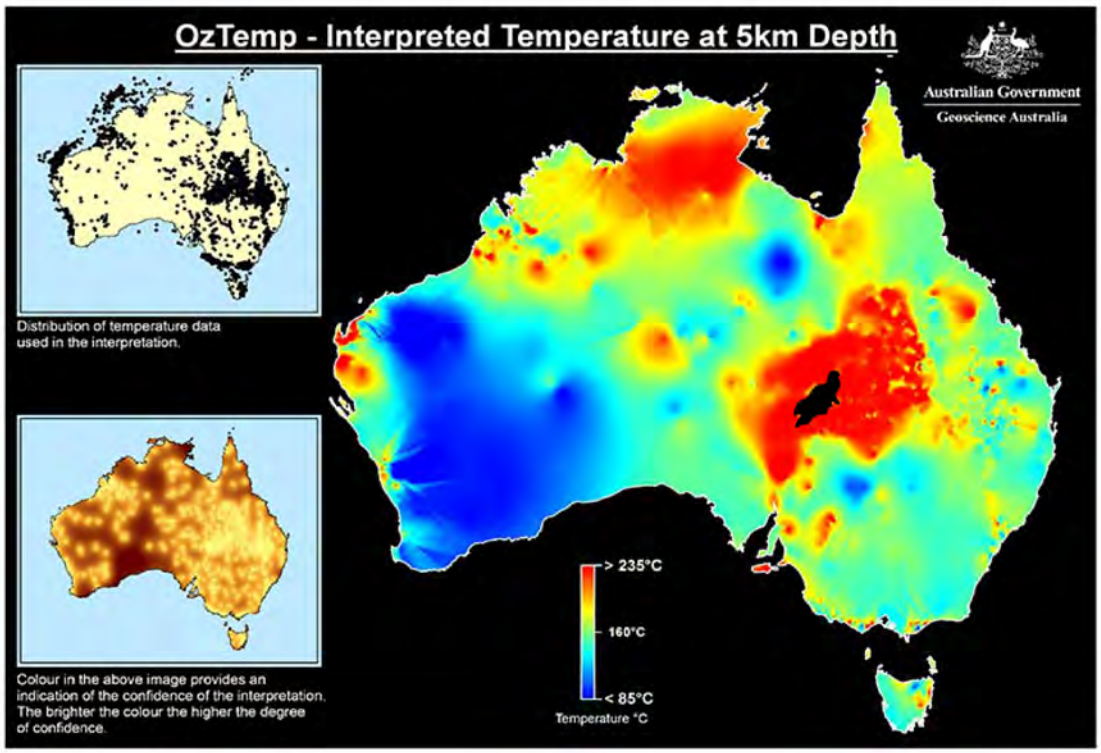

Figure 11: 5km crustal temperature profile across Australia, Cooper Basin indicated in black. Modelled by the Common Wealth of Australia, (2006) Available from www.ga.gov.au/energy/projects/geothermal-energy.html

The Cooper Basin project is located in a Carboniferous-Permian basin sequence and was initially a site of interest in the petroleum industry. This interest amassed a large amount of geological and geophysical data, including information on the high concentration of radiogenic elements in the underlying rocks granitic rocks. By 2003, the first well was drilled to a depth of 4.42 km penetrating the underlying granites by 3.67 km and attained a basal reservoir temperature of 250° C. Hydraulic fracturing required very high pressures to reach appropriate permeability levels with pumping pressures of 70 MPa and a

total influx volume of 20,000 m^3 at a flow rate of 26 l/s. Two production wells were subsequently drilled, reaching depths of 4.35 and 4.01 km. These wells were separated by 500 m and after further hydraulic fracturing and circulation tests, the production wells produced surface temperatures of ca. 210° C. A feasibility study was undertaken with a flow rate of 100 l/s producing surface temperatures of 245° C and attained a calculated LCOE of 6.2 c/KWh (Chopra and Wyborn, 2003). More recently, *Geodynamics Limited* reported their first successful test of their production well, with a flow rate of 35 l/s and pumping pressure of 29 MPa. This resulted in a basal reservoir temperature of 214° C and surface fluid temperature of 191° C, making it the most successful EGS plant thus far.

5.6 Summary and lessons learnt

Knowledge gained from the above mentioned plants played a vital role in initiating present-day commercial and experimental projects. Technological advancements made throughout these aforementioned projects greatly increased in both technical efficiency and overall energy capacity, illustrated in Figure 12; Table 1.

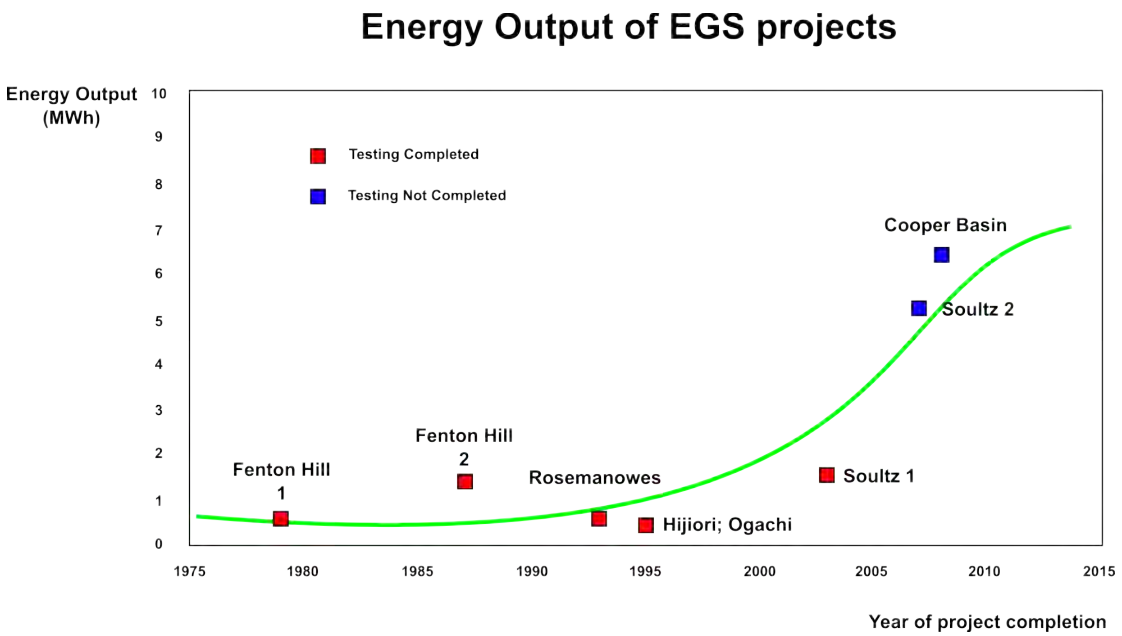

Figure 12: Status of past EGS projects and their development over time, AltaRock (internationalgeothermal.org)

Table 1: Breakdown and specifications of the abovementioned EGS plants, AltaRock (internationalgeothermal.org)

project	period	rock temp (°C)	res. depth (m)	well sep. (m)	flow rate (l/s)	water loss (%)	impedance (MPa/l/s)	therm. out. (MWth)	volume (m^3)
Fenton Hill	1973-79	232	3500	300	7	10	2.5	5	100
Rosemanowes	1980-93	80	2000	270	15	25	0.4	4	300
Hijiori	1985	270	2200	130	12	25	0.3	7	150
Soultz	1997	202	5000	700	100	0	0.12	50	20,000
Cooper Basin	2005	275	4500	300	50	0	0.10	75*	50,000*

Each of the technological advancements, and lessons, learnt from an individual project formed the basis for proceeding projects. The Fenton Hill project was the fundamental starting point proving that EGS was not just an idea, but also a possible alternative energy source. It provided evidence, supporting ideas that pressurised hydraulic fracturing could create an open fractured network adequately porous to allow fluid circulation and capable of sustaining electricity generation. It also highlighted various important aspects associated with hydraulic fracturing, most notably the importance of accurate fracture and stress field mapping and monitoring prior to fracturing. This would ensure that hydraulic fracturing was correctly orientated to gain maximum effect. Furthermore, it emphasised the need for maintaining an adequate flow pressure during hydraulic fracturing and general operation. This would ensure that the fractures would not collapse, causing an increase in the system impedance. However, also noting the need of a pumping pressure that is not excessively high, avoiding continuous growth of the system and the increase in overall water loss.

Fluctuations in the porosity and size of the fractured reservoir discovered at Fenton Hill formed the controlling factor in the Rosemanowes project as conscientiously varying the pumping pressures determined the success of maintaining an adequately porous fracture network. Regardless, project failure was related to a decrease of system pressure. This was further related to inaccurate pumping pressure calculations, compounded with a lithological profile that was simply insufficiently porous. This illustrates the need for accurate determination of the required pumping pressures that could maintain an adequately porous network, while avoiding irreversible fracture growth.

The application of an accurate pumping pressure is not the aspect that provides an important necessity, but also the accurate determination of the overall stress regime of the reservoir. The Hijiori and Ogachi projects discovered that delineating the stress regime incorrectly has detrimental effects when trying to achieve adequate fracture connectivity between wells. Considering a region with

a very complex geology and structural profile, accurate mapping and fracture orientation becomes challenging and provides another delineating factor in determining the success of the plant. These plants were restricted to using acoustic methods of determining the their respective stress regimes. However, these often had a high level of noise and poor accuracy. Current technological advancement does however allow for the use of ultrasonic imagining techniques, together with microseismicity monitoring and imaging programmes to ascertain the underlying stress regime with a much greater level of accuracy.

The Soultz and Cooper Basin projects have started a new phase of EGS exploration with several private companies, like *Geodynamics Limited* and *AltaRock Energy* exploring throughout Australia and USA, respectively. These projects now provide information illustrating the true economic potential of EGS as an alternative energy source. The Soultz project was the first project to demonstrate that an adequately porous fracture network can be created in a region with pre-existing fractures, through the implementation of proper stress orientation determination. The Cooper Basin illustrates additionally that an ideal geological environment for EGS is within radiogenically rich granite that is both uniform in composition and extensive in size. It also illustrates that hydraulic fracturing in a thrust environment leads to the development of ideal horizontal fractures.

The aforementioned private EGS companies, including their smaller counterparts, spurred on by added tax benefits and carbon reduction targets by an increasing number of countries will hold the key for EGS becoming a larger and successful alternative energy source in the world.

Chapter 6: Current status and future of Enhanced Geothermal Systems

The global combat toward climate change adaption and mitigation is led by a shift from traditional non-renewable energy sources to newer and technically more advanced alternative sources of energy. This shift largely involves solar, hydro, wind and biomass forms of energy, in addition to shale gas as a cleaner alternative to coal. The Earth does however also contain a large untapped source of geothermal energy. With the technology of extracting heat from the Earth for energy production being the main inhibiting factor, geothermal energy has never been a leading source of renewable energy. In an investigative report into the use and increase in all forms of geothermal usage, Lund et al., (2011) reported an 11.4 % energy increase every year, since 2005. This equates to an energy saving of 38 million tonnes of oil and consequently 107 million tonnes of carbon emissions. This figure alone greatly underscores the energy potential and effect geothermal energy could have on global energy security and climate change mitigation.

Considering climate change being one of most considerable the driving forces behind research and implementation of renewable energy, the recent Fukushima nuclear disaster in Japan has also illustrated a greater need for a safer alternative energy shift. Subsequent to this mammoth disaster, Japan signalled their shift away from relying on nuclear energy. In 2010, nuclear energy produced more than 13 % of the world's total energy, a number that increased at the beginning of this year with continued development of several new nuclear plants, including new build projects in South Korea (SHIN-WOLSONG) and Russia (BALTIISK-1). At the beginning of 2012, 13 countries relied on nuclear energy to provide more than 25 % of all their energy needs (Nuclear Energy Institute, 2012).

The immediate benefit of nuclear energy to CO_2 emissions is considerably evident in the USA, the world's largest producer of nuclear energy. The USA has avoided more than 11 billion metric tons of carbon emissions between 1995-2011. This reduction in carbon emissions has resulted however in the accruement of large quantities of spent nuclear waste. Figure 13 displays a map of the U.S. with the locations and amount of stored nuclear waste. In addition, U.S. regulations stipulate that each state producing nuclear energy must contribute to a nuclear waste fund. This fund is used to make provisions and runs an active monitoring system for the storage and regulation of nuclear waste. As of 2011, the cumulative monetary contributions toward the nuclear waste fund peaked over 35 billion dollars (Nuclear Energy Institute, 2012). More importantly, and regardless of the nuclear fund, the U.S. does not have many

permanent nuclear storage facilities. Currently, most spent nuclear fuel is stored in temporary facilities on site of nuclear reactors. These include wet storage pools in which spent nuclear fuel is stored in steel rods submersed in deep-water tanks capable of shielding most harmful radiation. With a shortage of onsite wet storage facilities, there are also dry storage facilities. These function by storing the spent nuclear fuel in steel tanks surrounded by an inert gas, such as boron. While these methods are adequate for shielding radiation emitted by the used nuclear fuel, they remain only a temporary solution. This problem is further compounded with the long half-lives of many spent nuclear fuel elements. These include highly toxic elements like Po^{239} with a half-life of 24,000 years and Po^{240}, 6,800 years.

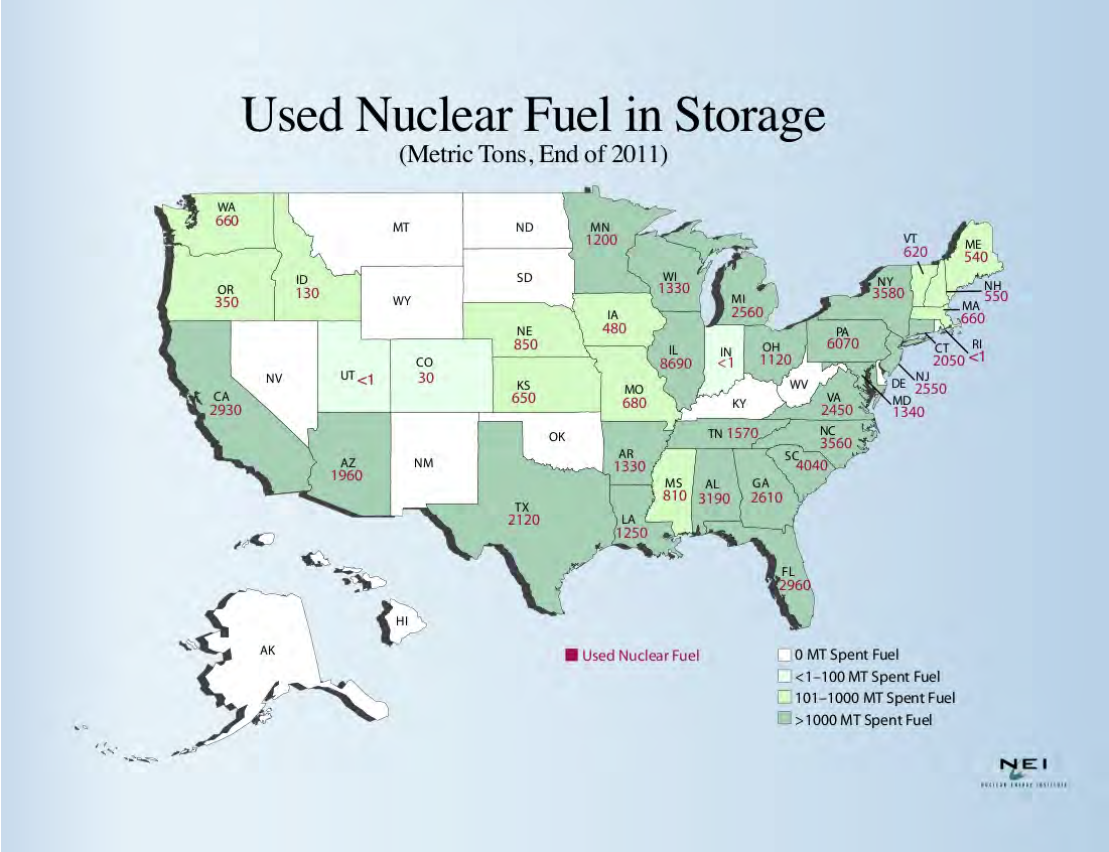

Figure 13: Stored used nuclear fuel in the U.S. December 2011. Nuclear Energy Institute, (2012)

In 2008, the U.S. Department of Energy addressed the issue of nuclear storage and began investigations into the construction of a 10 billion dollar long-term storage facility at Yucca Mountain, Nevada (Mascarelli, 2009). Herein it was postulated to build a deep storage facility within the mountain, capable of storing a large percentage of the U.S. spent nuclear fuel. However, budget cuts and concerns over the safety of the Yucca Mountain site casted many doubts and finally culminated in the suspension of the project in 2011. The preliminary findings were delivered in a technical evaluation report from the U.S. Nuclear

Regulatory Commission (U.S. NRC, 2011). The report concluded that the Yucca Mountains were not suitable for long-term storage and the project was discontinued. Thus failing to resolve the problem of spent nuclear waste in the USA.

France is the second largest producer of nuclear energy and is reliant on nuclear for 80 % of all its total energy requirements. This has led to the country developing a large supply of spent nuclear fuel and similarly faces the problem of inadequate long-term storage facilities. In 1999, France began investigations at the Bure lab. This investigation aims to store spent nuclear fuel 490 m underground into the surrounding rock. This rock storage system is found within an argillite layer that is both overlain and underlain by limestone formations. They aim to accomplish this by infusing the radioactive waste in glass, which is further encased in a steel cylindrical body. These cylinders will be buried 40 m into the argillite layer and sealed. After a thousand years, the steal casings would have corroded, leaving the radioactive waste in the rock itself. While some radionuclides may be able to defuse through the rock to the surface, it is assumed that these radionuclides would have decayed to a level rendering them harmless. These initial tests are expected to culminate in a final development plan and eventually to the construction of the storage facility by 2025 (Butler, 2010).

There is a clear dilemma when considering the trade-off between the insecurities of nuclear energy and its benefits toward GHG emissions and attaining a level of energy security. The recent Fukushima nuclear disaster clearly illustrates unprecedented safety shortfalls of nuclear energy. From being the forth-largest generator of nuclear energy and following the Fukushima nuclear disaster, Japan has announced that it will shift away from nuclear energy. This move was initiated with the introduction of a Renewable Energy Feed-in Tariff (REFIT) scheme (Inoue and Walet, 2012). Since alternative energy sources are expensive, most renewable energy projects rely heavily on government incentives. Spurred on by the Fukushima disaster Germany has also signalled a shift to renewable energy and has implemented one of the highest REFIT incentives. The Japanese ministry of Industry however, with its energy security under threat, has introduced aggressive REFIT schemes; double that of Germany (i.e. $/KWh 0.33-0.51). Since being elected as the new president of France, Francois Hollande is reaffirming his stance toward a much larger implementation of renewable energy (Leone, 2012). Being the second largest producer of nuclear energy and relying on nuclear for most of its energy needs, France also wants to decrease its reliance on nuclear power and shift toward alternative sources.

It appears that a global shift toward renewable energy may now become more aggressive as energy hungry nations discard their reliance of nuclear energy. These nations must then look for large-scale alternative energy sources. While these will include solar, hydro, wind and biomass, geothermal will likely become a bigger factor. In addition, with many nations devoid of active volcanism, they will have to consider the possibilities of EGS. Continued government incentives may therefore drive the shift toward harnessing the full potential of EGS throughout the world.

Figure 14 best illustrates the growth of broad geothermal energy till 2012, and represents the global geothermal energy production compared to the amount produced in the U.S. It also shows the current EGS development in the world. Being a relatively new technology and continuously benefitting from technological advancement, EGS is slowly gaining interest around the world. There are currently 16 countries employing EGS with the Geothermal Energy Association predicting this number to drastically increase as many countries realise their geothermal energy potential.

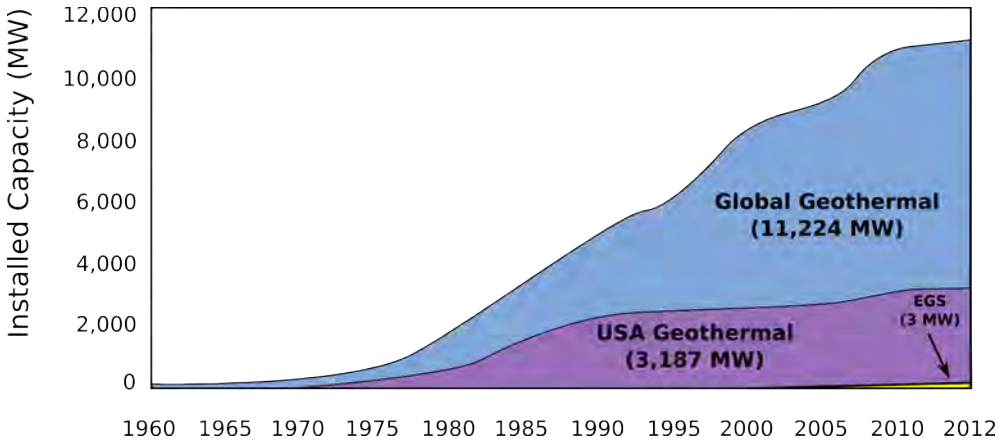

Figure 14: Graph illustrating the global geothermal production against the production in the USA, and global EGS development, after Geothermal Energy Association, (2012)

Chapter 7: Heat flow of South Africa

7.1 Available heat flow measurements in South Africa

Heat flow measurements in South Africa started in the late 1930's and focussed around the Witwatersrand Basin (WB) with gold mining operations beginning to enter the deep mining realm. During that period measuring heat flow was common practice in Europe and began to extend to the WB with European interest growing in mining and the geology of South Africa. Weiss, (1938); Krige (1939) sought to characterise the heat flow of South Africa and compare it to the known heat flow in Europe and America. Initial models suggested that the WB should contain a relatively high concentration of radioactive elements and therefore a presumable higher heat flow (Jeffreys, 1929). These early studies showed, in fact that the geothermal gradient in the WB was up to 30 % lower than those measured in Europe and America. According to Ballard et al., (1987) the low heat flow in the WB was however higher than similarly aged granitic terrains and had a marked increase in heat flow across its neighbouring Proterozoic mobile belts. Bullard, (1939) conducted a heat flow study across the WB to better characterise the temperature profile. In total, heat flow measurements were made on 49 samples from three boreholes within the WB. The average borehole depth reached 1.4 km where recorded temperatures were less than 50° C. One measurement, made at 2.1 km, yielded a temperature of 70° C. From these results Bullard, (1939) deduced that the WB was underlain by granite no thicker than 12 km. He also proposed that this granite should have a lower concentration of radioactive elements than previously thought.

The geological survey of South Africa (now the Council for Geoscience) continued detailed logging throughout what was then known as the Transvaal (now Gauteng Province). This survey focussed on the development of uranium concentration in the WB. The results of their survey also showed that the average heat flow was much lower than predicted. Bouwer, (1954) continued the heat flow investigations using a more sophisticated electronic measuring technique. This method was thought to have the capability of providing more accurate heat flow measurements. The deepest borehole measured down-hole temperature to a depth of 2.44 km within Witwatersrand quartzites and recorded a temperature of 54° C, while the underlying granites attained a maximum temperature of 50° C. Bouwer, (1954) did however find that the electric thermometer failed when measuring within dolomites. This was

attributed to the relatively low thermal conductivity of the dolomites, which fell out of the thermometer range.

Carte, (1955) also developed techniques to measure the thermal conductivity of rocks. He applied these techniques on selected rocks from the WB in an attempt to improve thermal profiles. However, many of the rocks sampled were highly altered and their original composition had varied to a large extent. This resulted in a decreased in the overall precision of his results.

Carte, (1969) completed the heat flow measurements beyond the boundaries of the WB. While the measurements around the gold fields confirmed low geothermal gradients, measurements made in the Namaqua-Natal mobile belt (NNMB) had a much higher geothermal gradient, up to 34° C/km (Carte and van Rooyen, 1969). Sclater and Francheteau, (1970) further investigated and modelled the disparity between the Archean craton and Proterozoic belts in North America. They considered a model based on the chemical and age differences between the two terrains. This model focused on the concentration of radioactive elements and the corresponding dissipation of the heat through the lithosphere, including the effect on groundwater circulation. They concluded that the heat flow of a terrain decreases at a constant rate proportional to the age of the terrain. This simplified model proposed that Archean rocks had more time to dissipate heat and therefore attain relatively colder signatures.

Chapman and Pollack, (1977) further investigated high heat flow values along the Kibaran Belt in Zambia. It was initially thought that the higher heat flow was due to the addition from radiogenic crust. They however found the heat flow signatures had little input from the crust and that the bulk of the heat input was associated with the relatively shallow asthenospheric mantle below the Western limb of the East African Orogen and consequential lithosphere thinning. The observations by Chapman and Pollack, (1977) complimented similar heat flow investigations by Ballard and Pollack, (1987). The latter performed 84 heat flow measurements across the Kaapvaal Craton and the surrounding Proterozoic NNMB. They discovered a heat flow difference of up to 25 mWm^{-2} between the craton and the NNMB. They further deduced that the low heat flow on the craton was predominantly due to the presence of the thick insulating cratonic root. This thick cratonic root resulted in a lower heat transfer from the asthenospheric mantle. Finally, they speculate that between 50-100 % of the heat input from the asthenospheric mantle was diverted to the adjacent mobile belts.

Jones, (1987) recorded the presently highest heat flow measurement in South Africa after he performed heat flow measurements in the NNMB and obtained a

value of 81 mWm^{-2}. He then continued investigations in 1992 by measuring the heat flow across a large portion of the southeast Kaapvaal Craton aiming to delineating its southern boundary (Jones, 1992), (Figure 15). From this transect he noted an increase from a cratonic heat flow of ca. 45 mWm^{-2} to ca. 80 mWm^{-2} over a distance of about 30 km. He concluded that the relative sharp change in heat flow within this relatively short distance best delineates the boundary between the Kaapvaal craton and the NNMB.

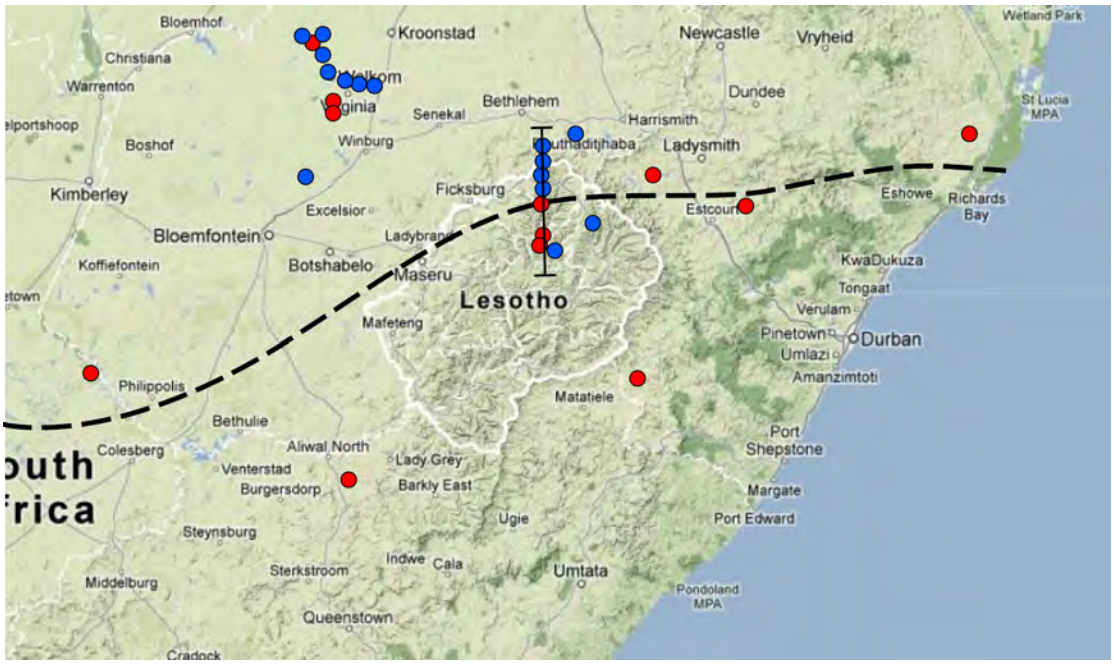

Figure 15: Edited Google map of the southeast part of the Kaapvaal craton, displaying borehole localities and the inferred boundary of the Kaapvaal craton, north of the dashed line, and NNMB, south of the dashed line, and Jones, (1992) heat flow transect across the inferred craton boundary. Modified after Jones, (1992)

Jaupart and Mareschal, (1999) amalgamated the heat flow variations throughout the Kaapvaal Craton. They compared heat flow data surrounding the Kaapvaal Craton against other Archean shields, most notably the Canadian Shield. They found that the heat flow of the mobile belts in South Africa are significantly higher than other similarly aged mobile belts by up to 20 mWm^{-2}. In addition, when removing the effect of crustal heat, they attained a representation of the mantle heat flow signature and found that the difference was small for the various Archean terrains. They noted that the Kaapvaal heat flow is on average 2 mWm^{-2} higher than the Canadian Shield. This suggests that the predominant heat flow variation is specifically due to the addition of radiogenic crust and not due to a large mantle heat flow.

7.2 Heat producing element potential of South Africa

Considering any potentially viable geothermal locations in South Africa is difficult since most heat flow measurements are restricted to the Wits Basin. Also, measurements made along promising mobile belt regions are limited in number. Another method in determining potential EGS sites in South Africa is by looking at surface concentration of heat producing elements. These heat producing elements undergo natural radiogenic decay, emitting heat, which is then trapped in the surrounding rock. Regions with high concentrations of heat producing elements provide another feature in delineating EGS target sites.

Andreoli et al., (2006) presented a mosaic of all radiometric gamma ray surface exposure data covering South Africa (Figure 16). This map displays measured U and Th concentrations over a large part of South Africa and provides a useful indication of those regions with higher heat producing potential. From the map, the authors concluded that the NNMB displays the highest levels of radiogenic enrichment, with U concentrations peaking above 1000 ppm. Other enriched areas include the Pilanesberg Complex that reaches U concentration levels of just below 1000 ppm, and the WB and Pongola basin which both amount to a U concentration of 500 ppm. Investigations undertaken by *Peninsula Energy Limited* around, Beaufort West also has confirmed high concentrations of U in the Karoo Basin. Shallow drilling was undertaken and measured U contents exceeding 2000 ppm between a depth of 1-2 m (Peninsula Energy Limited, 2012).

Orberger et al., (2011) investigated the anomalously high concentration of U in the black shales and conglomerates of the Archean Pongola Basin. They proposed that these signatures could be attributed to late stage chemical infiltration of low-temperature oxidising fluids. These oxidising fluids are possibly associated to detrital uraninite weathering. According to this theory, these chemical fluids remobilised U from an Archean granitic source material and sequestered it within the basin. This suggests that the source Archean rocks initially had a very high concentration of radiogenic heat producing elements.

There is a clear relationship between areas of higher radiogenic signature and those exhibiting higher heat flow. These regions are also the location of granitic magmatism, both Archean and much younger. This illustrates the importance of radiogenic input in aiding toward a higher crustal heat flow. Blackburn et al., (2011) suggests the possibility of using radiogenic data such as various U/Th-Pb isotopic data toward thermochronology to distinguish between terrains that are undergoing cooling, and those that have been reheated. Reheating could occur

through the addition of radiogenic rich crustal material or from the underlying mantle, both mechanisms rely on tectonic processes. Another application of thermochronology is toward determining the Pb retention time. This provides another method of determining the crustal cooling rate and ascertaining the heat producing concentration of a specific area. In regions lacking extensive heat flow measurements, this provides an alternative technique in determining possible EGS viability.

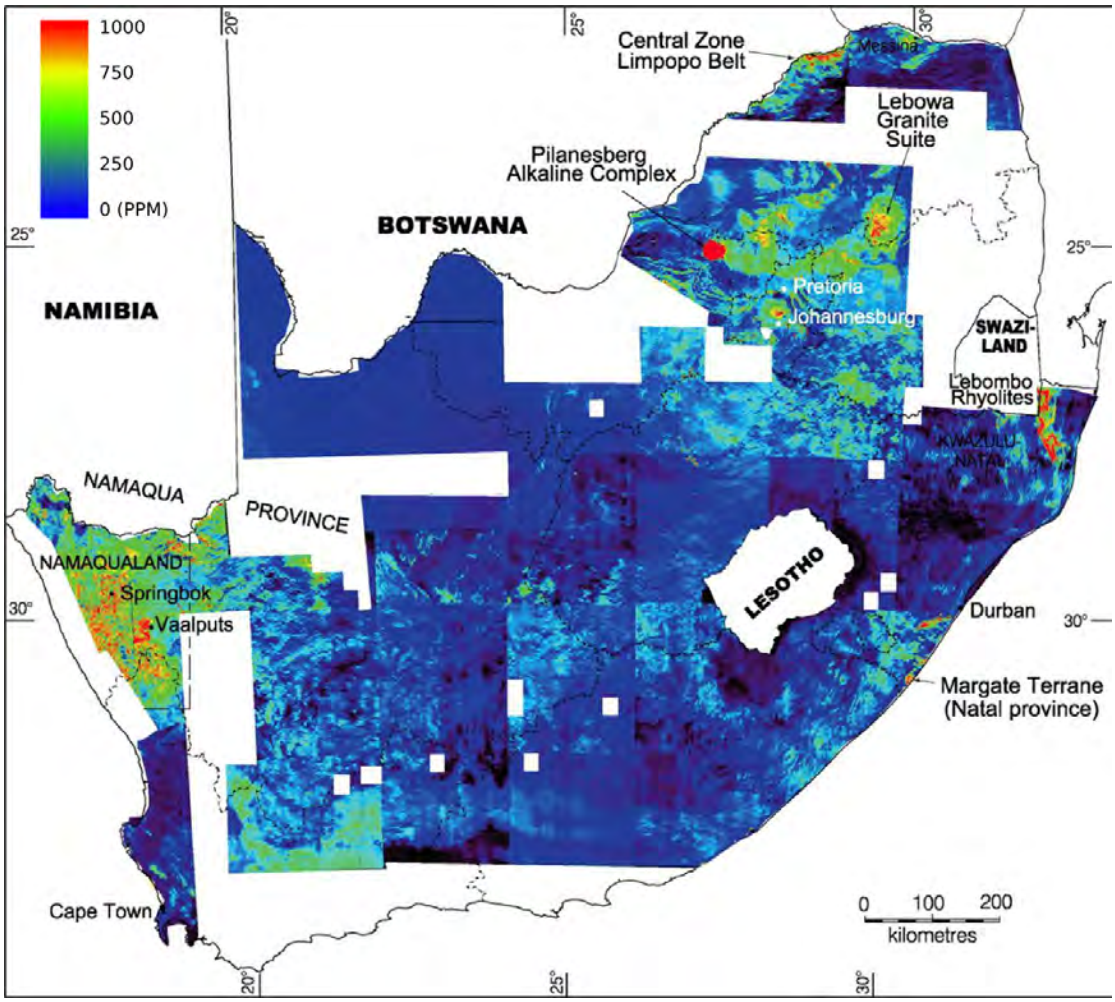

Figure 16: Gamma-ray exposure rate of K, U and Th in South Africa, measured in nanoGray/hour (nGy/h). Anomalies include Pilanesberg Alkaline Complex (U = 141 ppm; Th = 950 ppm); Limpopo Mobile Belt Central Zone (U = 90 ppm; Th = 500 ppm). Modified after Andreoli et al., (2006)

7.3 Effect of the Kaapvaal Craton on South African heat flow profile

7.3.1 Overview of the Kaapvaal Craton

The Kaapvaal Craton forms one of the most well preserved pieces of early continental fragments in the world. This craton developed over a period of ca. 1 billion years between 3.6-2.6 Ga and formed through processes similar to plate tectonics. These early tectonic processes included volcanic arc development and the amalgamation of discrete individual blocks along major suture zones (de Wit et al., 1992; Lowe, 1994; Poujol and Robb, 1999). The Archean period had a mantle with a higher temperature than presently and experienced accelerated oceanic crust development. There is however a clear crustal imbalance when accounting the present basaltic evidence on the existing cratons, including on Kaapvaal Craton. Herzberg and Rudnick, (2012) continued the early continental models by Jordan, (1975; 1978; 1988) and provides a possible explanation for this crustal disparity with thermal and petrological models. Their model suggests that some of the Archean oceanic crust acted as source material for a phase of partial melting. This result of the partial melting formed the earliest TTG continental crust. The remaining material separated according their density differences into a buoyant harzburgite layer and less buoyant eclogite layer. Thereafter, subsequent secular mantle cooling may have led to a notable decrease in the degree of partial melting within the mantle toward the end of the Archean (2.5 Ga) and a shift in style of continent formation (Keller and Schoene, 2012). This shift would have seen much less basalt formation and the formation of a more granitic composition, possibly accounting for the lack of basaltic material seen today.

The Kaapvaal Craton can be subdivided along two age-distinguishable crust domains, the eastern (Witwatersrand Block) and western (Kimberley Block) blocks (Figure 17). These discrete domains are separated by a major shear lineament, known as the Colesberg Lineament. Age determinations on both blocks show the Witwatersrand block, with a predominant granitic basement, is older (>2.9 Ga) than the Kimberley Block (<2.9 Ga) (Schmitz, 2004; de Wit et al., 2011; Zeh et al., 2011; Xie et al., 2012). De Wit and Tinker, (2004) performed eight deep seismic reflected profiles across the central region of the Kaapvaal Craton that provides a better illustration of the internal structure within the Kaapvaal Craton. The results of de Wit and Tinker, (2004) suggests that the craton represents a complex sequence of tectonically stacked crustal fragments, stacked along shallow and deep listric faults. These fragments were thrust along an eastward propagation pattern and amalgamated within the Neoarchean

period. The shallow geometry has also given rise to a relatively sharp and shallow Moho boundary below the craton.

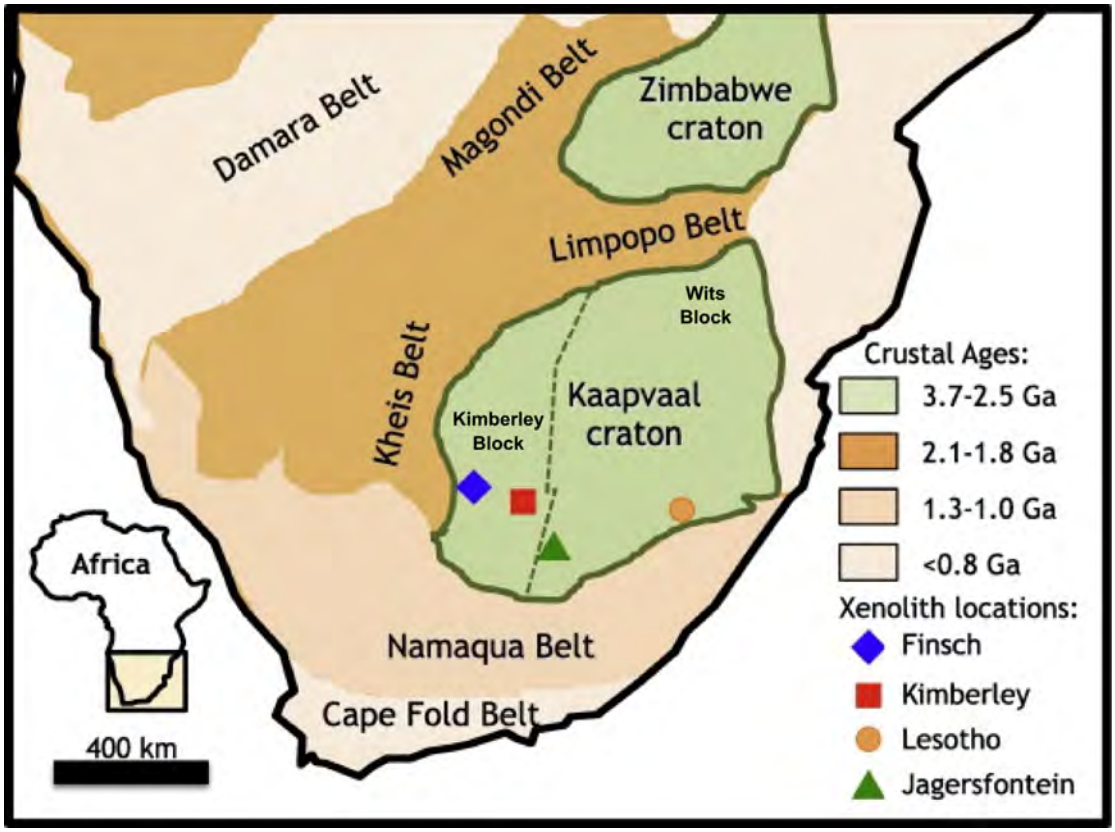

Figure 17: Simplified geological map of South Africa highlighting the Kaapvaal Craton and various crustal ages of the major orogenic belts Peslier et al., (2012)

7.3.2 Structure of the Kaapvaal Craton and its implication on heat flow

Geophysical investigations, such as seismic tomography illustrate high velocity signatures extending to depths of up to 250 km below the Kaapvaal Craton. These convey the presence of the thick underlying depleted mantle keel. Additionally, many of the relatively cold heat flow signatures have been measured in regions overlying the mantle keel. This suggests that the mantle keep may play a role in the development of the colder signatures observed throughout previous heat flow measurements. Many of the available heat flow measurements are restricted to areas overlying the craton and there is a lack of data along the surrounding terrains of the craton. Available data does however suggest much higher heat flow signatures along these neighbouring zones. Further suggesting that most of the heat flow is diverted by the craton and is concentrated along the surrounding zones.

Chevrot and Zhao, (2007) processed Rayleigh wave measurements recorded within the southern Africa Seismic Experiment across the Kaapvaal Craton. From their results, they define relatively slow seismic velocity signatures across the craton, extending into the surrounding Proterozoic mobile belts. They conclude that these slower signatures can be linked to heating of the lithosphere through crustal thinning and possibly Karoo magmatism. The results of Chevrot and Zhao, (2007) are consistent with James et al., (2004). The latter applied geological constraints on 3D seismic data using mantle xenoliths and estimated a much thinner crustal signature affecting the heat flow across the craton. This possibly suggests a larger mantle heat flow signature on the Kaapvaal Craton. Ballard and Pollack, (1987) further considered the variation between the heat flow on the craton and on the neighbouring mobile belts. They performed a series of heat flow measurements and concluded this disparity to either arise because: 1. A heat productivity composition and concentration variation between the cratonic and mobile belt material. 2. A larger effect from the underlying mantle root that deviates most of the mantle heat to the thinner mobile belts. 3. Possibly a combination of these two mechanisms.

Nguuri et al., (2001) and the Southern Africa Seismic Experiment elucidated the variation in crustal thickness below the Kaapvaal Craton (Carlson et al., 1996; 2000; de Wit et al., 2004). This experiment considered 81 seismic stations across the Kaapvaal Craton that recorded and processed seismic events to ascertain a better understanding of the Moho underlying the craton and produce a crustal thickness map across South Africa (Figure 18). The map illustrates that thicker crust underlies the mobile belts, contrary to previous views the mobile belts has a much thinner crustal profile. These areas also comprise of the countries hot springs with highest surface temperatures. These hot springs appear to fall within the suture zones between the mobile belts and craton. Two exceptions are hot springs within Lesotho. According the crustal map, these springs are located on the craton. These values however correlate with observations by Jones, (1992) who concluded that this region represents the southern boundary of the Kaapvaal Craton. While the inferred cratonic boundary of Ballard and Pollack, (1987) and Jones, (1992) vary, Hartnady, (1985) had earlier considered these anonymous hot springs. The latter had hypothesized that this heat flow signature was related to an underlying mantle hot spot. He continued by attributing the anonymously high altitude of the region and thick basaltic rocks to be a result of the proposed hot spot. However, Jones, (1992) highlighted the lack of available supporting data and was able to dispel this hypothesis.

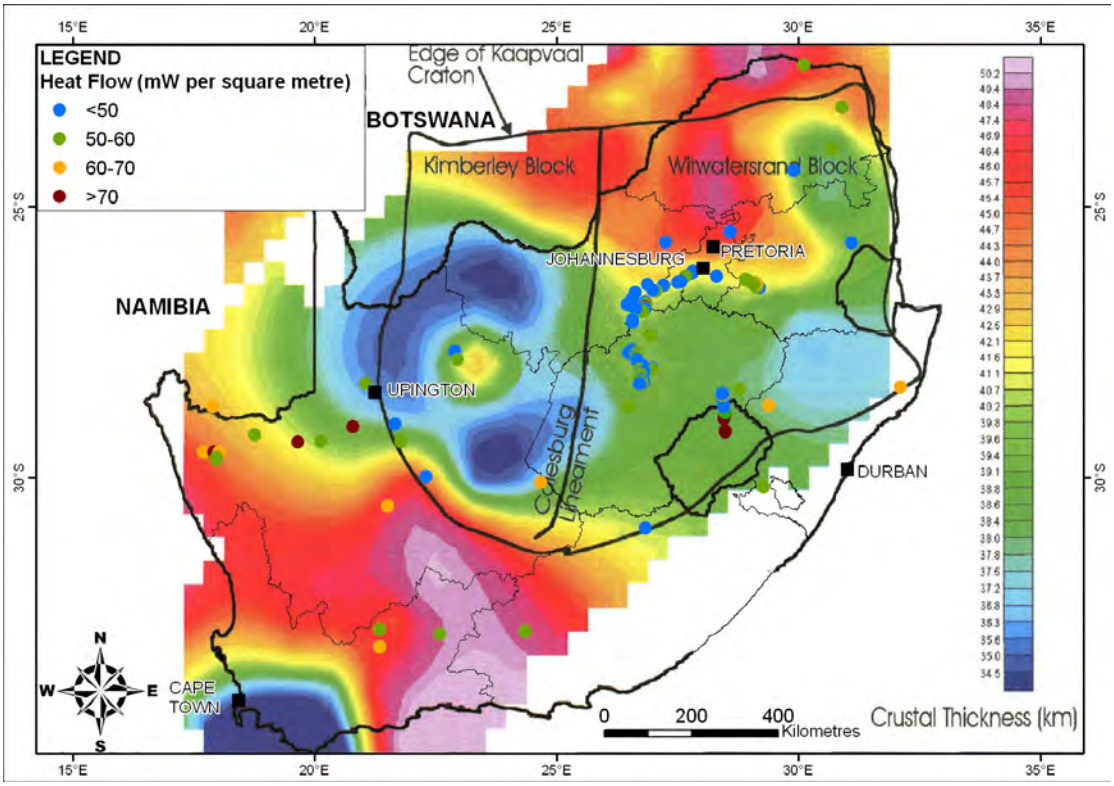

Figure 18: Crustal thickness profile of South Africa, showing the locations of some selected hot springs, modified after Doucouré and de Wit, (2002)

Complimentary to the southern Africa Seismic Experiment was the southern African Magnetotelluric Experiment (SAMTEX). This project was launched in 2003 to thoroughly investigate and delineate the structure beneath the Kaapvaal and Zimbabwe Cratons and their surrounding terrains. The experiment benefited from 330 instrumental sites using long period measurements at a third of the sites with a high depth penetration of more than 300 km, over a total distance of 5000 km. Comparing data from the SAMTEX and seismic data from the Kaapvaal craton, Hamilton et al., (2006) considered electrical anisotropy within the Kaapvaal Craton. They discovered that the anisotropy is clearly defined at crustal depths for both the MT and seismic data and are related to large-scale geological structures. The findings of Hamilton et al., (2006) corroborates that of Silver et al., (2004). The latter related seismic anisotropy to large-scale deformational events and the development of distinct mantle fabric. These deformational events firstly created compression-related mantle fabric and subsequent extensional-related reactivation zones. These deformational events include: 1. An orogeny before 2.9 Ga leading to the development of a mantle fabric within the Zimbabwe Craton. 2. An orogeny at 2.9 Ga along the west of the Kaapvaal Craton. 3. The Limpopo Orogeny and the development of the three distinctive zones of the Limpopo Mobile Belt. 4. The Magondi Orogeny at 2.0 Ga, leading to the reactivation along the Limpopo Mobile Belt and the emplacement of the Bushveld Complex. 5. The Kheis Orogeny that led to the

deposition of the Soutpansberg Group. Silver et al., (2004) also concluded that the geometry of the mantle fabric related to these orogenic periods would later create a control for later magmatic intrusions and the further evolution of the Kaapvaal and Zimbabwe Cratons.

Fouch et al., (2004) also elucidated the mantle structure beneath the Kaapvaal and Zimbabwe Cratons using seismic tomography. Their results display a correlation between the mantle structure and the regional surface geology, similar to results from Hamilton et al., (2006). Figure 19 shows an example of the results of Fouch et al., (2004) from the Cape Fold Belt to within the Zimbabwe Craton. According to Jones, (1992) the relative position of the Kaapvaal and Zimbabwe Cratons provides a barrier disrupting the convective heat flow from the mantle, focussing it along the cratons bordering mobile belts.

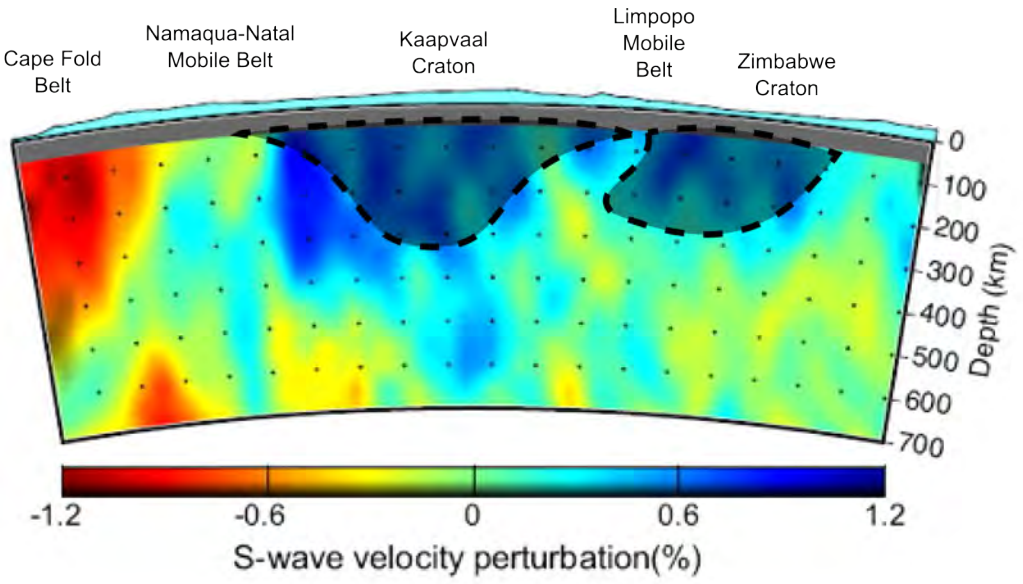

Figure 19: Modified image of S-wave cross-section across the Kaapvaal Craton. Two blocks highlight approximate location of the Kaapvaal and Zimbabwe Cratons. Modified after Fouch et al., (2004)

Bird et al., (2006) modelled the propagation of the East African Rift (EAR) southward using numerous stress and strain patterns. In addition, they generated a modelled heat flow map (Figure 20). This map compiles available heat flow data from the EAR southward to the Kaapvaal Craton. This shows that while the anonymously high heat flow measurements evident in the NNMB are clear, as based on published data (Pollack et al., 1993), there is no clear anomaly shown in the LMB. However, this likely reflects the lack in available published data in this region.

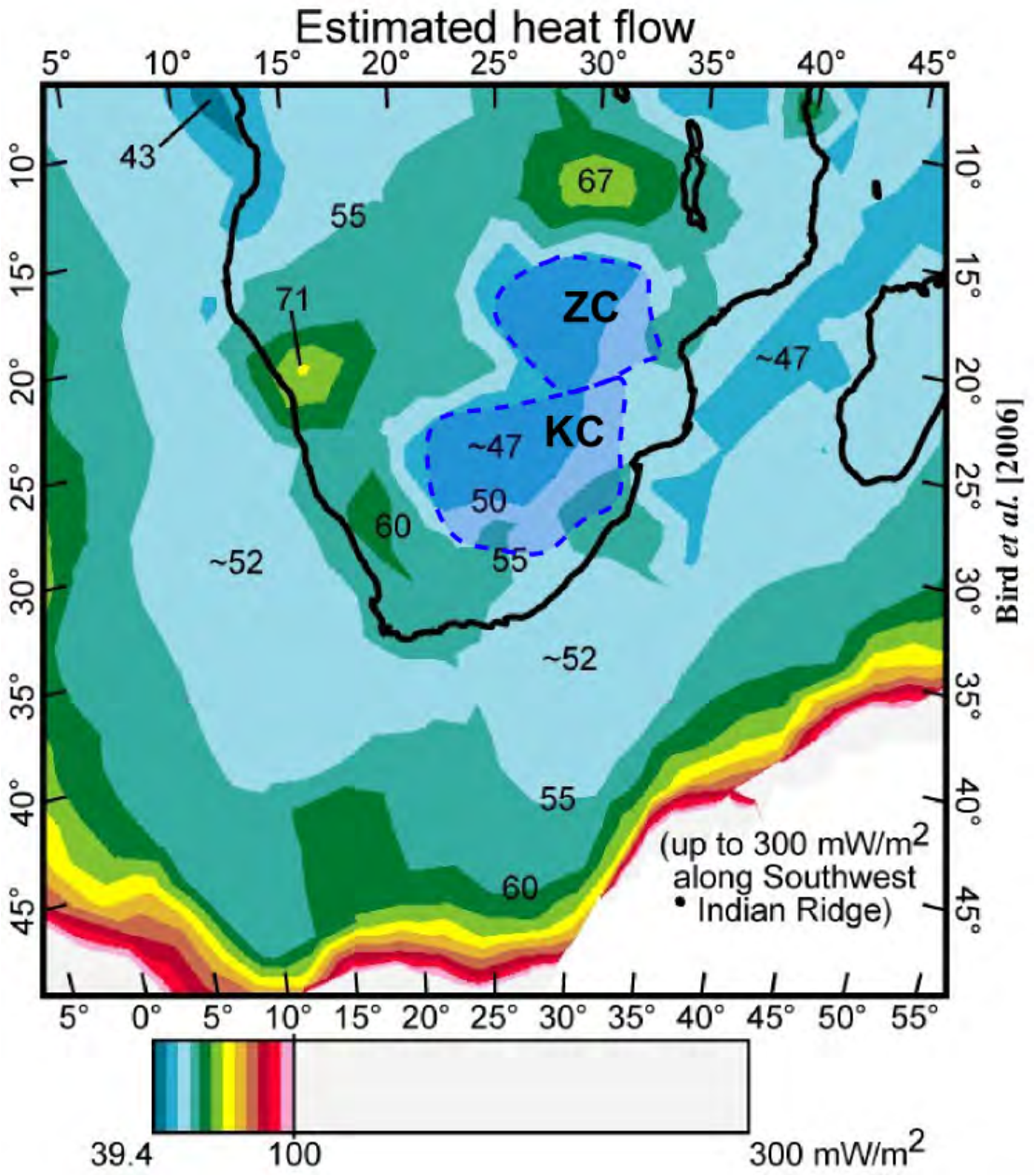

Figure 20: Modelled heat flow map of southern Africa. Contour intervals delineate 5 MW/m² variations, ZC = Zimbabwe Craton; KC = Kaapvaal Craton, Bird et al., (2006)

7.4 Geothermal potential map of South Africa

A geothermal potential map is generated using all available heat flow data in South Africa (Figure 21). This is calculated using Inverse Distance Weighting (IDW) within Quantum GIS. It considers a total of 120 heat flow measurements recorded throughout South Africa, however concentrated around the Wits Basin. The region overlying the Kaapvaal Craton forms the lowest potential area, while the bounding Namaqua-Natal Mobile Belt shows the highest potential signatures. The western extent of the Kaapvaal Craton is not entirely constrained due to a lack of data in this region.

The target Makuleni area is within the Limpopo Mobile Belt. According to the potential map the Limpopo Mobile Belt does not form a highly prospective region. However this is because the calculation depends of very few data points. Similarly, the Cape Fold Belt is limited for data and therefore appears less prospective. Ideally, a much larger amount of data should be acquired to improve the regional cover and precision of the calculation.

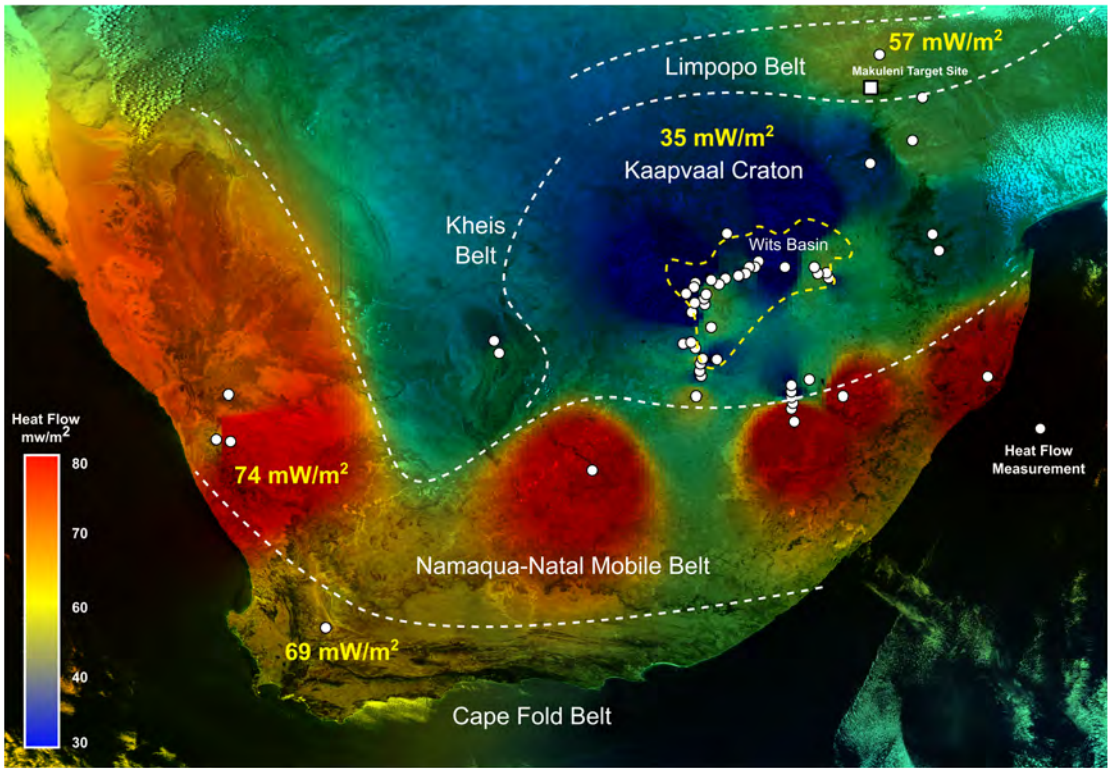

Figure 21: Geothermal potential map created within Quantum GIS using available heat flow data, various data point represented by the white dots

Chapter 8: The Makuleni target site, Limpopo Province

8.1 General overview of the Makuleni target site

8.1.1 Poverty in the Vhembe District of the Limpopo Province

The Limpopo Province is separated into five district municipalities. The Makuleni target site is located in the northern most and vastly rural Vhembe District (Figure 22). May et al., (1995); Lancaster et al., (1997) provide guidelines for delineating a poverty index in South Africa. They note several aspects under consideration when delineating this, and these include: 1. Weighting the average national income level, with a poverty limit based on low monthly income. 2. Discerning a level of fundamental well being, based on social and food security. This study considers a primary poverty index corresponding to a gross income on the 40th percentile of the national mean income. Since South Africa is a developing nation with a relatively low mean income rate, the 20th percentile of mean income rate is considered as an ultra-poverty index. Based on this and according to Pauw, (2005) the Limpopo Province is one of the most poverty-stricken provinces in South Africa, with a poverty rate of just under 70 %. This exceeds the national poverty rate that stood just below 50 % in 2011[17].

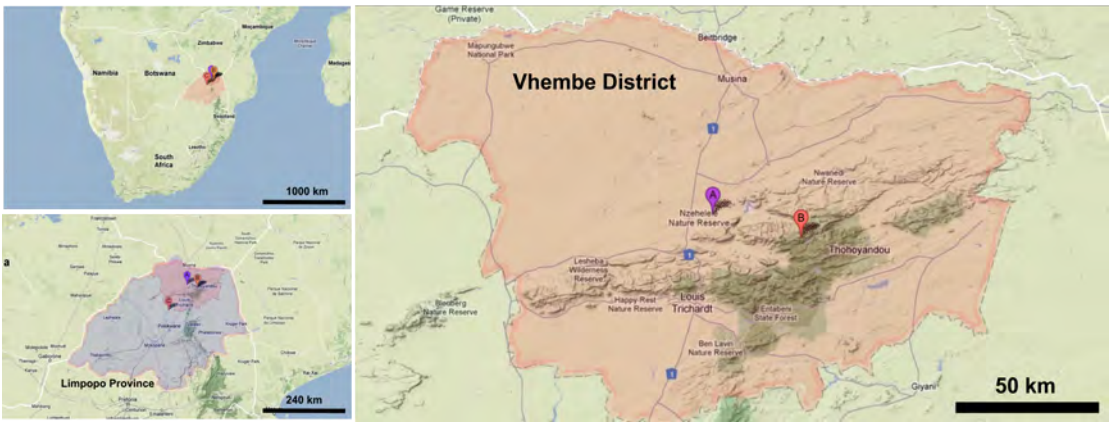

Figure 22: Overview of the Vhembe District Municipality, A; and the Makuleni target site, B; within the Limpopo Province, C

[17] Information published in the Mail and Guardian, September 2011. Based on a collaborative research programme funded through the EU. More information available from: http://mg.co.za/article/2011-09-16-poverty-and-inequality-in-south-africa.

8.1.2 Current energy sources within the Vhembe Municipality

The Integrated Development Plan (IDP) Document, 2007 estimated that 70 % of rural areas in South Africa are yet to be connected on the National Energy Grid (NEG). Despite the expansion of the NEG many rural households still could not connect to the NEG because they lack adequate housing infrastructure. According to the results of the Census 2011 (Figure 23), the majority of the Vhembe municipal district resides in adequate housing. These values include the larger towns and residential areas. There is however a substantial 10 % of the population that resides in rural dwellings. These are concentrated in the smaller villages throughout the Vhembe District and include the Makuleni and its neighbouring villages.

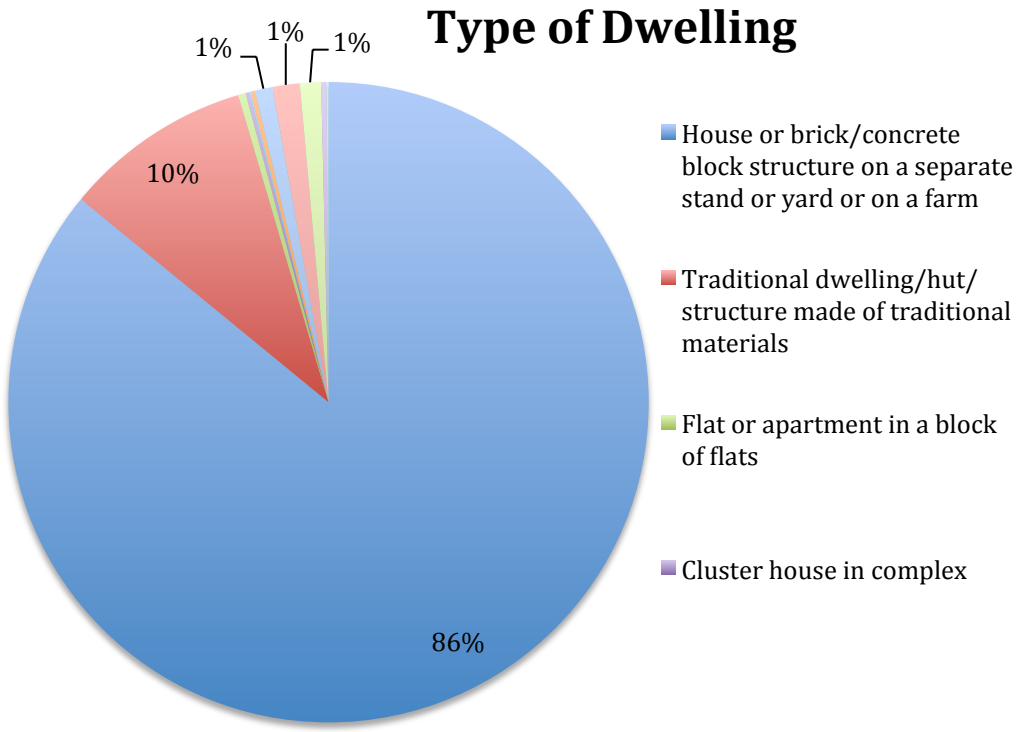

Figure 23: Type of dwelling and the number of people residing in each household in the Vhembe District Municipality. Census, 2011

Despite a marked lack of adequate housing infrastructure, the NEG has extended into the Makuleni and its neighbouring villages. Many of these villages now have access to and benefit from Eskom's basic free energy policy. Under this policy rural households receive 50 KWh of electricity at the beginning of each month. Figure 24 illustrates the various energy sources and their usages in the Vhembe District. These values include developed residential areas, however illustrates that while electricity is commonly used as the dominant lighting source, wood still forms the most prominent cooking fuel. The use of more rudimental forms of cooking fuel represents the more rural communities, like the Makuleni village.

This reiterates that while these villages have access to electricity, a large number of the rural population still finds the cost of electricity exorbitant and do not benefit from installed infrastructure.

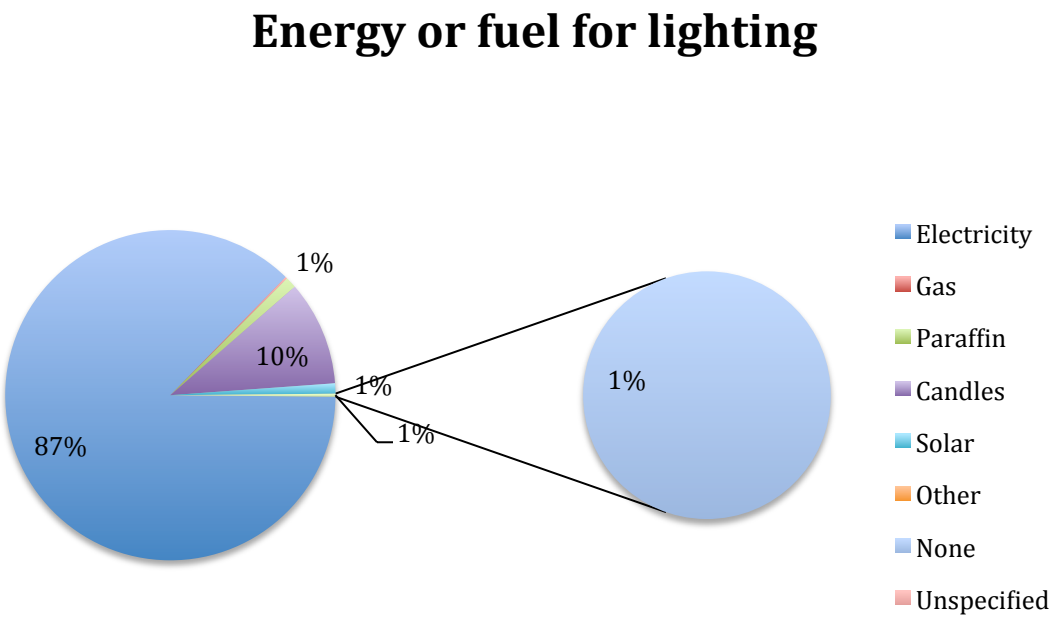

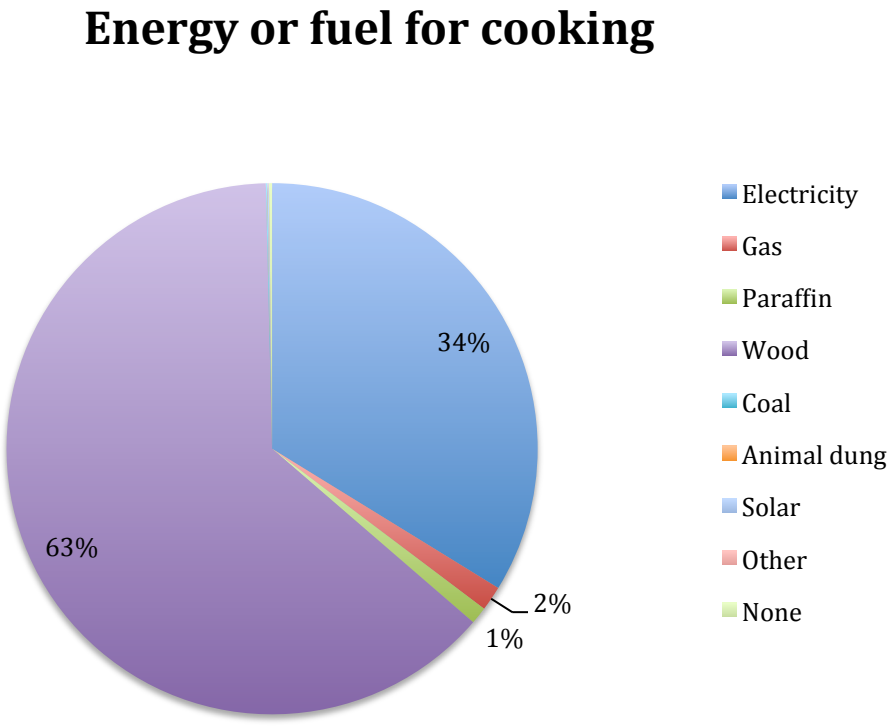

Figure 24: Breakdown of the various energy sources and usage per household in the Vhembe District Municipality. Census, 2011

8.1.3 Water sources throughout the Vhembe Municipality

With more than 80 % of the Vhembe District having adequate housing, a large portion of the population can benefit from the municipal water scheme and borehole water supply Figure 25. The rural and areas with a predominance of traditional housing, including the Makuleni village, rely on the large dams and river systems throughout the Soutpansberg mountain range. Hydrogeological is essential to ascertain any impact to the groundwater supply and it's possible implication to the surrounding population.

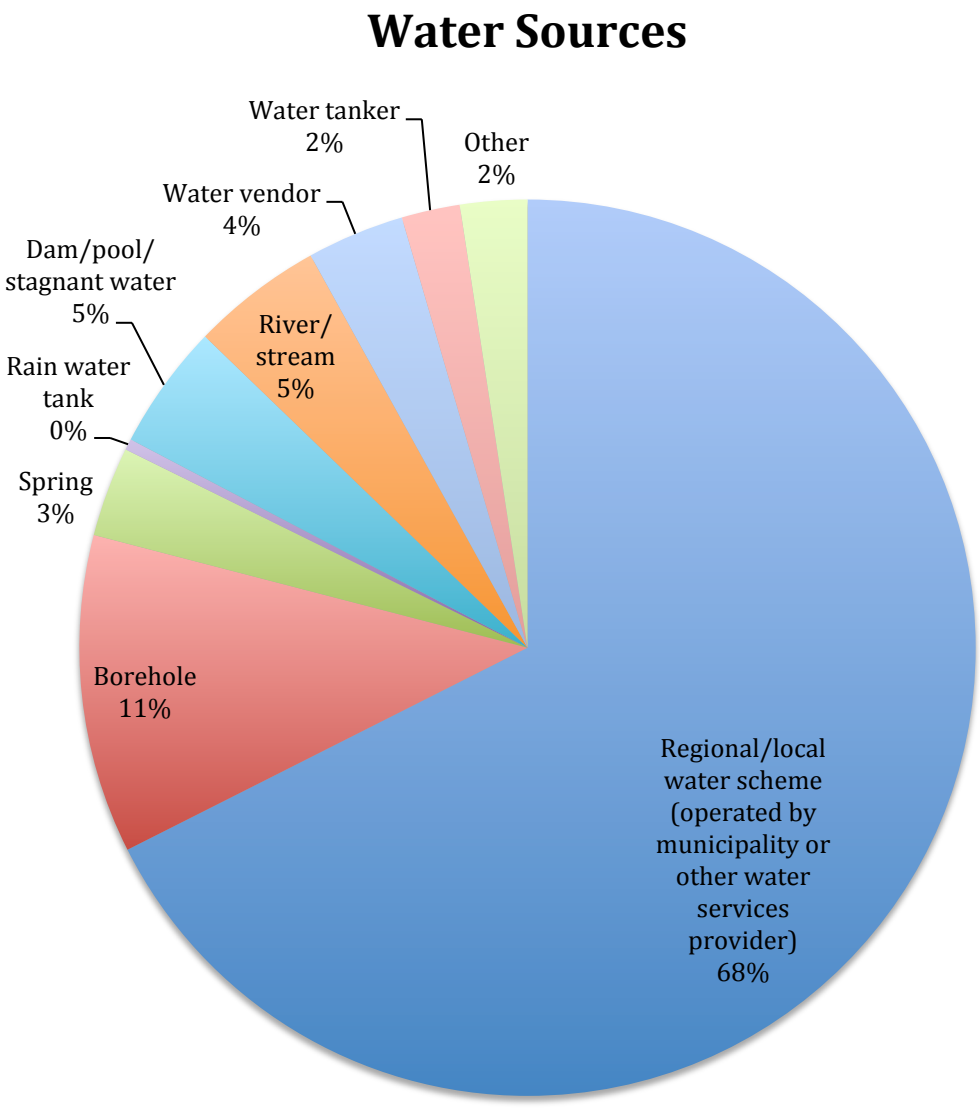

Figure 25: Various population water supply sources in the Vhembe Municipal District. Census, 2011

8.1.4 Benefits of an EGS plant in the Makuleni area

Figure 26 illustrates a map of the target Makuleni and its neighbouring villages. By scrutinising a Google Earth image within a spatial analysis, estimating the energy requirements for each household is possible. Based on a site visit each household is estimated to have approximately 10 people, with a calculated total of 1,000 households. These numbers are further quantified with Limpopo's rural settlement expansion, as defined from the 1996 and 2001 census comparative document (Statistics South Africa: Census 2001) and the latest Census 2011 results. The spatial analysis calculates that each household in the Makuleni and surrounding villages will have an average energy consumption of ca. 50 KWh per month. This includes for lighting, cooking and heating applications. These values are corroborated by Davis, (1998); Aitken, (2007); Louw et al., (2008) who have performed various energy calculations to determine average rural energy usage.

The EGS plant is proposed to attain a maximum power output of 75 MW. However before reaching full capacity, it will rely on the results from a 1 MW demonstration plant. The demonstration plant will serve to better ascertain the exact amount of production wells and size of fractured reservoir required. The low energy needs of the rural households suggest that the demonstration plant could produce enough energy to sustain of the Makuleni village. The problem of inadequate households will however remain a limiting factor yielding all households from benefiting.

One of the key benefits possible with the development of an EGS plant in the Makuleni village is the impact on South Africa's carbon emissions. Total CO_2 emissions per KWh of energy produced by South African coal-fired power plants is ca. 0.96 $kgCO_2$/KWh (Eskom Factor Report, 2011). With the final completion of the Medupi and Kusile coal-fired plants in 2015 and 2018, respectively, South Africa will struggle generate a substantial decrease in the CO_2 emissions without several renewable energy options. Successful development of a 75 MW EGS plant in the Makuleni Village, South Africa will have the potential of saving 1.5 gCO_2/KWh.

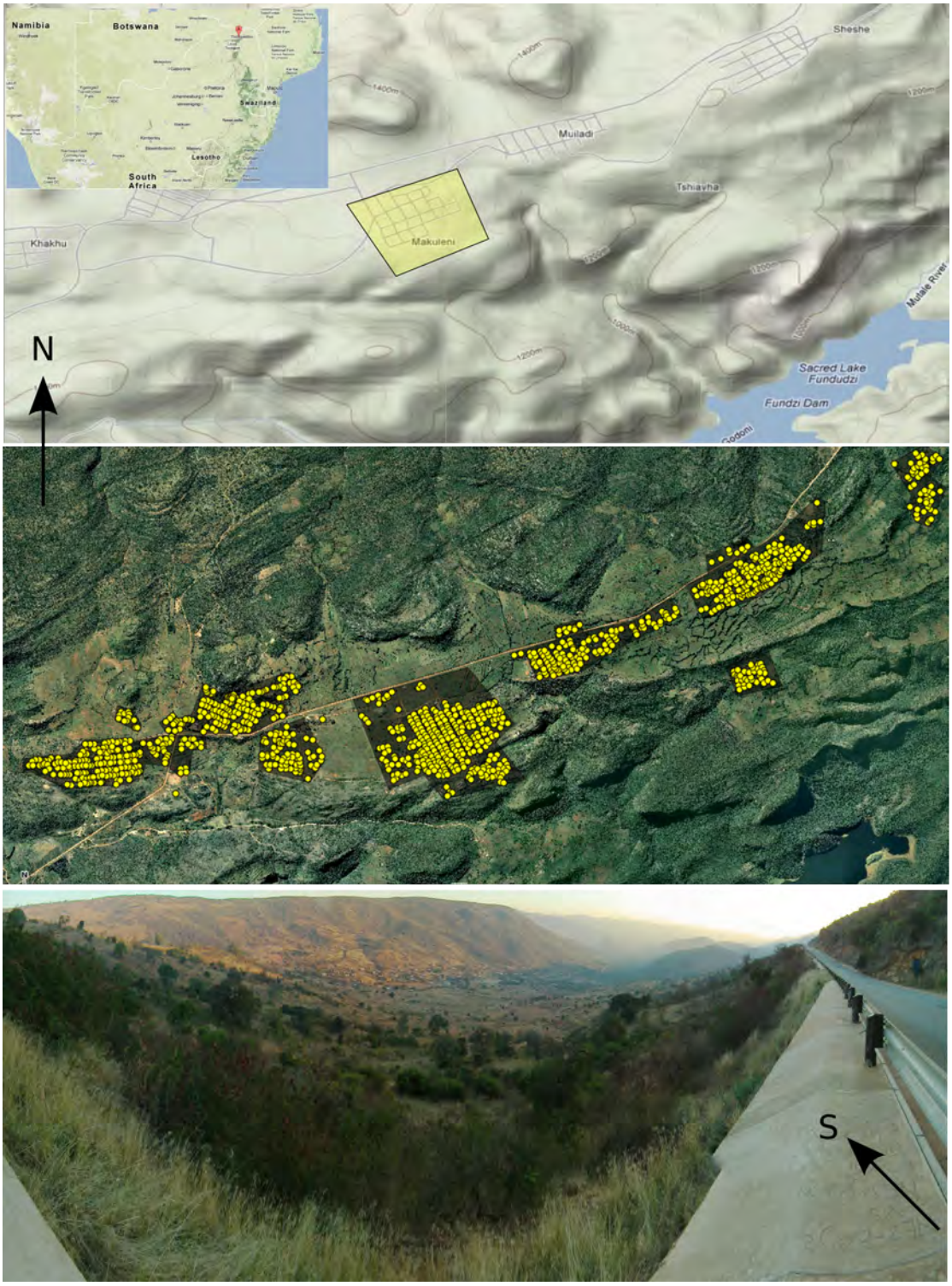

Figure 26: Google map of the Makuleni and surrounding villages, top; Google Earth map with spatial analysis data points of each household, middle; Makuleni valley and Google map overview, bottom

8.2 Geology overview of the Makuleni target site

The Makuleni target site is located in the 1.85 Ga Soutpansberg Group of the Limpopo Province (Cheney et al., 1990; Barton and Pretorius, 1997). The Soutpansberg mountain range unconformably overlies Limpopo Archean TTG rocks (Brandl, 1986; 1987; Brandl and Kroener, 1993). The TTG sequence contributes a large amount to the radiogenic signature recorded by Andreoli et al., (2006), Figure 16. The Soutpansberg Group (Figure 28) was deposited as a syn-rift sequence in a half-graben basin structure with alternating phases of sedimentary deposition and volcanic outpouring (Bumby et al., 2001; Crow and Condie, 1990; Bumby et al., 2002). This deposition occurred during a late-stage period of regional extension following the collision of the Kaapvaal and Zimbabwe cratons (Schaller et al., 1999). The Limpopo Mobile Belt (LMB) formed during the collision of Kaapvaal and Zimbabwe cratons, with the Soutpansberg Group deposited in the southern region of this orogenic belt. The northern boundary of the Soutpansberg separates the southern and middle regions of the LMB with a prominent shear zone, known as the Palala Shear Zone (PSZ) (Jansen, 1975). The PSZ illustrates a complex Archean history with several phases of deformation and the development of a strong mylonitic fabric, while metamorphism is minimal in the Soutpansberg rocks.

The Soutpansberg displays a complex network of normal faults and numerous dolerite dykes and sills characterising the area with many fault-controlled hot springs (Figure 18; Figure 28) (Olivier et al., 2008; Nyabeze et al., 2010). The hottest spring records a surface temperature of 70° C (Nyabeze et al., 2010; Tekere, 2011). This spring is located on the Siloam fault where groundwater circulation appears to reach a maximum depth of 2 km. This would suggest that at greater depths, a possible basal reservoir temperature could be attained capable of sustaining low-enthalpy EGS production.

The Makuleni target site area overlies the Funduzi Formation, attaining a maximum thickness of 2,800 m in some places. This comprises of argillaceous and arenaceous clastic sediments with minor pyroclastic volcanic rocks and a thin sequence of basalt. The Funduzi overlies a much thicker sequence of the Wyllies Poort Formation, attaining a maximum thickness of 4,000 m near the lake Funduzi. This includes sandstones, quartzites and conglomerates. This in turn overlies a thick sequence of Sibasa basalts, attaining a maximum thickness of 3,300 m. Below the Sibasa and at the base of the Group is a thin sequence of the Tshifhefhe Formation, attaining a maximum thickness of 5 m. These include basalts, shales and conglomerates. Toward the north, the Soutpansberg Group is separated from the Karoo Supergroup by the Bosbokpoort fault. At some places

this fault displays a downward throw of up to 10 m. The fault runs adjacent to the extension of the EAR and displays numerous shallow hot springs and high concentration of hydrothermal copper mineralisation.

A 3D schematic of the geological profile underlying the target area is displayed in (Figure 27). Three wells represent the proposed working system of the demonstration EGS plant. The blue well provides a down flow conduit for the influx of the cold working fluid, and two yellow wells serve as up flow production lines for the development of the renewable energy. The geology has been simplified into two discrete sequences: (1) Soutpansberg volcano-sedimentary sequence that has been split into the three lower groups expected below the target site, (2) the basement granite-gneiss of the Hout River-Goutplaats Gneiss suite. Schematically overlain with the geology is an illustration of the vertical fractures and associated dyke and sill development. In addition, a temperature profile is shown and corresponds with values estimated within the model.

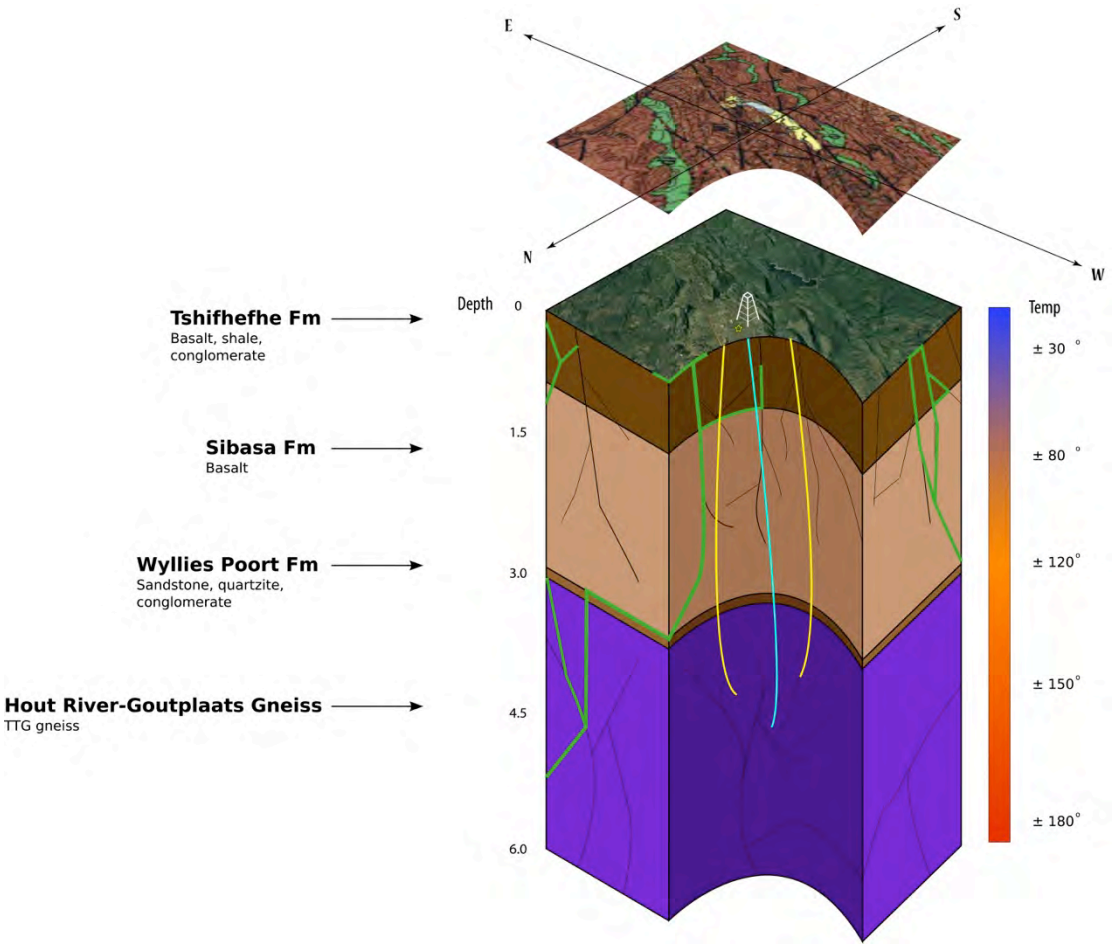

Figure 27: Simplified geological model of the EGS target site and estimated temperature profile

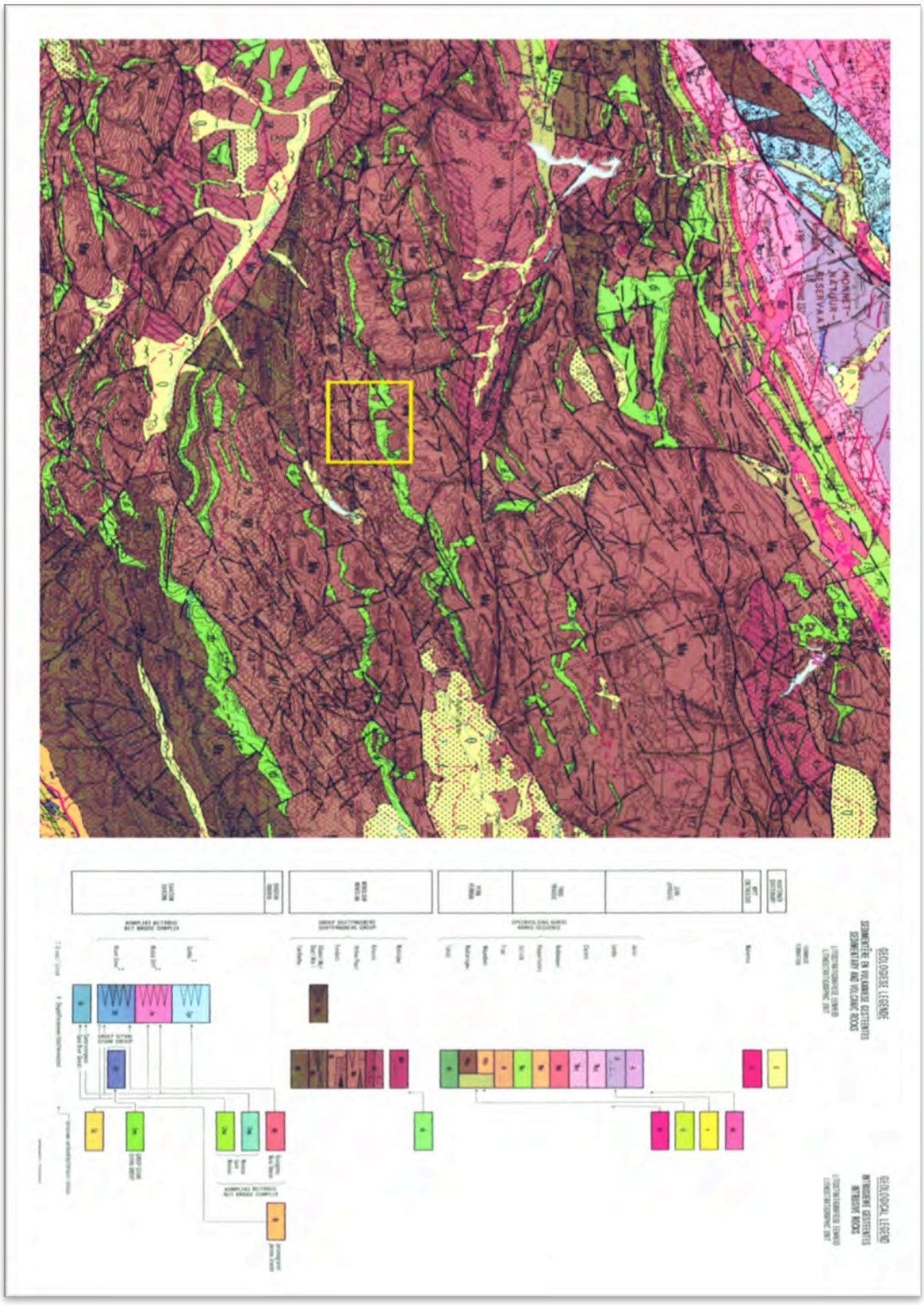

Figure 28: Geological map surrounding the target area, clipped from the Messina and Alldays 1:250,000 geological maps, Brandl, (1981); Brandl and Pretorius, (2000), respectively

8.3 The Limpopo Mobile Belt

The Limpopo Mobile Belt (LMB) (Figure 29) is a 150,000 km^2 high grade metamorphic terrain interpreted to have formed during the amalgamation of the Kalahari Shield. This was a consequence to the collision between the Kaapvaal and Zimbabwe Cratons (Coward et al., 1976; van Reenen et al., 1992; Rigby et al., 2008). The LMB can further be subdivided into three distinctive zones, namely the northern (NMZ) and southern (SMZ) marginal zones and the central zone (CZ) (Cox et al., 1965). The NMZ and SMZ are predominately composed of reworked fragments of the adjacent Zimbabwe and Kaapvaal Cratons, respectively, and are each separated from the cratons by steeply dipping ductile shear zones. The CZ is distinctive and consists of diverse supracrustal sequence and is furthermore separated from the marginal zones by two major strike-slip shear zones.

Kramers et al., (2001) investigated the heat flow disparity between the marginal zones of the LMB. These investigations included the Southern Marginal Zone (SMZ), Northern Marginal Zone (NMZ) and Central Zone (CZ). They found that the SMZ shows a much lower heat flow than the NMZ and correlated this difference to a contrast in the crustal composition of their adjacent cratons. The Kaapvaal Craton underlies the SMZ, while the Zimbabwe Craton underlies the NMZ. They deduce that the Kaapvaal Craton has lower concentration of heat producing elements than the Zimbabwe craton.

The NMZ is made up of reworked granite-greenstone remnants from the Zimbabwe Craton. These include charnockites, enderbites with lesser ultramafics, iron formations and metapelites (Rigby et al., 2008). The NMZ was later subjected to late-stage thrusting resulting in the formation of a strong mylonitic fabric, evident throughout the charno-enderbites (Ridley, 1992). Frei et al., (1999) performed age determinations on a suite of syn and post-tectonic porphyritic granites and microgranites crosscutting the NMZ. Their results constrained the age of NMZ to 2.67-2.52 Ga. In contrast, the SMZ consists of reworked and metamorphosed material of its adjacent Kaapvaal Craton and is subdivided into a northern high-grade granulite zone and a southern rehydrated granulite zone. A retrograde ortho-amphibolite isograd zone separates these zones. Barton and van Reenen, (1992) constrained the age of the SMZ to 2.67-2.66 Ga by dating the syn-tectonic charno-enderbites and granodiorites of the Matok intrusive complex.

These marginal zone rocks form the basement throughout a large part of the Limpopo Province and are the target lithology for EGS exploitation. These

consists of the 2.8-3.3 Ga Hout River and Goutplaats Gneisses, which has been proposed by Brandl, (2006) to be grouped together as the Hout River-Goutplaats Gneiss. These are a highly strained and deformed sequence of porphyritic biotite-bearing gneisses and migmitites. They also display a high degree of brittle fracturing, rendering them ideal for fluid circulation.

The CZ is a completely distinctive zone when compared with the NMZ and SMZ. This zone consists of some of the earliest known supracrustal sequences including quartzites, magnetite quartzites and calc-silicates. These supracrustal rocks have been deformed and metamorphosed to granulite facies. Zeh et al., (2008) performed U-Pb dating on detrital zircons from the quartzites to attain ages of between 3.88-3.91 Ga, making these the oldest detrital minerals in South Africa. The CZ was later intruded by several different phases of granulites, including the TTG Sand River Gneiss Suite, Messina Suite and younger granites of the Bulai and Singelele Suites of Gneiss.

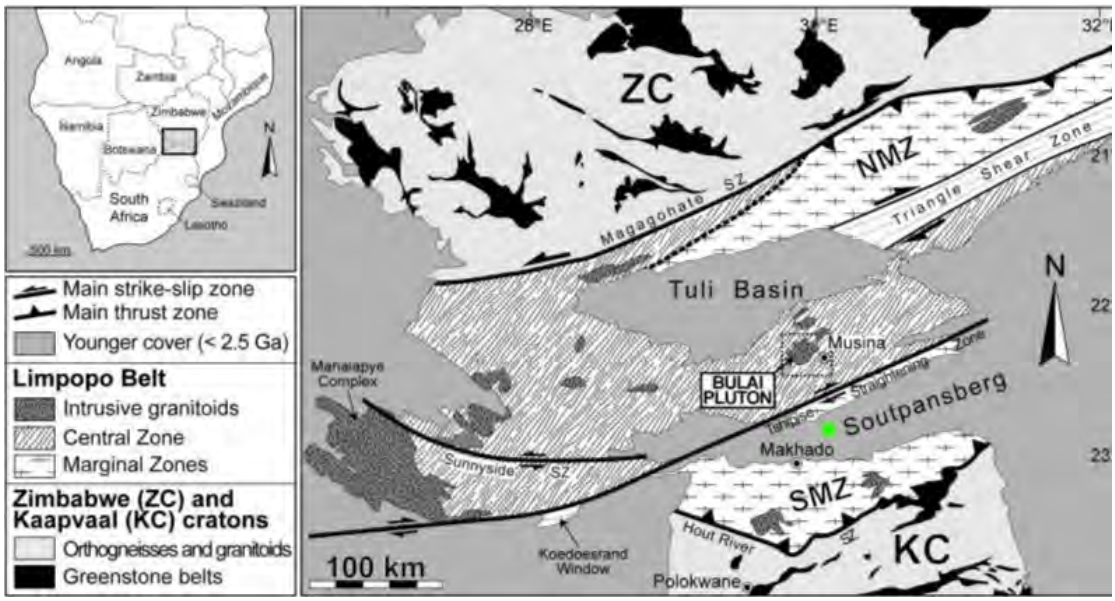

Figure 29: The Limpopo Mobile Belt with Makuleni target site, demarcated in green, note that "younger cover" includes the Soutpansberg Group, after Laurent et al., (2011); modified after Boshoff, (2006)

8.4 Structural and deformational overview of the target area

The LMB is one of the oldest orogenic belts in the world displaying a complex deformational history (Holzer et al., 1998; Rigby et al., 2008), compounded by several phases of granitic intrusions. The LMB experienced extensive sedimentation (Bumby et al., 2004) providing a thick insulating cover for the underlying granite-gneiss sequence. The deformational history of the LMB can be divided into three distinctive periods as described by Holzer et al., (1998). The earliest event occurred at 3.2 Ga and represents a phase of large magmatic outpouring associated with the Sand River and Messina Gneiss Suites. This event was overprinted by the next major magmatic led deformational event associated with the emplacement of the Singelele, Bulai and Alldays Gneisses at 2.65 Ga (Zeh et al., 2007; 2008). The final and most notable deformational event occurred at 2.0 Ga and signifies a heightened period during the amalgamation of the Zimbabwe and Kaapvaal cratons. Following this amalgamation was a decrease in the overall compressional stress regime and the start of an extensional regime. During this period rift basin formed throughout the Limpopo Province and signalled the beginning of the Soutpansberg deposition, in addition to extensive normal faulting.

An extensive fracture network within the targeted Limpopo rocks probably formed during the extension phase Limpopo Orogeny. However, it can be assumed that many of these fractures had enough time to heal themselves and subsequently sealed. Having sealed, the healed fractures would remain as the ideal zones for reactivation. The early Cretaceous Kalahari epeirogeny provided a period of intense continental uplift and would have induced reactivation along these incipient fractures. The exact causation of the Kalahari epeirogeny remains elusive, however de Wit, (2007) provides evidence for three corresponding events associated with this period. These include: 1. A large-scale exhumation and weathering period associated with the breakup of Gondwana. 2. A high degree of basaltic magmatism and the emplacement of two large igneous provinces. 3. An increase in kimberlitic intrusions throughout the Kaapvaal Craton. All these events contribute toward the anonymously high altitude of most of the Kaapvaal craton and likely the consequential reactivation of numerous fractures in the targeted granite-gneiss terrain.

8.5 Hydrogeology of the target area

Holland and Witthüser, (2011) performed an investigation of the factors controlling groundwater and borehole productivity in the Limpopo Province. Considering the crystalline bedrock in which the groundwater aquifers are developed, they apply a concept of two distinguishable zones overlying each other as the main controlling factor of the groundwater flow. The upper zone is considered as having a high porosity, but low permeability. This zone is dominated by clay-rich, highly weathered material. This zone then overlies a lower zone that is highly fractured and jointed with a lower porosity, but higher permeability. This second zone occurs within the basement granite-gneisses. They also described the presence of a thin weathered regolith overlying most of the Limpopo region. The regolithic layer result in a larger impedance of groundwater flow and therefore the fractures within the underlying bedrock plays the dominant role in the groundwater flow (Figure 30).

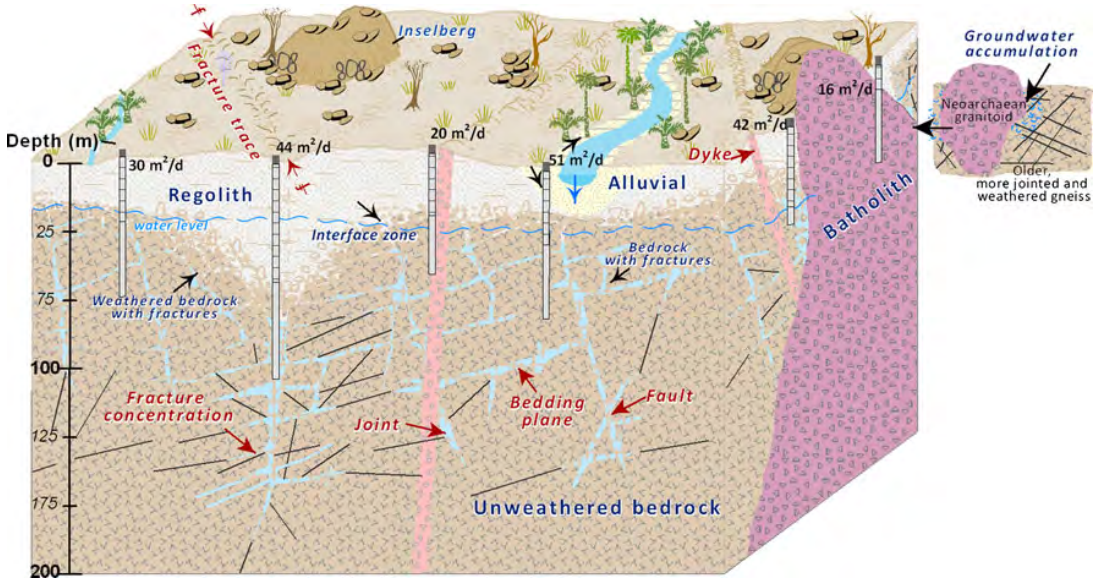

Figure 30: A conceptualised model of groundwater aquifers in the Limpopo Province, Holland and Witthüsser, (2011)

The target Hout River-Goutplaats Gneiss is described as having a relatively deep (>100 m) fractured groundwater aquifers. These deep aquifers are further described as being relatively fresh, unweathered and being well interconnected. This suggests that hydraulic fracturing can be successful in creating an adequately porous and well connected reservoir. However, care will have to be taken in maintaining a closed system to reduce system water loss to surrounding aquifers.

Holland and Witthüser, (2011) also recorded numerous transmissivities throughout their field area (Figure 31). Transmissivity considers the hydraulic conductivity and saturated thickness of an aquifer to illustrate the ability for an aquifer has to transmit fluids (Weight and Sonderegger, 2001). Most of the transmissivity readings fall between 4-40 m^2/day. These provide average transmissivities for the region. A few outliers do however reach values of more than 150 m^2/day. Pump tests sustained over a day resulted in yields of up to 1.5 l/s, which, according to Clarke (1985), this can be considered as a good yield. Most of the lower transmissivity readings are related to granitic inselbergs, while higher readings are commonly measured along the contact zones surrounding these bodies. Measurements of the major granite-gneiss units show that the Hout River-Goutplaats Gneiss displays some of the highest transmissivities of the surrounding units. This would imply that the Hout River-Goutplaats is adequately porous and could potentially sustain EGS development.

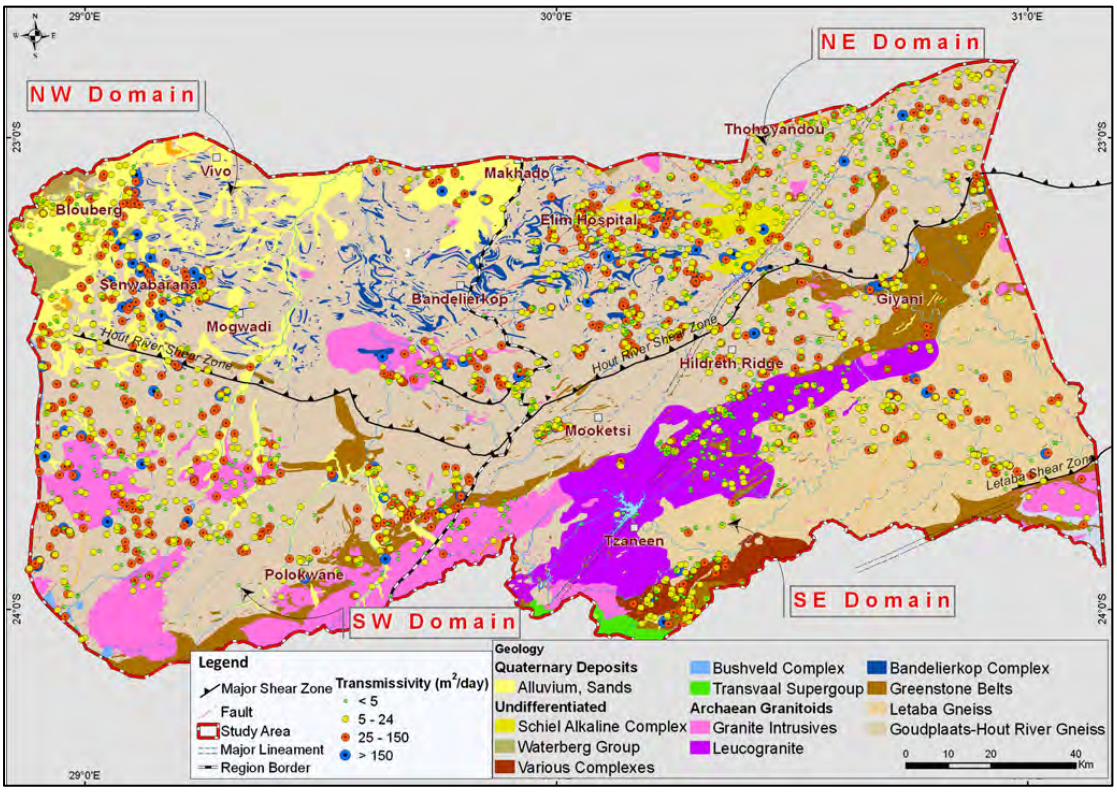

Figure 31: Spatial distribution map of the Holland and Witthüsser, (2011) study area illustrating transmissivity values. Note the Makuleni target site is located just outside the delineated region toward the north of Makhado

Chapter 9: Enhanced Geothermal System economic model

9.1 Model development background

An economic model was developed for a hypothetical EGS pilot plant along the Limpopo Mobile Belt, surrounding the Makuleni village (Figure 32). The model calculates the unit cost of electricity (Levelised Cost of Electricity) and was completed during a summer research fellowship within the Young Scientists Summer Programme (see Appendices). The model focuses on attaining the viability for EGS in South Africa as a function of various geological and engineering parameters equated to determine the total energy capable of being produced, weighed against the total cost required for developing an EGS plant. Short et al., (1995) conducted a similar study for the U.S. Department of Energy and created an evaluation method for energy sources within the U.S. The aim of this research was to standardise the valuation and calculation the viability of a specific energy source. Many of the equations used by Short et al., (1995) still form the basis of energy, and econometric calculations, and similar mathematical formulas are adopted here. Huenges, (2010) provides a detailed account of EGS exploration and development and his broad outline of EGS development is incorporated within this study.

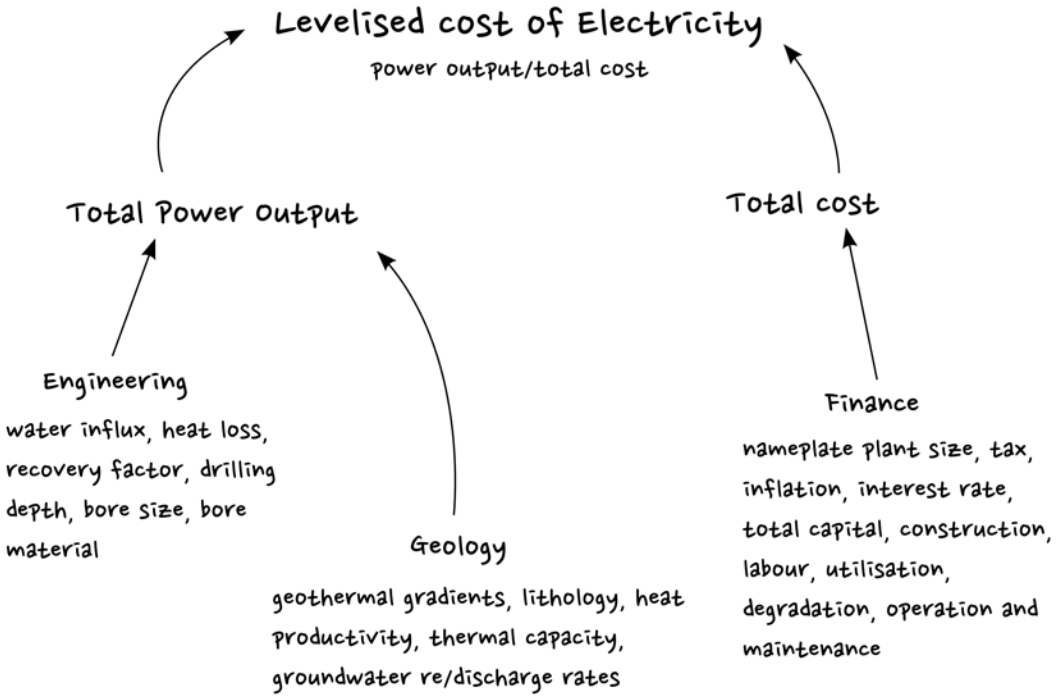

Figure 32: Flow diagram of the economic model structure and various data parameters

The main data sources incorporated within the model include similar EGS projects in Soultz, France (Asanuma et al., 1999; Cuenot et al., 2010; Genter et al., 2010; Muller et al., 2010; Schill et al., 2010; Hébert et al., 2011) the Cooper Basin, Australia (Chopra and Wyborn, 2003; Chopra, 2005; Cooper et al., 2010) and renewable energy research performed by Credit Suisse on several alternative energy sources (Credit Suisse, 2009) and EGS financial modelling by (Sanyal et al., 2007; 2009). Further data incorporated is geological data from extended fieldwork within the Limpopo region and developmental costs of construction and generation of a power plant with data from the African Development Bank (African Development Bank Medupi Power Project Appraisal Report, 2009). The LCOE modelling assumes the development of a conceptualised EGS plant within the Limpopo Mobile Belt of South Africa and is subjected to all financial and economical constraints of development in South Africa and all associated local costs accrued.

The various parameters defined within the scope of this research were incorporated and run through the Levelised of Electricity (LCOE) model. This model was created within Microsoft Excel and aims toward obtaining the economic viability of harnessing EGS within the Limpopo Province. Variations in the geological conditions regarding heat flow, heat productivity, the various lithologies and their thicknesses were taken into account and formulated toward estimating the likely basal reservoir temperature that could be achieved. These factors were subsequently used to estimate the total energy capacity of the plant. Economic parameters consider all costs associated with the construction and maintenance of the hypothesised plant. All economic and financial costs are appended to South African economic rates and standards, as of March 2011.

The hypothesised EGS plant has a nameplate size of 75 MW producing from a triplet well system. A maximum reservoir depth of 6 km is considered with a reservoir volume of ca. 1000 m^3. Two key scenarios are forecasted and include: 1. LCOE without an added REFIT incentive, 2. LCOE with an added REFIT incentive.

Table 2: Input parameters of the LCOE model with the various data sources. Further information in List of Definitions and Table 3 (Appendix A.1) and Table 4 (Appendix A.2)

Parameter	Unit	Amount	Source
capital cost per KW	USD/KW	38,666,367	calculated within the model
nameplate size	KW	75,000	calculated within the model
total capital costs	USD	2,900,000,000	Augustine, 2006; ADB, Appraisal report: Medupi, 2009
lifetime	years	30	Credit Suisse, 2009
O&M per MW	USD/MW	25	calculated within the model
construction time	months	36	Chopra, 2005; Credit Suisse, 2009
utilisation factor	%	95	Chopra, 2005; Credit Suisse, 2009
annual degradation	%	0.5	Chopra, 2005; Credit Suisse, 2009; Genter et al., 2010
tax rate	%	40	SARS, 2011
annual inflation rate	%	6	SA Reserve Bank, 2011
PTC (REFIT)	USD/MW	250	NERSA, 2009
interest rate	%	6	SA Reserve Bank, 2011
yearly payment	USD	26,105,922	calculated within the model
geotherm 1	°C/km	50	geologically modelled
thickness 1	km	2	geologically modelled
geotherm 2	°C/km	25	geologically modelled
thickness 2	km	4	geologically modelled
thermal drawdown	%	0.15	geologically modelled
geothermal heat loss	%	0.5	geologically modelled
number of wells	#	3	Chopra, 2005; Credit Suisse, 2009; Genter et al., 2010
well depth	km	6	Chopra, 2005; Credit Suisse, 2009; Genter et al., 2010
influx temperature	°C	55	Olivier et al., 2008; Tshibalo et al., 2010; Tekere et al., 2011
flow rate	kg/s	50	Chopra, 2005; Credit Suisse, 2009; Genter et al., 2010
aquifer volume	m^3	248,918,838	GRIP Database, 2011
fracture zone depth	m	171	GRIP Database, 2011
fracture zone volume	m^3	59,811,468	GRIP Database, 2011
exploitation volume	m^3	8,100,323	GRIP Database, 2011
natural discharge	m^3	2,395,866	GRIP Database, 2011
natural recharge	m^3	15,141,318	GRIP Database, 2011
drought recharge	m^3	11,032,151	GRIP Database, 2011

9.2 Levelised Cost of Electricity (LCOE)

Levelised Cost of Electricity (LCOE) is a method used to determine the viability of an electricity-generating source. This uses a number of equations that considers all financial constraints related to the preliminary work, to construction, operation and maintenance and finally decommissioning of a plant. The financial factors are then weighed against the total energy and electricity produced. The result is a value that expresses whether an energy source may prove economical or not. The LCOE calculated in this model is expressed as $cents[18] per kilowatt of energy produced within a year ($c/KWh). The interface of the model with input parameters is shown in Appendix A.1: Table 3

The LCOE model depends on the overall costs associated with construction and the operation and maintenance of a prospective EGS plant in South Africa, weighed against the total prospective amount of energy capable of being generated. An outline of the calculations used in determining the LCOE is displayed in Appendix A.3: Table 4 and Table 5. This can be defined by the general equation:

$$\mathbf{LCOE} = \frac{\mathbf{TC}}{\mathbf{TE}}$$

Equation 1: LCOE = levelised cost of electricity; TC = total costs; TE = total energy

A prominent cost factor affecting the model is associated with the initial planning and development of the EGS plant. This includes all costs associated with prospecting phases before and during the construction. Several of the key factors are highlighted below:

9.2.1 Labour costs

Developing and construction costs used within the model have been estimated from similar development of coal-fired power plants within South Africa (African Development Bank, project appraisal report: Medupi, 2009). This allowed for accurate estimation of South Africa civil costs associated with labourers, including all transport and housing allowances and other South African labour-related regulations. (See appendix A.2: Table 4)

[18] Dollar value calculated as based on the rate in March 2011.

9.2.2 Generation costs

The cost of the turbines and all electrical equipment used for electricity generation and grid parity cost for feeding electricity back into the national energy grid are also incorporated within the model. In addition, another highly prominent cost factor involves the initial deep drilling and hydraulic fracturing processes (see Appendix A.2: Table 4). These values have been estimated using similar deep drilling project cost in the U.S. and other similar international EGS projects (Augustine, 2006). The total capital cost per KW of electricity produced is formulated as follows:

$$\mathbf{C(kw)} = \frac{\mathbf{C}}{\mathbf{N}}$$

Equation 2: C(MW) = capital cost per MW of electricity; C = total capital costs; N = nameplate plant size

9.2.3 Operation and maintenance costs

The operation and maintenance parameter accounts for continuous cost applied throughout the lifetime of the plant. This is associated with the various phases of planned maintenance and operational downtime thereof. This is calculated using a defined operation and maintenance cost per year weighed against the total energy production of that same year. This considers both the South African tax and inflation rates and is equated as follows:

$$\mathbf{OM} = \sum_{\mathbf{t=2}}^{\mathbf{t=n}} \mathbf{OM(t)} * \mathbf{(1+i)} * \mathbf{P(t)} * \mathbf{(1-T)}$$

Equation 3: OM = overall operation and maintenance; t = year; n = lifetime of the plant; OM(t) = defined operation and maintenance value per MWh; i = South African annual inflation rate; P(t) = annual electricity production; T = South African tax rate

9.2.4 Plant utilisation and efficiency

The utilisation factor illustrates the overall efficiency of the plant by equating the plant utilisation with an annual depreciation associated with turbine and well corrosion. This factor has an influence on the overall efficiency of the plant and the sustainability of energy production over the lifetime of the plant, and is calculated as follows:

$$\mathbf{U} = \sum_{\mathbf{t=2}}^{\mathbf{t=n}} \mathbf{U(t)} * \mathbf{(1 - D)}$$

Equation 4: U = overall plant utilisation factor; U(t) = defined yearly utilisation factor; t = year; n = lifetime of the plant; D = annual degradation of the plant

9.2.5 Renewable energy production incentive

The initial development and shift toward renewable energy in South Africa led to the National Energy Regulator of South Africa introducing the first phase of a renewable energy feed-in tariff (REFIT). This provides incentives for projects producing renewable energy and feeding it back in the national energy grid. Initially, provision was only given to wind, hydro and certain forms of solar renewable schemes. These forms of renewable energy were included on the basis that they had been investigated and further developed with pilot projects providing promising results. More recently however, the second phase of the REFIT scheme (National Energy Regulator of South Africa, 2009) will look into the incorporation of other renewable schemes, including geothermal. The inclusion of geothermal within the REFIT scheme will have a major implication on the overall cost of the any geothermal energy plant and therefore a range of possible production tax credit incentives is incorporated within the model and calculated as follows:

$$\mathbf{PTC} = \mathbf{PTC(t)} * \mathbf{E(t)} * \mathbf{1000}$$

Equation 5: PTC = overall production tax credit; PTC(t) = defined yearly production tax credit; E = electricity produced

9.3 Total electricity production

The total amount of potential electricity produced in an EGS plant relies on two important factors: 1. The geological variants affecting the target site. 2. The engineering parameters associated with harnessing the energy.

9.3.1 Geological parameters

The geological parameters depend mostly on the lithological profile underlying the target site. This extends from the surface to the maximum depth of the geothermal reservoir. This profile determines the variation in heat productivity, conductivity and overall geothermal gradient along the length of the wells and into to the geothermal reservoir. The calculations are shown in Appendix A.3: Table 6. A geological profile that allows for successful EGS harnessing requires basal plutonic rocks that have a high concentration of heat producing elements and an extensive fracture network. The plutonic rocks require a thick overlying sequence of sediments that insulates the heat produced. The overlying sediments attains its own high heat flow signature through conductive contact with the underlying plutonic rocks, in addition to commonly having its own internal heat production. This results in a geothermal disparity between the sediments and plutonic rocks. This disparity leads to fluctuation in the heat flow profile, factored into the model. The heat flows are simplified according the targeted plutonic rocks and overlying insulating sediments. This results in a 2-phase heat flow profile that fits tangential to the respective heat flows of the plutonic and sedimentary rocks.

An adequately porous reservoir is required within the target plutonic rocks and needs to have the capacity of sustaining thorough fluid circulation. Thorough circulation is necessary to allow the geothermal fluid to be heated to required critical levels. The system should ideally remain closed and sustain an adequate pressure gradient between the production and geothermal wells. The available heat flow data was used together with geological thicknesses, predicted well depth and a thermal loss coefficient of the surrounding geology to determine the expected basal reservoir temperature, calculated as follows:

$$\mathbf{Tb} = \sum_{\mathbf{n=1}}^{\mathbf{l=n}} \frac{(\mathbf{G} * \mathbf{t})}{\mathbf{d}} * (\mathbf{1} - \mathbf{L})$$

Equation 6: Tb = expected basal reservoir temperature; l = lithology; n = number of lithological units; G = geothermal gradient; t = thickness of the lithological unit; d = well depth; L = thermal loss coefficient

9.3.2 Engineering parameters

The engineering parameters consider the amount of heat available for exploitation and estimate the total amount of electricity capable of being harnessed. This calculation is one of the most important as the total amount of energy represents the nameplate plant size, and this value defines the overall efficiency and viability of the plant. Due to the lack of adequate heat flow data within the Limpopo Province, the model incorporates several possible basal reservoir temperatures. These basal reservoir temperatures are based on the surrounding geothermal gradients and variations in the possible geological profile.

Further input parameters include the initial and final temperature of the working fluid together with the heat capacity and the overall flow rate within the system. Appendix A.3: Table 7 outlines the calculations used to determine the total energy that could be harnessed. Variation in the composition of the working fluid can plays a major role in the overall energy production. The model assumes the use of water as the main geothermal fluid. However, experiments suggest that supercritical CO_2 as a working fluid decreases the boiling temperature and pressure and has an influence on the overall efficiency of the system. An additional factor is also considered for the total heat loss during the extraction process. This is a factor of the total well depth and the total heat productivity of the surrounding geology. These factors are equated in a modified version of the heat-energy theorem, as follows:

$$\mathbf{Energy} = \left[\mathbf{R} * \mathbf{1000} * \mathbf{C} * \left(\left(\mathbf{Tb} * (\mathbf{1} - \mathbf{Rf})\right) - \mathbf{Ti}\right)\right] * \mathbf{0.001}$$

Equation 7: R = system flow rate; C = heat capacity factor; Ti = input temperature of the working fluid; Tb = reservoir temperature; Rf = final recovery factor

9.4 Groundwater sustainability

Harnessing geothermal energy from the EGS mechanism requires a substantial amount of water for operation. Failure to create an entirely sealed reservoir will result in poor water recovery rates and require continuous addition. An economically viable reservoir can be up to 1000 m^3 in volume with flow rates reaching 50 l/s. These factors place a large burden on water supply, which further needs to consider the population and other industrial and agricultural usage. Developing a preliminary groundwater sustainability model is vital for

calculating the impact an EGS plant may have on the surrounding water supply and population needs.

Hydrogeological data was acquired from the Department of Water Affairs and the Groundwater Resource Information Project in the Limpopo Province. The model estimates the value of water required to run the proposed EGS plant and weighs it against the current local exploitation values, together with the natural recharge and discharge rates. This includes periods of normal rainfall, and periods of drought. These calculations are illustrated in more detail in Appendix A.3: Table 6.

A population coefficient is also taken into account, and considers an increase in the surrounding population. Population growth will impact the water supply and possible exploitation levels. The idealised EGS system is a closed system, with high efficiency and minimal water loss. An additional coefficient is however added within the equation to account for water loss associated with the pumping and generation of energy. The abovementioned parameters are equated as follows:

$$\mathbf{W} = \sum_{\mathbf{t=1}}^{\mathbf{t=n}} [\mathbf{Rn} - \mathbf{Ry} - \mathbf{Gl} - \mathbf{Dn} - (\mathbf{Dp} * (\mathbf{1} + \mathbf{ip}))]$$

Equation 8: W = estimated required water supply; t = year; n = lifetime of the plant; Rn = natural recharge rate; Ry = yearly plant water flow rate required; Gl = geothermal water loss coefficient; Dn = human population required discharge; ip = human population increase factor over plant lifetime

Chapter 10: Results

10.1 Enhanced Geothermal System Levelised Cost of Electricity

10.1.1 Model results vs. other models

The LCOE modelled results of a proposed EGS plant within the Makuleni target site are shown in Figure 33 and compared with other international EGS projects:

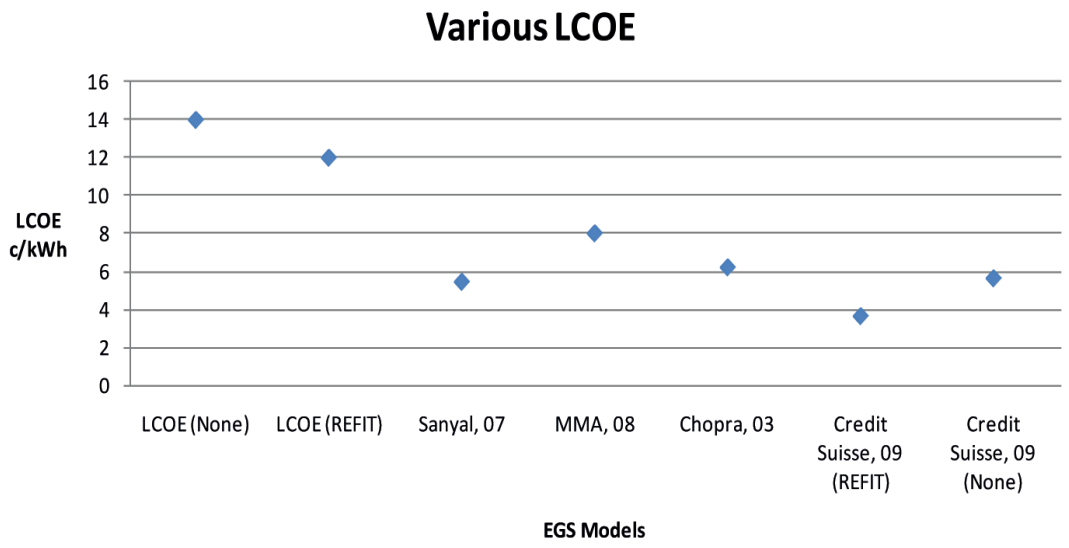

Figure 33: A graph comparing the calculated LCOE result within this study against other similar economic models of EGS

The first result as represented by "LCOE (None)" is the modelled result for a scenario excluding any Renewable Energy Feed-In Tariff (REFIT). This would best simulate an EGS plant under the current scheme in South Africa, lacking any REFIT or other tax incentive for geothermal energy.

"LCOE (REFIT)" is the same model parameters, however includes a REFIT of $25/MWh. This incentive is the standard REFIT for EGS in Germany and is inclusive of a carbon tax credit for renewable energy production.

Sanyal, (2007) represents the modelled LCOE results from the Desert Peak EGS plant in Nevada, USA.

MMA, (2008) represents the modelled calculations performed by MacLennan Megasanik Associates for the Australian Geothermal Association during their continued research into the viability of developing several EGS plants within Australia.

Chopra, (2003) are the results as determined for the first successful EGS project in the Cooper Basin, South Australia.

The final two points illustrated are the modelled results as determined by a Credit Suisse report on renewable energy with the first point including a REFIT and carbon tax credit, which is excluded from the final point.

10.1.2 Calculated energy potential versus other renewables

The calculated LCOE and energy capacity of this study is compared with other energy options, including renewable and non-renewable sources in Figure 34. The LCOE of EGS in South Africa considers both the REFIT and non-REFIT scheme against coal, gas and nuclear forms of energy as calculated by Credit Suisse (2009). The red points represent the LCOE of each form of energy, while the corresponding blue points represent the total energy capacity of each source.

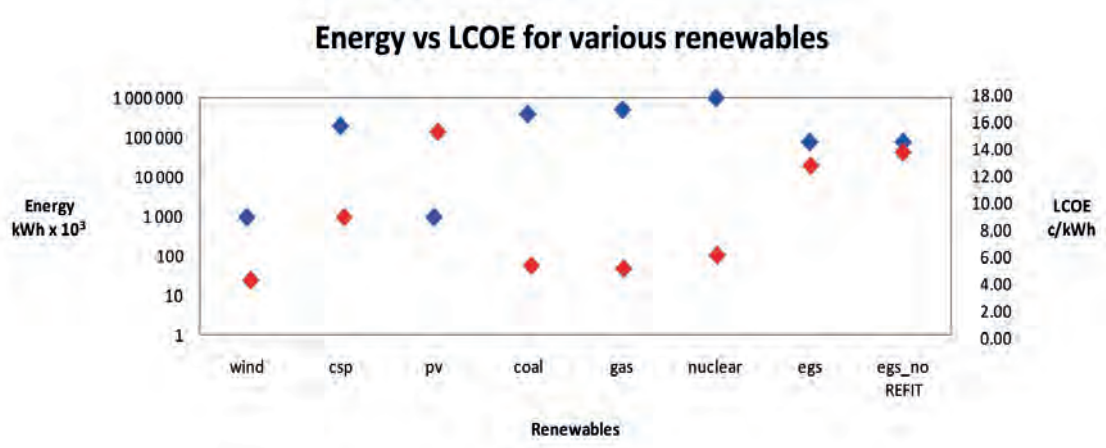

Figure 34: A comparison of the calculated LCOE against other renewable energy options. Renewable energy calculations determined by Credit Suisse, (2009)

10.2 Model sensitivity analysis

10.2.1 Energy potential versus depth

The effect on the LCOE of an increase in the basal reservoir temperature and the consequential increase in the overall energy capacity of the system is shown in Figure 35. The red curve represents the scenario excluding REFIT, while the blue curve illustrates a scenario including a $25/MWh REFIT. This calculation restricts the drilling depth to 6 km with no further variation. The temperature range best estimates the expected basal reservoir temperature as determined within the model.

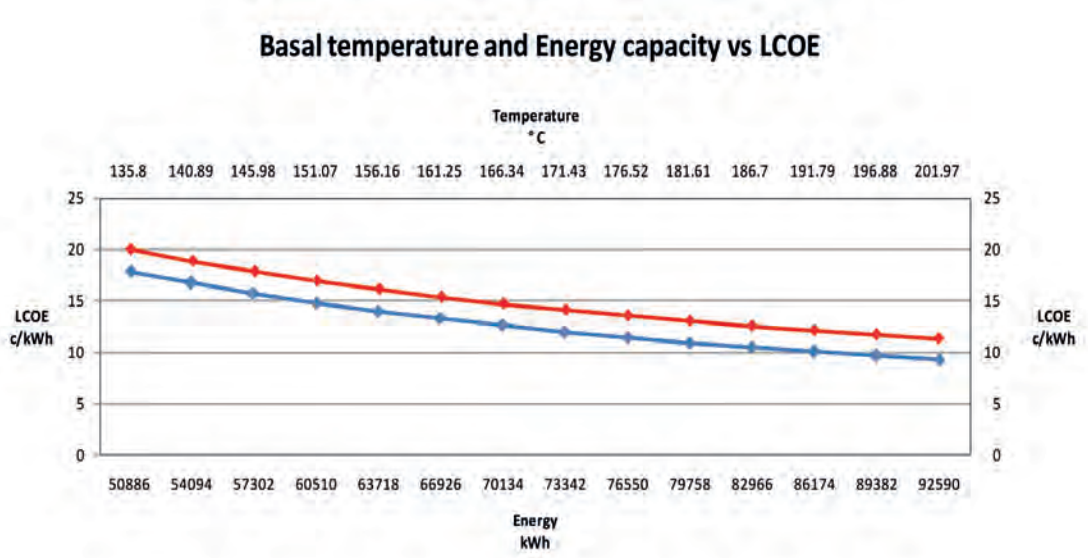

Figure 35: A graph showing the effect on the LCOE with an increase reservoir temperature, and consequential increase in energy capacity. The red line represents a scenario without an added REFIT; the blue line represents a scenario with an added $25/MWh REFIT

10.2.2 Cost versus incentives

Renewable energy is an expensive alternative source of energy that relies on governmental incentives to be deemed significantly economically viable. The effect of a REFIT on the LCOE is shown in Figure 36. The LCOE represents the as absolute value of the incentive the government is expected to pay a corporation for the production of renewable energy.

With no current concession provided for the production of renewable energy through geothermal mechanisms, this estimates the effects of a REFIT range from 0 to a maximum of $30/MWh (300$c/KWh) of energy produced.

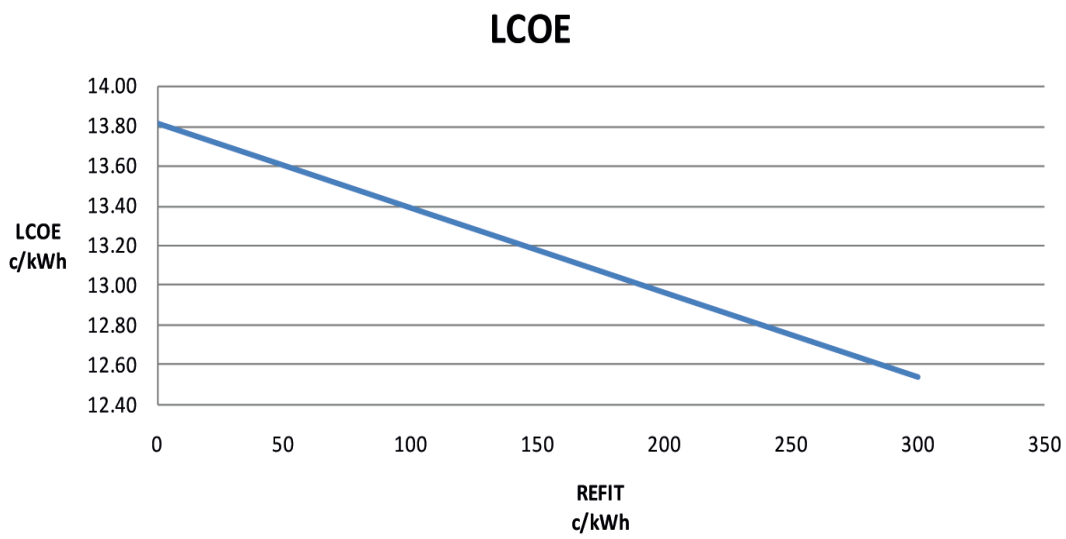

Figure 36: A graph showing the effect of an added REFIT on the LCOE

10.2.3 Cost versus drilling depth

The effect of an increasing drilling depth on the LCOE is shown in Figure 37. This considers increasing drilling costs with depth as determined from Augustine, (2006). These values are compounded with current and previous inflation rates to attain a comparable evaluation for the current time period.

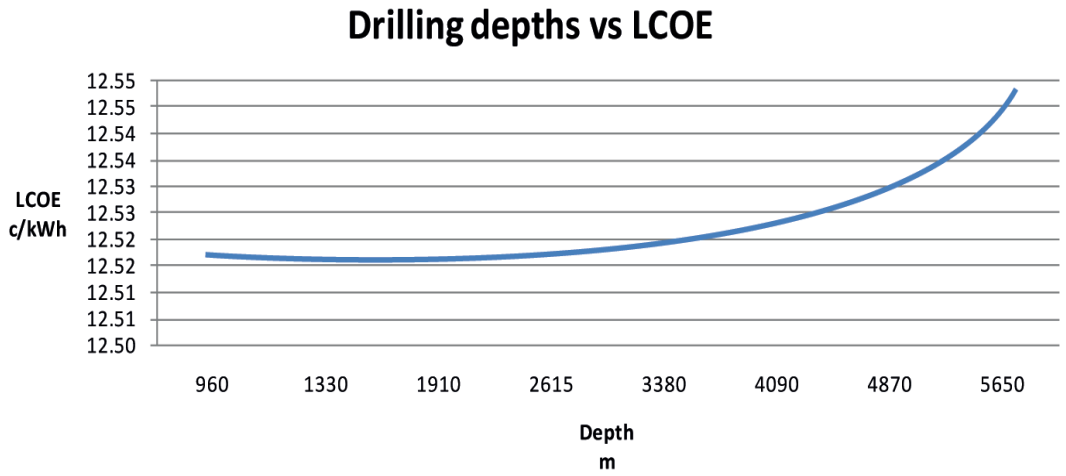

Figure 37: A graph showing the effect of increased drilling depth on the LCOE

10.3 Enhanced Geothermal System sustainability

The model calculates total energy capable of being produced from any production well, at any depth and for a certain basal reservoir temperature. However, over the lifetime of the plant a thermal drawdown of the reservoir could result in a decrease of the total energy production. Figure 38 shows the calculated result for the total reduction in heat as indicated by the red curve, against the consequential decrease in the overall energy production as indicated by the blue curve. The thermal drawdown rate is estimated according the age and heat productivity of the Limpopo rocks and further appended against those of other EGS granites.

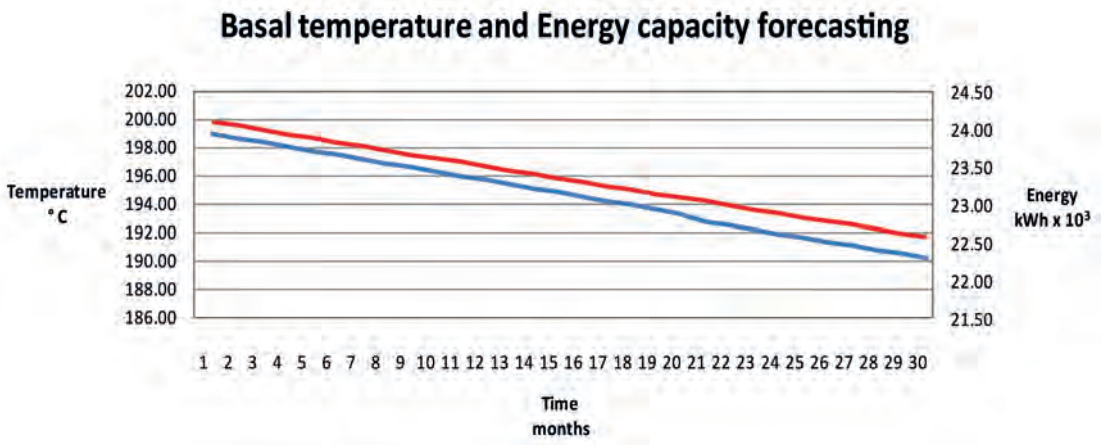

Figure 38: A graph showing the forecasted decrease in reservoir temperature (Red) and the associated decrease in energy production (Blue)

10.4 Groundwater sustainability

Water is the main constituent of the working fluid within the proposed EGS plant system and therefore forms an important component within the model. The Makuleni target site is situated where one of the main potable water sources is groundwater. The overall effect of an EGS plant on the groundwater volume is calculated in the model and the results are displayed in Figure 39.

A large concentration of the water exploited for human use is attained from groundwater aquifers stored within fracture zones and incorporated below surface sand layers. Using data from the Department of Water Affairs[19] and the Groundwater Resource Information Project[20] that monitors several thousand

[19] Available from: Department of Water Affairs, Limpopo: www.dwaf.gov.za.
[20] Available from: http://griplimpopo.co.za.

boreholes throughout the Limpopo Province. The model calculates the overall amount of water being exploited for human and industrial usage, and weighs this against the overall recharge rates. Both periods of drought and flooding are also included. These calculations are forecasted over the lifetime of the EGS plant, including a coefficient for human settlement increase associated to the development of the Limpopo Province.

The results of this forecast is illustrated by the red line in Figure 39, while the overall required water consumption of the EGS plant is illustrated by the blue line. Based on these results the idealised closed system of the EGS plant will be sustainable over its lifetime.

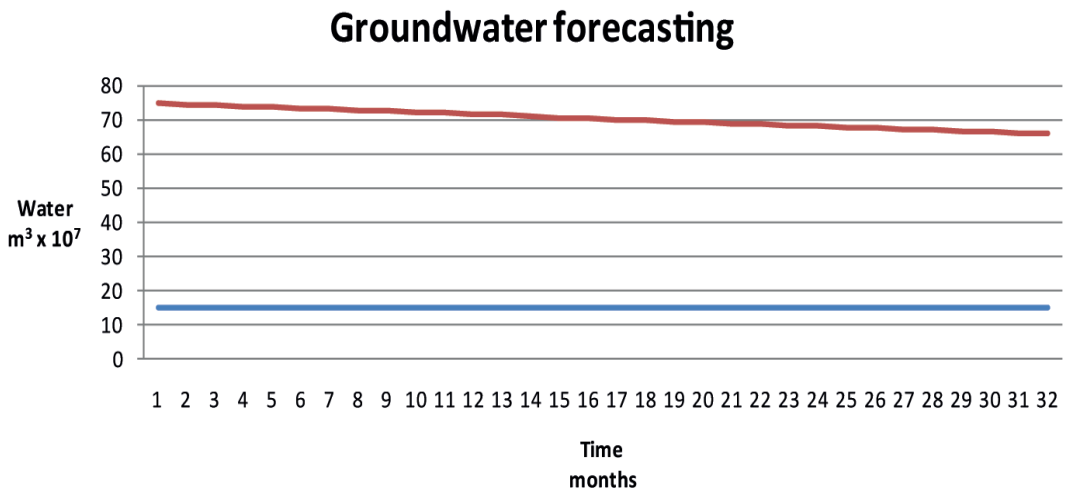

Figure 39: A graph illustrating the forecasted effect an EGS plant in the Makuleni village will have on the groundwater supply over the lifetime of the plant. The red line represents the total recharge rate and the blue line represents the water supply required by the plant

Chapter 11: Discussion

11.1 Enhanced Geothermal System in South Africa

11.1.1 Summary and lessons of previous EGS projects

While EGS has only been developed over the last 25 years, numerous lessons have been learnt from the various studies conducted in the past. Early EGS projects benefitted from "hot spots" related to recent volcanism, with target sites, for example, at the base of calderas (i.e. Fenton Hill, Hijiori and Ogachi). The French and Australian projects however aimed to explore the possibilities of developing this technology in areas devoid of volcanism. They proposed the use of ultra-deep reservoirs in crystalline rock. The crystalline rock would have a high concentration of heat producing elements and subsequent high degrees of heat flow associated thereof.

The Los Alamos National Laboratory was the first to develop the concept of harnessing energy from hot dry rocks (West, 1974; Tester and Albright, 1979; Murphy et al., 1981). From this research, it was soon realised that the heat stored in deep crystalline rocks, notwithstanding those in areas with active volcanism, might supply what appears a tantamount of infinite renewable energy, capable of sustaining the world's energy needs. In response, and together with several partners, the Fenton Hill project was launched and maintained a singular aim of realising the potential of the hot dry rock concept. This project showed great success and continued further to provided a basis for preceding projects. Between the consequential projects in the United Kingdom (Batchelor, 1982) and Japan (Brown et al., 1999; Kuriyagawa and Tenma, 1999), as well as other projects in Germany (Clauser, 1997; Schellschmidt et al., 2010) and Switzerland, the process of hydraulic fracturing was better developed and incorporated. The importance of developing an adequately fractured reservoir was highlighted and most projects encountered numerous problems with controlling the reservoir growth. Common problems stemmed from the overall growth of the fractured reservoir that generally expanded in unexpected directions during hydraulic fracturing, contrary to what models had predicted (Parker, 1989; Shin et al., 2000). This was often the result of the local stress regime being initially modelled incorrectly, as was experienced in the United Kingdom and Japan. Understanding the overall, and more importantly the deep-seated stress regime became of the utmost importance. The underlying stress

regime controls the design and development of the geothermal reservoir and the success generating an adequately fractured and porous conduit (Albright and Pearson, 1982).

Another common issue associated with the fractured network was the overall increase in the system impedance, as encountered in France (Genter et al., 2010; Baillieux et al., 2011). This occurred due to a change in the overall flow rate. It was discovered that the overall porosity and jointing within the fractured reservoir showed a high sensitivity to variations in the system flow rate. In the case where the flow rate was decreased, spacing between joint sets and overall fracture porosity also decreased substantially. By contrast, when the flow rates were kept high for prolonged periods, the reservoir continued to grow, often leading to high concentration of fluid loss. This was evident in the Japanese project where fluid losses amounted to as much as 70 % and was attributed to large variation of the overall flow rate. Many of these earlier problems were addressed by the beginning of the Soultz project (Baria et al., 1998; 1999), and later the Cooper Basin project (Chopra and Wyborn, 2003).

11.1.2 The Makuleni EGS target site

The present day success of the Soultz and Cooper Basin projects provide a basis for possible incorporation of EGS within South African renewable energy research and development. This could be potentially viable along one of the relatively high heat flow zones in its ancient mobile belts. Based on available heat flow data within the Kaapvaal Craton, the Namaqua Natal Mobile Belt (NNMB), Cape Fold Belt (CFB) and Limpopo Mobile Belt (LMB) displays the highest heat flow in South Africa (Jones, 1987; 1992). These display relatively high concentrations of radiogenically enriched granites providing a heat source (Andreoli, 2006). In addition, having suffered a complex deformational history (Thomas et al., 1994; Holzer et al., 1998), some of these granites and gneisses contain an ideal natural fracture system, and complex stress regime associated to continental collisions and intra-continental deformation. These factors would indicate that South Africa has the potential target sites to possibly harness geothermal energy from EGS. This study considered the Makuleni and its surrounding villages on the border between the southern marginal and central zones within the LMB as a hypothetical target site for EGS exploration. To better ascertain the economic viability of such a venture, an economic model was developed to calculate the unit cost of electricity generated from this hypothetical plant. This model considers various economical, geological and engineering parameters constraining the production of energy through EGS.

The LMB target site is similar to the Cooper Basin target site, with a deep basement sequence of granites and gneisses and showing evidence of a relatively high concentration of radioactive elements (Kramer et al., 2001). However, the concentrations at the Cooper Basin far exceed those of the LMB. The Soutpansberg Group overlies the basement Limpopo gneisses and together these contribute toward relatively high upper crustal heat flow. This high heat flow is evident with the numerous hot springs, none more than the Siloam hot spring attaining a maximum surface temperature of ca. 70° C near the Makuleni village (Nyabeze et al., 2010; Tekere, 2011). The granites in the NNMB show higher heat flow signatures that those of the LMB. In contrast, the LMB is overlain by a thick insulation sedimentary sequence in the form of the Soutpansberg (Bumby et al., 2004). While thick Karoo rocks do cover most of the NNMB, those areas providing high heat flow signatures are devoid of any cover. Additional work throughout the NNMB, especially areas with thick Karoo cover, may provide further potential EGS sites in South Africa.

Based on a Quantum GIS spatial analysis of the target area and surrounding villages, an initial pilot plant producing a total of 1 MW of energy would be sufficient to supply the village households with renewable energy, however constrained by a broader lack of adequate infrastructure of many households. Since the expansion of the energy grid within the rural regions of the Vhembe District Municipality, the expected costs associated with connecting the geothermal plant to the National Energy Grid will be minimal. Assuming the success of any prospective pilot plant and the development of a full scale 75 MW EGS plant as modelled, the target area and surrounding villages will greatly benefit from continuous employment and further economic benefits associated with a possible renewable energy feed-in tariff. The model estimates the generation of the 75 MW of energy to be produced from a minimum of 3 production wells from a single large reservoir at a maximum depth between 5-6 km. The reservoir is expected to reach a size of 1000 m^3 and be restricted to a maximum water loss rate of 10 %. The development of a 75 MW EGS plant will also have the potential of saving ca. 1.5 gCO_2/KWh. This highlights its potential toward South Africa's mitigation and adaption of climate change.

11.2 The cost of a 75 MW EGS plant in South Africa

Considering the exclusion of any REFIT incentives, the LCOE is calculated with the energy cost to be greater than 14 $c/KWh. 7 $c/KWh more than the current coal generated electricity. However, under the same circumstances, with an added REFIT of $25/MWh, comparable with the REFIT regulations in Germany, the LCOE drops to approximately 12 $c/KWh, which becomes a comparable renewable energy option i.e. only 1 $c/KWh more than solar photovoltaic, however having up to 25 MW lower energy capacity. When considering how these results weigh against other similar models for similar EGS plants, the results are comparable with calculated case scenario deviating no more than 4 $c/KWh from other model projections. As the combat against climate change intensifies nations will face stringent penalties for failing to meet GHG reduction targets. The legal implementations of GHG reduction is becoming more aggressive following the COP18 summit, especially when considering the amendment made to the Kyoto Protocol, extending it for another 8-year commitment period. This amendment occurs together with a newer climate change agreement expected to be resolved in 2015. The 2015 resolution is expected to have legal implementations likely resulting in financial penalties for big GHG emitters, like South Africa. This will further force the cost of all forms of renewable energy sources in South Africa to decrease.

The calculated LCOE of the hypothetical EGS plant in the Makuleni and surrounding villages suggest that it would be one of the most expensive renewable energy projects in South Africa. However, assuming its success, it would have the capacity to produce a large concentration of renewable energy, second only to a large-scale concentrate solar power (CSP) project. However, it should be noted that CSP does not only provide a larger energy capacity, but it provides it at a substantially lower cost. Another aspect to bear in mind is that a large scale CSP plant generating 75 MW of energy will require a total surface area of 1,500,000 m^2 (Mendelsohn et al., 2012), while the Soultz EGS plant covers an area of 105,000 m^2 having a lesser impact on land usage.

Statistics from the Nuclear Energy Institute, (2012) illustrates that the U.S. has avoided over 11 million metric tons of CO_2 emissions from the implementation of nuclear energy. Despite attaining a high level of energy security, the U.S. has also devoted 35 billion dollars toward a nuclear spent fuel fund that still has no long-term storage solution. In addition, since the Fukushima disaster several nations have signalled their intention to shift away from nuclear. These include the U.S., Germany, France and Japan, all of which fall within the top 5 nuclear producing

nations. Presently, this has resulted in greater research and technological advances made in the fields of renewable energy, including EGS.

The high cost of the EGS plant calculated in this model assumes the prospect of an EGS plant in an area with a relative lower heat production and heat flow rate than other international target sites. Many of these sites boast some of the highest heat flow in areas lacking any active volcanism, i.e. the Cooper Basin, Australia. With the lower heat flow rate estimated within the target area, the model is based on the calculations assuming a drilling depth between 5-6 km. Deeper drilling should cause a substantial increase to the overall project costs. The model suggests that continued increase of the drilling depth below 2 km results in an steeply increasing trend of the LCOE, however this increase from 2-6 km only results in an overall 1-2 $c/KWh.

The total energy capable of being produced from an EGS plant within the LMB depends predominantly on the basal reservoir temperature encountered. With a shortage of heat flow and geothermal gradient data, the model relies on information as gathered from the surrounding hot springs and high radioactive granites to attain predictions of reservoir temperatures against depth. The calculated basal reservoir temperature illustrates that EGS will only be viable and sustainable for a lifespan of 30 years at the Makuleni target site if a basal temperature of between 150-200° C is attained at a depth of between 5-6 km. The closest hot spring to the Makuleni target site is found along the Siloam Fault. Here groundwater naturally flows down to a maximum depth of approximately 2 km and returns to the surface at a temperature of ca. 70° C. This provides evidence suggesting the anomalously high heat flow in the region and furthermore corroborates the modelled calculations that suggest the minimal required basal reservoir temperatures can be reached within 6 km.

11.3 LCOE model sensitivity

The most prominent factor affecting the energy capability of a prospective EGS system is the maximum reservoir temperature. In turn this directly influences the depth of drilling, which makes it a controlling factor on the LCOE. In addition, with the lack of recent volcanism in the LMB, a geothermal reservoir at a greater depth is required to maximise the amount of energy producible. The cost of drilling increases substantially and is further compounded with the cost of additional deep hydraulic fracturing to increase reservoir permeability. The model does however estimate that the cost of drilling affects the LCOE to a lesser extent than the addition of a REFIT incentive. An added REFIT provides a cost

relief for energy produced and therefore has the ability of deeming the project viable in the event of high energy production rates.

An increasing government REFIT causes the overall LCOE to decrease steeply as indicated on Figure 36. When considering an appropriate REFIT scheme for inclusion toward the possible EGS plant, various figures were incorporated within the LCOE modelling and showed that the most appropriate REFIT value is one similar to that in place in Germany, where an allocated amount of $25/MWh is applied. Geothermal is not currently under consideration within the National Energy Regulator of South Africa (NERSA) framework of consideration, this is mostly due to the lack of commercial geothermal energy projects in the country. A provision is however in place to include geothermal and other renewable energy options that are not currently under consideration and in the event of successful commercial application, a much larger governmental tax incentive would be considered. The development of renewable energy is becoming aggressive and the technology of low-enthalpy EGS is advancing toward the use of low temperature resources. With certain organic fluid compositions and specific fluid flow rates, EGS plants can become economically viable at temperatures as low as 100 (Kohl and Speck, 2004), making it more probabilistic in many global regions.

11.4 EGS sustainability in South Africa

Based on the data of the Department of Water Affairs and the Groundwater Resource Information Project in the Limpopo Province, the average rate of aquifer recharge is adequate to sustain an EGS plant in the Vhembe District Municipality within the Limpopo Province. Furthermore, the modelled results, based on the average recharge and discharge rates as experienced during possible periods of drought, compounded with a coefficient for the increase in demand on the groundwater supply over the lifetime of the plant, shows favourable results for sustaining an EGS plant and having a low impact to the surrounding communities. Assuming a regular thermal decrease in the basal reservoir, the model predicts that there would not be a great drop in the overall production temperature of the geothermal reservoir over a period of 30 years, and would amount to less than 1 MWh of the total energy production.

Chapter 12: Conclusion and recommendations

Under the threat of climate change the international community is becoming aggressive in shifting toward alternative energy sources. This is spurred on through the results of numerous Conferences Of the Parties, or COP meetings. Through all their slow progress and apparent failures, it was at the COP 17 conference where first signs of strict regulations were seriously discussed for nations failing to meet GHG reduction targets. Most developed nations have already succeeded in reducing their GHG emissions while maintaining a high level of energy security. However, this has been largely due to the accelerated development of nuclear energy. The lack of adequate facilities for the storage of spent nuclear fuels is a large concern, however, of even greater threat is the ever-present danger of nuclear disaster. This was none more evident than at Chernobyl and even more disastrous, Fukushima. This brings two main factors to light: 1. The importance of reducing GHG emissions and accelerating the combat against climate change. 2. The implementation of safer alternative energy sources.

South Africa is an economic powerhouse in Africa and has since been grouped within the BRICS group of nations of emerging economies globally. A side effect of this economic growth is that South Africa has also become the leading GHG emitter on the African continent and the 12th largest CO_2 emissive nation in the world. This occurred because of South Africa's large reliance on coal-generated forms of energy. The South African Government has signalled the nations intent toward the combat against climate change. This has taken the form of various policies and regulations for, not only research and development of renewable energy, but also their implementation. An example of this is the White Paper on Renewable Energy, (2003; 2012), which emphasises the need for renewable energy development. Eskom's large-scale photovoltaic water heating system for houses, together with regulations for the implementation of such technology to all new building projects clearly illustrates the nations course of action.

Despite the intent of the South African Government, the country still lacks adequate energy security. Energy security plays a vital role for further economic and social development and with South African renewable energy in an infant stage, the Energy Sector has licensed the construction of two new large-scale coal-fired power plants. These plants will increase South Africa's energy production with another 8000 MW of energy, but this will also prove detrimental to the nations combat against climate change. With consensus on the financial

burden countries will be faced with expected by 2015 and fully implemented by 2020, South Africa can expect stiff penalties for increasing CO_2 emissions.

This thesis considers the possibilities of implementing EGS as an intermediary solution as South Africa shifts toward larger scale renewable energy generation. Current renewable projects that include wind, hydro, solar and biomass will not be capable of sustaining South Africa's energy needs alone. The heat stored within the Earth is thought to contain enough energy to sustain the world's energy requirements. While many areas devoid of active volcanism and tectonism have not considered tapping into the Earth's heat energy, EGS provides a mechanism to exploit the low-enthalpy energy of South African "cool" geology.

To ascertain the possibilities and probabilities of South Africa considering EGS as an alternative energy source this study develops an economical model based on net present values. This model considers a hypothesized EGS plant in the Makuleni village, Vhembe District Municipality, Limpopo Province. This area has numerous fault-controlled hot springs recording the highest surface temperatures in the country. While these temperatures are far from capable of hydrothermal energy (>200°), they do allow for low-enthalpy geothermal mining (>100°). The hypothesized EGS plant is estimated to produce 75 MW of electricity over a period of 30 years. Based on a spatial analysis, this would suffice for the surrounding communities and have a surplus that could be fed back into the National Energy Grid.

LCOE calculations in this thesis suggest that the cost of an EGS plant in South Africa would be very expensive (14 c/KWh), e.g. more than double that of conventional coal-fired energy (7 c/KWh). However, when adding a REFIT incentive, the cost decreases substantially. In addition, when an accord is reached on financial penalties countries will have to face for failure to decrease their GHG emissions, South Africa will be looking at expanding the renewable energy development beyond wind, hydro, solar and biomass.

This research can conclude that: Enhanced Geothermal Systems in South Africa is possible and could provide an intermediary solution, initially for 30 years as South Africa makes further progress in a long-term shift to renewable energy. In addition, research shows that EGS has the potential for simultaneous carbon sequestration. This could further decrease South African GHG emissions and curb impending penalties for the failure to do so.

From this research several key recommendations can be drawn:

- In light of the fact that global fight against climate change is becoming more aggressive and developing nations will not be exempt from new legislation against failure to meet GHG reduction targets. South Africa will have to investigate the economic, social and environmental cost of being the leading carbon emissive nation in Africa.

- As an emerging economy of the world, South Africa will have to shift from traditional coal-generated forms of energy and implement large-scale renewable energy technologies.

- Enhanced Geothermal Energy in conjunction with a binary generation system can generate energy from low-enthalpy sources and has the possibilities of simultaneous sequestration. This could be a technology assisting in South Africa's shift to renewable energy security.

- EGS is a very costly form of renewable energy; its viability relies on governmental tax incentives.

- South Africa's geology, in general, of the Kaapvaal Craton in particular has a relatively cold heat flow signature with a thick underlying mantle keel. However, there are zones with areas of higher heat flow. These areas could form the ideal location for low-enthalpy EGS exploitation.

- There is simply not enough crustal heat flow data in South Africa to adequately define the quantitative viability of EGS with a high level of accuracy. This report relies on measurements made mostly in the 19th century, and could subsequently be over or underestimating the true value of EGS as a resource in South Africa. Therefore, further research and especially data acquisition is required towards further exploitation and potential development of the first pilot EGS plant in Africa, to truly ascertain the value of EGS in South and the rest of Africa.

Acknowledgements

I would like to provide my greatest appreciation to Professor Maarten de Wit for allowing me to perform this research and his continuous support and assistance throughout this period. I wish to extend my thanks for the unwavering funding awarded by the Department of Science and Technology, National Research Foundation, and the !Khure Afrika and Inkaba ye Afrika programmes. Without the above-mentioned assistance, this research would not have reached fruition.

I would also like to thank and mention the International Institute for Applied Systems Analysis and my mentor Professor Tony Patt who assisted me throughout the economic modelling, forming the backbone of this research. I would also like to mention my fellow peers who participated at the Young Scientists Summer Programme in Vienna for their continuous support and assistance.

Finally, I would like to especially thank my family for their positive influence, and my colleagues at the Council for Geoscience, Limpopo Unit for their continuous support throughout my tenure.

References

Adams, M.C., Moore, J., Bjornstad, S., McCulloch, J., Buck, C. (2005). Fluid-mineral equilibria and injection in EGS – Effect of injecting groundwater. Proceedings: 30th Workshop on Geothermal Reservoir Engineering Stanford University, SGP-TR-176

African Development Bank. (2009). Project Appraisal Report: Medupi power project

Aitken, R. (2007). Housegold energy use: a comparison of household energy consumption and expenditure across three provinces. Journal of Energy in Southern Africa, **18**, 20-28

Albright, J.N., Pearson, C.F. (1982). Acoustic emissions as a tool for hydraulic fracture location: Experience at the Fenton Hill hot dry rock site. Society of Petroleum Engineers, **22**, 523-530

AltaRock Energy. (2010). Increasing geothermal production using EGS systems. 2010 California Geothermal Forum, UC Davis Mondavi Studio, May 10, 2010

AltaRock Energy. (2010). Newberry EGS Demonstration: Project history. http://altarockenergy.com/projects.htm. Last accessed: July 2012

Andre, L.V., Audigane, P., Azaroual, M., Menjoz, A. (2007). Numerical modelling of fluid-rock chemical interactions at the supercritical CO_2 – liquid interface during CO_2 injection into a carbonate reservoir, the Dogger Aquifer (Paris Basin, France). Energy Convention Magmatism, **48**, 1782-1797

Andreoli, M., Hart, R., Ashwal, L., Coetzee, H. (2006). Correlations between U, Th and metamorphic grade in the western Namaqualand Belt, South Africa, with implications for radioactive heating of the crust. Journal of Petrology, **47**, 1095-1118

Asanuma, H., Liu, H., Niitsuma, H., Baria, R. (1999). Identification of structures inside basement at Soultz-sous-Foret (France) by triaxial drill-bit vertical seismic profiling. Geothermics, **28**, 355-376

Augustine, C. (2006). A comparison of geothermal with oil and gas well drilling costs. Proceedings: 31st Workshop on Geothermal Reservoir Engineering. Stanford University

Axelsson, G. (2008). Production capacity of geothermal systems. Presentation at the Workshop for Decision Makers on Direct Heating Use of Geothermal Resources in Asia. Tianjin, China, 11-18 May, 2008

Baglow, N. (2005). A geological description of sheets 2329 CD Pietersburg and 2329 DC Mankweng. Explanation: Sheets 2329 CD and 2329 DC (1:50 000). Council for Geoscience South Africa, 10-19

Baillieux, P., Schill, E., Dezayes, C. (2011). 3D Structural regional model of the EGS Soultz site (northern upper Rhine Graben, France): Insights and perspectives. Proceedings: 36th Workshop on Geothermal Reservoir Engineering, Stanford University

Baisch, S., Carbon, D., Dannwolf, U., Delacou, B., Devaux, M., Dunand, F., Jung, R., Koller, M., Martin, C., Sartori, M., Secanell, R., Voros, R. (2009). Deep heat mining Basel-seismic risk analyses. SERIANEX Group, Department fur Wirtschaft, Soziales und Umwelt des Kantons Basel-Stadt, Basel.

Ballard, S. and Pollack, H.N. (1987). Diversion of heat by Archean cratons: A model for southern Africa. Earth and Planetary Science Letters, **85**, 253-264

Ballard, S., Pollack, H.N., Skinner, N.J. (1987). Terrestrial heat flow in Botswana and Namibia. Journal of Geophysical Research, **92**, 6291-6300

Barth, M., Titus, J. (1984). Greenhouse effect and sea level rise: a challenge for this generation. Van Nostrand, New York, OSTI: 6429665

Baria, R and Green, A.S.P. (1989). Microseismics: A key to understanding reservoir growth. In Hot Dry Rock Geothermal Energy, Proceedings: Cambourne School of Mines International Hot Dry Rock Conference, Roberson Scientific Publications, London, pp 363-3771

Baria, R., Baumgartner, J., Gerard, A., Jung, R. (1998). European Hot Dry Rock georthermal research programme 1996-1997. Contract N: JOR3-CT95-0054, Joule 3 Programme, final report EUR 18925 EN, pp 151

Baria, R., Baumgartner, J., Gerard, A., Jung, R., Garnish, J. (1999). European HDR research programme at Soultz-sous-Forêts (France) 1987-1996. Geothermics, **28**, 655-669

Baria, R., Michelet, S., Baumgartner, J., Dyer, B., Nicholls, J., Hettkamp, T., Teza, D., Soma, N., Asanuma, H., Garnish, J., Megel, T., Kohl, T., Jueperkoch, L. (2005). A 5000 m deep reservoir development at the European HDR site at Soultz, Prcoeedings: 30th Workshop on Geothermal Reservoir Engineering, Stanford University

Baria, R., Jung, R., Tischner, T., Teza, D., Baumgartner, J., Dyer, B., Hettkamp, T., Nicholls, J., Michelet, S., Sanjuan, B., Soma, N., Asanuma, H., Garnish, J. (2006). Creation of an HDR/EGS reservoir at 5000 m depth at the European HDR project, Proceedings: 31st Stanford Geothermal Workshop, Stanford University

Barton, J.M., van Reenen, D.D. (1992). When was the Limpopo Orogeny? Precambrian Research, **55**, 7-16

Barton, J.M., Pretorius, W. (1997). Soutpansberg age (1.85 Ga) magmatism and metallogenesis in southern Africa: a result of regional rifting. Abstract: International Symposium on Plumes, Plates and Mineralisation. University of Pretoria

Batchelor, A.S. (1982). The stimulation of a Hot Dry Rock geothermal reservoir in the Cornubian Granite, England. Proceedings: 8th Workshop on Geothermal Reservoir Engineering, Stanford University

Batchelor, A.S., Baria, R., Hearn, K. (1983). Monitoring the effect of hydraulic stimulation by microseismic event location: a case study. SPE 58th Annual Technology Conference, San Francisco, October, SPE 12109

Batchelor, A.S. (1986). Reservoir behaviour in a stimulated Hot Dry Rock system. Proceedings: 11th Annual Workshop on Geothermal Reservoir Engineering, Stanford University

Baticci, F., Genter, A., Huttenloch, P., Zorn, R. (2010). Corrosion and scaling detection in the Soultz EGS power plant, upper Rhine Graben, France. Proceedings: World Geothermal Congress 2010, Bali Indonesia

Belcher, R., Kisters, A. (2006). Syntectonic emplacement and deformation of the Heerenveen batholith: Conjectures on the structural setting of the 3.1 Ga granite

magmatism in the Barberton granite-greenston terrain, South Africa. Geological Society of South Africa Special Papers, **405**, 211-231

Bickle, M.J. (1978). Heat loss from the Earth: A constraint on Archean tectonics from the relation between geothermal gradients and the state of plate production. Earth and Planetary Science Letters, **40**, 301-315

Bird, P., Ben-Avraham, Z., Schuber, G., Andreoli, M., Viola, G. (2006). Patterns of stress and strain rate in southern Africa. Journal of Geophysical Research, **111**, B08402

Björnsson, J., Helgason, T., Palmason, G., Stefansson, V., Jonatansson, H., Mariusson, J.M., Fridleifsson, I.B., Thorstainsson, L. (1998). The potential role of geothermal energy and hydropower in the world energy scenario in year 2020. Paper 3.1.07. Proceedings of the 17k WEC Congress, Houston (Texas), **5**, 69-87

Blackburn, T., Bowring, S., Schoene, B., Mahan, K., Dudas, F. (2011). U-Pb thermochronology: creating a temporal record of lithosphere thermal evolution. Contributions to Mineral Petrology, DOI 10.1007/s00410-011-0607-6

Boshoff, R., van Reenen, D.D., Smit, C.A., Perchuk, L.L., Kramers, J.D., Armstrong, R. (2006). Geological history of the central zone of the Limpopo Complex: the west Alldays area. The journal of Geology, **114**, 699-716

Bouwer, R.F. (1954). Bore-hole temperatures in the Klerksdorp and Orange Free State areas. Union of South Africa Department of mines

Brandl, G. (1981). Messina: 1:250,000 geological map. Geological Survey of South Africa

Brandl, G. (1986). The geology of the Pietersburg area: explanation of sheet 2328. Geological Survey of South Africa, Pretoria, 43 pp

Brandl, G. (1987). The geology of the Tzaneen area: explanation of sheet 2330. Geological Survey of South Africa, Pretoria, 55 pp

Brandl, G., Kroener, A. (1993). Preliminary results of single zircon studies from various Archean rocks of north-eastern Transvaal. Abstract: 16th colloqium of African Geology, Mbabane, Swaziland, **1**, 54-56

Brandl, G., Pretorius, S.J. (2000). Alldays: 1:250,000 Geological map. Geological Survey of South Africa

Brown, D., DuTeaux, R., Kruger, P., Swenson, D., Yamaguchi, T. (1999). Fluid circulation and heat extraction from engineered geothermal reservoirs. Geothermics, **28**, 553-572

Bullard, E.C. (1939). Heat Flow in South Africa. Proceedings: Royal Society London, **173**, 474-502

Bumby, A.J., Eriksson, P.G., van der Merwe, R., Brummer, J.J. (2001). Shear-zone controlled basins in the Blouberg area, Northern Province, South Africa: syn- and post-tectonic sedimentation relating to ca. 2.0 Ga reactivation of the Limpopo Belt. African Earth Sciences, **33**, 445-461

Bumby, A.J., Eriksson, P.G., van der Merwe, R., Steyn, G.L. (2002). A half-graben setting for the Proterozoic Soutpansberg Group (South Africa): evidence from the Blouberg Area. Sedimentary Geology, **147**, 37-56

Butler, D. (2010). France digs deep for nuclear waste. Nature, **466**, 804-805

Carlson R., Grove, T., de Wit, M., Gurney, J. (1996). Program to study crust and mantle of the Archean craton in southern Africa. Eos Transactions. AGU, **77**, 273-277

Carlson, R.W., Pearson, D.G., Boyd, F.R., Shirey, S.B., Irvine, G. (1999). Re–Os systematics of lithospheric peridotites: implications for lithosphere formation and preservation. In: Gurney, J.J., Gurney, J.L., Pascoe, M.D., Richardson, S.H. (Eds.), The J.B. Dawson Volume. Red Roof Design, Cape Town, 99–108

Carlson, R., Boyd, F., Shirey, S., Janney, P., Grove, T., Bowring, S., Schmitz., Dann, J., Bell, D., Gurney, J., Richardson, S., Tredoux, M., Menzies, A., Pearson, D., Hart, R., Wilson, A., Moser, D. (2000). Continental growth, preservation and modification in southern Africa. GSA Today, **10**, 1-7

Carte, A.E. (1955). Thermal conductivity and mineral composition of some Transvaal rocks. American Journal of Science, **253**, 482-490

Carte, A.E. and van Rooyen, A.I.M. (1969). Further measurements of heat flow in South Africa

Cartwright, A. (2008). Stockholm Environment Institute: Global climate change and adaption-A seal-level rise risk assessment. Prepared for: The City of Cape Town Environmental Resource Management Department. R030800032

Chamorro, C., Mondéjar, M., Ramos, R, Segovia, J., Martin, M, Villamañán. (2011). World geothermal power production status: Energy, environmental and economic stduy of high enthalpy technologies. Energy, in press, corrected proof available online 18 July 2011

Chandrasekharam, D., Bundschuh, J. (2008). Low-enthalpy geothermal resources for power generation. CRC Press/Balkema. ISBN 978-0-203-89455-2

Chapman, D.S and Pollack, H.N. (1977). Heat flow and heat production in Zambia: Evidence for lithosphere thinning in central Africa. Department of geology and mineralogy, The University of Michigan, Ann Arbor, Michigan (USA)

Cheney, E.S., Barton, J.M., Brandl, G. (1990). Extent and age of the Soutpansberg sequences of south Africa. South African Journal of Geology, **93**, 644-675

Chevrot, S., Zhao, L. (2007). Multiscale finite-frequency Rayleigh wave tomography of the Kaapvaal craton. Geophysics Journal International, DOI:10.1111/j.1365-246X.2006.03289.x

Church, J., White, N. (2006). A 20th century acceleration in global sea-level rise. Geophysical Research Letters, **33**, 1602pp

Cocherie, A., Guerrot, C., Fanning, M., Genter, A. (2004). Datation U-Pb des deux facies granite de Soultz (Fosse Rhenan, France). C.R Geoscience, **336**, 775-787

Cooper, G., Beardsmore, G., Waining, B., Pollington, N., Driscoll, J. (2010). The relative costs of engineered geothermal systems exploration and development in Australia. Proceedings: World Geothermal Congress 2010, Bali, Indonesia, 25-29 April 2010

Chopra, P., Wyborn, D. (2003). Australia's first hot dry rock geothermal energy extraction project is up and running in granite beneath the Cooper Basin, NE, South Australia. Magmas to mineralisation: The Ishihara Symposium, GEMOC Macquarie University

Chopra, P. (2005). Status of the geothermal industry in Australia, 2000-2005. Proceedings: World Geothermal Congress 2005, Antalya, Turkey, 24-29 April 2005

Chorowicz, J. (2005). The East African rift sytem. Journal of African Earth Sciences, **43**, 379-410

Cladouhos, T.T., Osborn, W.L., Petty, S., Bour, D., Iovenitti, J., Callahan, O., Nordin, Y., Perry, D., Stern, P.L. (2012). Newberry volcano EGS demonstration – Phase 1 results. Prcoeedings: 37th workshop on geothermal reservior engineering, Stanford university, SGP-TR-194

Clarke, L. (1985). Groundwater abstraction from crystalline complex areas of Africa. Quarterly Journal of Engineering Geology, **18**, 25-34

Clarke, C., Sullivan, J., Harto, C., Han, J., Wang, M. (2012). Life cycle environmental impacts of geothermal systems. Proceedings: 37th workshop on Geothermal Reservoir Engineering Stanford University

Clauser, C. (1997). Geothermal energy use in Germany-status and potential. Geothermics, **26**, 203-220

Cooper, G.T., Beardsmore, G.R., Waining, B.S., Pollington, N., Driscoll, J.P. (2010). The relative costs of engineered geothermal system exploration and development in Australia. Proceedings: World Geothermal Congress 2010 Bali, Indonesia

Coward, M.P., James, P.R., Wright, L. (1976). Northern margin of the Limpopo mobile belt, southern Africa. Geological Society of America Bulletin, **87**, 601-611

Cox, K.G.,Johnson, R.L., Monkman, L.J., Stillman, C.J., Vail, J.R., Wood, D.N. (1965). The Geology of the Nuanetsi Igneous Province. Philosophical Transactions of the Royal Society of London, A **257**, 71-218

Credit Suisse. (2009). Alternative energy sector, How much does is cost? pp. 26

Crow, C., Condie, K.C. (1990). Geochemistry and origin of early Proterozoic volcanic rocks from the Transvaal and Soutpansberg successions, South Africa. Precambrian Research, **47**, 17-26

Cuenot, N., Dorbath, L., Frogneux, M., Langet, N. (2010). Microseismic activity induced under circulation conditions at the EGS project of Soultz-sous-Forets (France). Proceedings: World Geothermal Congress, Bali Indonesia

Cypser, D., Davis, S. (1998). Induced seismicity and the potential for liability under U.S. law. Tectonophysics, **289**, 239-255

Damiani, D., Litynski, J., McIlvried, H., Vikara, D., Srivastava, R. (2001). The US department of Energy's R&D program to reduce greenhouse gas emissions through beneficial uses of carbon dioxide. Greenhouse Gases: Science and Technology, **2**, 9-16

Davies, R. (2011). Methane contamination of drkinking water caused by hydraulic fracturing remains unproven. Proceedings of the National Academy of Sciences of the United States of America, **108**, E871

Davis, M. (1998). Rural household energy consumption: The effects of access to electricity-evidence from South Africa. Energy Policy, **26**, 207-217

de Laguna, W., Tamura, T., Weeren, H.O., Struxness, E.G., McClain, W.C., Sexton, R.C. (1968). Engineering development of hydraulic fracturing as a method for permanent disposal of radioactive wastes. Oak Ridge National Laboratory, Technical Report: W-7405-ENG-26

de Ronde, C., de Wit, M. (1994). Tectonic history of the Barberton greenstone belt, South Africa: 490 million years of Archean crustal evolution. Tectonics, **13**, 983-1005

de Wit, M., de Ronde, C., Tredoux, M., Roering, C., Hart, R.A., Armstrong, R., Green, R., Perberdy, E., Hart, R.J. (1992). Formation of an Archaean continent. Nature, **357**, 553-562

de Wit, M., Richardson, S., Ashwal, L. (2004). Kaapvaal Craton Special Volume. South African Journal of Geology, **107**, 324pp

de Wit, M., Tinker, J. (2004). Crustal structures across the central Kaapvaal craton from deep-seismic reflection data. South African Journal of Geology, **107**, 185-206

de Wit, M. (2007). The Kalahari epeirogeny and climate change: differntiating cause and effect from core to space. South African Journal of Geology, **110**, 367-392

de Wit, M., Furness, H., Robin, B. (2011). Geology and tectonostratigraphy of the Onverwacht Suite, Barberton Greenstone Belt, South Africa. Precambrian Research, **186**, 1-27

Doi, N., Kato, O., Muramatsu, Y. (1990). On the Neo-granite and geothermal reservoir in the pre-Tertiary rocks at the Kakkonda geothermal field, Iwater Prefecture. Annual Meeting Geothermal Research Society of Japan, 6pp

Doucouré, C.M. and de Wit, M.J. (2002). Temporal variation in rigidity and mechanical behaviour of old thick continental lithosphere. South African Journal of Geology, **105**, 39-50

Douglas, B. (1991). Global sea level rise. Journal of Geophysical Research, **96**, 6981-6992

Duchane, D. (1993). Geothermal Energy, Encyclopedia of Chemical Technology, Wiley, New York, **12**, 512-539

Dziggel, A., Otto, A., Kisters, A.F.M., Meyer, F.M. (2007). Tectono-metamorphic controls on Archaean gold mineralisation in the Barberton greenstone belt, South Africa: an example from the New Consort gold mine. In Van Kranendonk, M., Smithies, R.H., Bennet, V. (Eds.) Earth's oldest Rocks. Developments in Precambrian Geology, Elsevier, **15**, 699-727

Econometrix. (2012). Karoo Shale Gas Report. Special report on economic considerations surrounding potential shale gas resources in the southern Karoo of South Africa. Available from www.static-shell/static/zaf/downloads/ aboutshell/econometrix/econometrix_report.pdf

Edkins, M., Marquard, A., Winkler, H. (2010). South Africa's renewable energy policy roadmaps. For the United Nations Environmental Programme Research Project: Enhancing information for renewable energy technology deployment in Brazil, China and South Africa. University of Cape Town Energy Research Center, Final Report June 2010

Edmunds, W.M., Andrews, J.N., Burgess, W.G., Kay, R.L., Lee, D.J. (1984). The evolution of saline and thermal groundwaters in the Carnmenellis granite. Mineralogical Magazine, September 1984, **48**, 407-424

Eskom Annual Report (2008). Including Eskom Forecast: coal statistics, 2007

Eskom Factor Report (2011). Available from: http://www.eskomfactor.co.za/eskom-factor-environmental.php

Frei, R., Schoenberg, R., Blenkinsop, T.G. (1999). Geochronology of the late Archaean Razi and Chilimanzi suites in Zimbabwe; implications for the late Archaean tectonics of the Limpopo Belt and Zimbabwe Craton. South African Journal of Geology, **102**, 55-63

Fridleifsson, I.B., Freeston, D.H. (1994). Geothermal energy research and development. Geothermics, **23**, 175-214

Fouch, M.J., James, D.E., VanDecar, J.C., van der Lee, S. (2004). Mantle seismic structure beneath the Kaapvaal and Zimbabwe cratons. South African Journal of Geology, **107**, 33-44

Genter, A., Dezayes, C., Gentier, S., Ledesert, B., Sausse, J. (2002). Conceptual fracture model at Soultz based on geological data. 4th HDR Forum, Strasbourg, France, 1998, pp 93-102

Genter, A., Goerke, X., Graff, J., Cuenot, N., Krall, G., Schindler, M., Ravier, G. (2010). Current status of the EGS Soultz geothermal project (France). Proceedings: World Geothermal Congress 2010, Bali, Indonesia, 25-29 April 2010

George, R., Rogers, N., Kelley, S. (1998). Earliest magmatism in Ethiopia: evidence for two mantle plumes in one flood basalt province. Geology, **26**, 923-926

Giardini, D. (2009). Geothermal quake risks must be faced. Nature, **462**, 848-849

Gornitz, V. (1991). Global coastal hazards from future sea level rise. Global and Planetary Change, **3**, 379-398

Hamilton, M., Jones, A., Evans, R., Evans, S., Fourie, C., Garcia, X., Mountford, A., Spratt, J., the SAMTEX MT Team. (2006). Electrical anisotropy of South African

lithosphere compared with seismic anisotropy from shear-wave splitting analyses. Physics of the Earth and Planetary Interiors, **158**, 226-239

Harris, C., Vogeli, J. (2010). Oxygen isotope composition of garnet in the Peninsula granite, Cape Granite Suite, South Africa: constraints on melting and emplacement mechanisms. South African Journal of Geology, **113.4**, 401-412

Hartnady, C.J. (1985). Uplift, faulting, seismicity, thermal spring and possible incipient volcanic activity in the Lesotho-Natal region, SE Africa: The Quathlamba hotspot hypothesis. Tectonics, **4**, 371-377

Hébert, R., Ledésert, B., Bartier, D., Dezayes, C., Genter, A., Grall, C. (2010). The Enhanced Geothermal System of Soultz-sous-Forêts: A study of the relationships between fracture zones and calcite content. Journal of Volcanology and Geothermal Research, **196**, 126-133

Hébert, R., Ledésert, B., Genter, A., Bartier, D., Dezayes, C. (2011). Mineral precipitation in geothermal reservoir: the study case of calcite in the Soultz-sous-Forêts Enhanced Geothermal System. Proceedings: 36th Workshop on Geothermal Reservoir Engineering Stanford University

Herzberg, C., Rudnick, R. (2012). Formation of cratonic lithosphere: An integrated thermal and petrological model. Lithos, **149**, 4-15

Hochstein, M. (2005). Heat transfer by hydrothermal systems in the East African Rifts. Proceedings: World Geothermal Congress, Antalya, Turkey

Holland, M., Witthuser, K. (2009). Factors that control sustainable yields in the Archean basement aquifers of the Limpopo Province. Basement aquifers of Southern Africa: Report to the Water Research Commission. WRC Report No. TT 428-09, 57 pp

Holland, M., Witthuser, K. (2011). Evaluation of geologic and geomorphologic influences on borehole productivity in crystalline bedrock aquifers of Limpopo Province, South Africa. Hydrogeology Journal, **19**, 1065-1083

Holm, A., Blodgett, L., Jennejohn, D., Gawell, K. (2010). Geothermal energy: international market update. Geothermal Energy Association

Holzer, L., Frei, R., Barton, J.M., Kramers, J.D. (1998). Unraveling the record of successive high grade events in the Central Zone of the Limpopo Belt using Pb single phase dating of metamorphic minerals. Precambrian Research, **87**, 87-115

Hooijkaas, G.R., Genter, A, Dezayes, C. (2006). Deep-seated geology of the granite intrusions at the Soult EGS site based on data from 5 km-deep borehole. Geothermics, **35**, 484-506

Hori, Y., Kitano, K., Kaieda, H., Kiho, K. (1999). Present status of the Ogachi HDR project, Japan and future plans. Geothermics, **28**, 637-645

Howard, G.C, Fast, C.R. (1970). Hydraulic fracturing. New York, Society for Petroleum Engineers of AIME. pp 210

Hubbert, M.K., Willis, D.G. (1957). Mechanics of hydraulic fracturing. Transactions of the American Institue for Mineral Engineering, **210**, 153-163

Huenges, E. (2010). Geothermal Energy Systems: Exploration, Development and Utilization. Wiley-VCH2010, ISBN 978 527 40831 3

Huq, S., Reid, H., Konate, M., Rahman, A., Sokona, Y., Crick, F. (2004). Mainstreaming adaption to climate change in Least Developed Countries (LDCs). Climate Policy, **4**, 25-43

Idaho National Laboratory (2006). The future of geothermal energy: impact of enhanced geothermal systems (EGS) on the United States in the 21st century. Prepared for the U.S. Department of Energy

IGA News. (2009). Newsletter of the Internation Geothermal Association. Quarterly No. 78. Available from www.geothermal-energy.org. Last accessed: May 2012

Inoue Y., Walet, L. (2012). Reuters: Japan approved on Monday icentives for renewable energy that could unleash billions of dollars in clean-energy investoment and help the world's third=giggest economy shoft away from a reliance on nuclear power after the Fukushima disaster. Available from www.reuters.com. Last accessed: july 2012

IPCC. (2007). Fourth Assessment Report (AR4), Synthesis Report. Cambridge University Press.

Jacobs, M. (2012). Climate policy: Deadline 2015. Nature, **481**, 137-138

James, D., Boyd, F., Schutt, D., Bell, D., Carlson, R. (2004). Xenolith constratints on seismic velocities in the upper mantle beneath southern Africa. American Geophysical Union, **5**, DOI:10.1029/2003GC000551

Jansen, H. (1975). The Soutpansberg Trough (Northern Transvaal)-an aulacolagen. Transvaal Geological Society of South Africa, **78**, 129-136

Jaupart, C and Mareschal, J.C. (1999). The thermal structure and thickness of continental roots. Lithos, **48**, 93-114

Jeffreys (1929). The Earth, Cambridge

Jones, M.Q.W. (1987). Heat flow and heat production in the Namaqua mobile belt, South Africa. Journal of Geophysical Research, **92**, 6273-6289

Jones, M.Q.W. (1992). Heat flow anomaly in Lesotho: implications for the southern boundary of the Kaapvaal Craton. Geophysical Research Letters, **19**, 2031-2034

Jones, N. (2011). United States investigates fracking safety: Energy department to scrutinise hydraulic fracturing for natural gas. Nature, published online 12 May 2011, doi: 10.1038/news.2011.282. Last accessed: May 2012

Jordan, T. (1975). The continental tectosphere. Reviews of Geophysics, **13**, 1-12

Jordan, T. (1978). Composition and development of the continental tectosphere. Nature, **274**, 544-548

Jordan, T. (1988). Structure and formation of the continental tectosphere. Journal of Petrology, Special Volume (1), 11-37

Keller, C., Schoene, B. (2012). Statistical geochemistry revels disruption in secular lithosphere evolution about 2.5 Ga ago. Nature, **485**, 490-495

Kiryukhin, A. (1993). High temperature fluid flow in the Dachny field of the Mutnovsky hydrothermal system, Russia. Geothermics, **22**, 49-64

Kohl, T., Speck, R. (2004). Electricity production by geothermal hybrid-plants in low-enthalpy areas. Proceedings: 29th Workshop on Geothermal Reservoir Engineering. Stanford University, SGP-TR-175

Kramers, J.D., Kreissig, K., Jones, M.Q.W. (2001). Crustal heat production and style of metamorphism: a comparison between two Archean high grade provinces in the Limpopo Belt, southern Africa. Precambrian Research, **112**, 149-163

Krige (1939). Proceedings of the Royal Society of South Africa, **173**, 450-474

KRISP Working Group. (1991). The Kenya Rift: pure shear extension above a mantle plume. Nature, **345**, 223-227

Kröner, A., Jaeckel, P., Brandl, G. (1999). Single zircon ages for felsic to intermediate rocks from the Pietersburg and Giyani greenstone belts and bordering granitoid orthogneisses, northern Kaapvaal Craton, South Africa. Journal of African Earth Sciences, **30**, 773-793

Kuriyagawa, M., Tenma, N. (1999). Development of hot dry rock technology at the Hijiori test site. Geothermics, **28**, 627-636

Lancaster, G., Ray, R., Valenzuela, R. (1999). A cross country study of equivalence scales and expenditure inequality on unit record household budget data. Economic Development and Cultural Change, **48**, 177-208

Laurent, O., Martin, H., Doucelance, R., Moyen, J., Paquette, J. (2011). Geochemistry and petrogenesis of high-K “sanukitoids” from the Bulai pluton, Central Limpopo Belt, South Africa: Implications for geodynamic changes at the Archaean-Proterozoic boundary. Lithos, **123**, 73-91

Ledesert, B., Hebert, R.L., Grall, C., Genter, A., Dezayes, C., Bartier, D., Gerard, A. (2009). Calcimetry as a useful tool for a better knowledge of flow pathways in the Soultz-sous-Forets Enhanced Geothermal System. Journal of Volcanology and Geothermal Research, **181**, 106-114

Lee, M.K., Brown, G.C., Webb, P.C., Wheildon, J., Rolling, K.E. (1987). Heat flow, heat production and thermo-tectonic setting in mainland UK. Journal of the Geological Society, **144**, 35-42

Leggett, J. (2011). China's Greenhouse Gas Emissions and Mitigiation Policies. Congressional Research Service, Prepared from memnbers and committees of Congress. R41919, available from http://www.fas.org/sgp/crs/row/R41919.pdf, last accessed: 11 December 2012

Leone, S. (2012). Hollande vicotry signals shift in France's renewable energy policy. RenewableEnergyWorld.com. Avaiable from: www.renewableenergy world. Com. Last accessed: July 2012

Livingstone, D.A. (1975). Late Quaternary climatic change in Africa. Annual review of Ecology and Systematics, **6**, 249-280

Louw, D. (1994). Accretionary history of the Archean Barberton greenstone belt (3.55-3.22 Ga) southern Africa. Geology, **22**, 1099-1102

Louw, K., Conradie, B., Howells, M., Dekenah, M. (2008). Determination of electricity demand for newly electrified low-income African household. Energy Policy, **36**, 2814-2820

Lovelock, B., Cope, D., Balstar, A. (1982). A hydrothermal model of the Tongonan geothermal field. Proceedings: Pacific Geothermal Conference, Auckland, 259-264

Lund, J.W., Freeston, D.H., Boyd, T.L. (2011). Direct utilisation of geothermal energy 2010 worldwide review. Geothermics, **40**, 159-180

Majer, E.L. and Peterson, J.E. (2007). The impact of injection on seismicity at The Geysers, California Geothermal Field. International Journal of Rock Mechanics & Mining Sciences, **44**, 1079-1090

Mascarelli, A.L. (2009). Funding cut for US nuclear waste dump. Nature, **458**, 1086-1087

Matsunaga, I., Tao, H., Tenma, N. (2000). Geochemical evaluation of the Hijiori HDR reservoir at Yamagata, Japan. Proeedings: World Geothermal Congress 2000, Japan, pp 3787-3792

May, J., Carter, M., Posel, D. (1995). The composition and persistence of poverty in rural South Africa: an entitlement approach. Land and Agriculture Policy Centre, Policy Paper No. 15

McLaren, S., Sandiford, M., Hand, M. (1999). High radiogenic heat-producing granites and metamorphism- An example from the western Mount Isa inlier, Australia. The Geological Society of America, **27**, 679-682

McLennan Magasanik Associates Pty Ltd. (2008). Installed capacity and generation from geothermal sources by 2020. Report to Australian Geothermal Energy Association, August 2008

McLennan, S.M., Taylor, S.R. (1996). Heat flow and the chemical composition of continental crust. The Journal of Geology, **104**, 369-377

Mendelsohn, M., Lowder, T., Canavan, B. (2012). Utility-scale concentrating solar power and photovoltaics projects: A technology and market overview. National Renewable Energy Laboratory. NREL/TP-6A20-51137

Montgomery, C.T., Smith, M.B., NSI Technologies. (2010). Hydraulic fracturing: history of an enduring technology. Journal of Petroleum Technology (Society of Petroleum Engineers), **62**, 26-32.

Mukheibir, P., Ziervogel, G. (2007). Developing a municipal adaption plan (MAP) for climate change: the city of Cape Town. Environment and Urbinization, **19**, 143-158

Muller, J., Bilkova, K., Genter, A., Seiersten, M. (2010). Laboratory results of corrosion tests for EGS Soultz geothermal wells. Proceedings: World Geothermal Congress 2010, Bali, Indonesia

Muraoka, H. (1993). A picture of future geothermal resources from the viewpoint of magma. Journal Japan Geothermal Energy Association, **30**, 100-126

Murphy, H.D., Tester, J.W., Grigsby, C.O., Potter, R.M. (1981). Energy extraction from fractured geothermal reservioirs in low-permeability crystalline rock. Journal of geophysical research, **86**, 7145-7158

Mutale Municipality. (2007). Draft IDP document (March 2007): Mutale Revised Report-March 2007 pp 20-21

Nageo, T., Uyeda, S. (1989). Heat flow measurements in the northern part of Honshu, northeast Japan, using shallow holes. Tectonophysics, **164**, 301-314

Nägler, T.F., Kramers, J.D., Kamber, B.S., Frei, R., Prendergast, M.D.A. (1997). Growth of subcontinental lithospheric mantle beneath Zimbabwe started at or before 3.8 Ga: Re-Os study on chromites. Geology, **25**, 983-986

NERSA. (2009). Renewable Energy Feed-In Tariff phase 2. NERSA consultation paper, July 2009, pp9

Neumann, N., Sandiford, M., Foden, J. (2000). Regional geochemistry and continental heat flow: implications for the origin of the South Australian heat flow anomaly. Earth and Planetary Science Letters, **138**, 107-120

Nguuri, T.K., Gore, J., James, D.E., Webb, S.J., Wright, C., Zengeni, T.G., Gwavava, O., Snoke, J.A. (2001). Crustal structure beneath southern Africa and its implications for the formation and evolution of the Kaapvaal and Zimbabwe cratons. Geophysics Research Letters, **28**, 2501-2504

Nicholls, R.J., Hoozemans, F.M.J. (1996). The Mediterranean: vulnerability to coastal implications of climate change. Ocean & Coastal Management, **31**, 105-132

Nuclear Energy Institute. (2012). Resource and statistics. Available on: www.nei.org. Last accessed: July 2012

Nyabeze, P.K., Venter, J.S., Olivier, J., Motlakeng, T.R. (2010). Characterisation of the thermal aquifer associated with the Siloam hot spring in Limpopo, South Africa. Proceedings: Water Resource Management, 2010

Nyblade, A. (1999). Heat flow and the structure of Precambrian lithosphere. Developments in Geotectonics, **24**, 81-91

Oldfield, S. (2000). The centrality of community capacity in state low-income housing provision in Cape Town, South Africa. International Journal of Urban and Regional Research, **24**, 858-872

Olivier, J., Venter, J.S., Jonker, C.Z. (2011). Thermal and chemical characteristics of hot water springs in the northern part of the Limpopo Province, South Africa. Water SA, **37**, 427-436

Olivier, J., van Niekerk, H.J., van der Walt, I.J. (2008). Physical and chemical characteristics of thermal springs in the Waterberg area in Limpopo Province, South Africa. Water SA, **34**, 163-174

Orberger, B., Hofmann, A., Wirth, R., Tudryn, A., Megneng, M. (2011). Uranium mineralisation in carbonaceous chert pebbles from Mesoarchean Mozaan Group conglomerates (~3 Ga, Pongola Basin, South Africa): trap or source rock? Society for Geology Applied to Mineral Deposits. 11th SGA Biennal Meeting "Let's talk ore deposits" Conference, Antofagasta: Chille (2011)

Osborn, S., Vengosh, A., Warner, N., Jackson, R. (2011). Methane contamination of drinking water accompanying gas-well drilling and hydraulic fracturing. Proceedings of the National Academy of Sciences of the United States of America, **108**, 8172-8176

Parker, R.H. (1989). Hot Dry Rock geothermal energy, Phase 2B final report of the Cambourne School of Mines Project. Pergamon Press, ISBN 008037929

Parker, R.H. (1991). Problems in the development of artificial geothermal energy exploitation in Cornwall. Proceedings of the Ussher Society, **7**, 316-320

Pauw, K. (2005). A profile of the Limpopo Province: Demographics, poverty, inequality and unemployment. PROVIDE Background Paper 2005: 1(9). Available from:http://www.elsenburg.com/provide/documents/BP2005_1_9%20Demographics%20LP.pdf

Peninsula Energy Limited. (2012). High-grade uranium confirmed at site 45 Karoo, South Africa. Available from www.infomine.com/index/pr/PB205271. PDF. Last accessed: July 2012

Peslier, A., Woodland, A., Bell, D., Lazarov, M., Lapen, T. (2012). Metasomatic control of water contents in the Kaapvaal cratonic mantle. Geochimica et Cosmochimica Acta, **97**, 213-246

Pine, R.J. and Batchelor, A.S. (1984). Downward migration of shearing in jointed rock during hydraulic injections. Internation Journal of Rock Mechanics Mining Sciences and Geomechanics Abstracts, **21**, 249-263

Pistone, S., Stacey, R., Horne, R. (2011). The significance of CO_2 solubility in geothermal reservoirs. Proceedings: 36th Workshop on Geothermal Reservoir Engineering, Stanford University, SGP-TR-191

Pollack, H.N., Chapman, D.S. (1977). On the regional variation of heat flow, geotherms, and lithospheric thickness. Tectonophysics, **38**, 279-296

Pollack, H.N., Hurter, S.J., Johnson, J.R. (1993). Heat flow from the Earth's interior: Analysis of the global data set. Geophysics, **31**, 267-280

Potter, R.M., Robinson, E.S., Smith, M.C. (1974). Method of extracting heat from dry geothermal reservoirs, U.S. Patent #3,786,858

Pruess, K. (2006). Enhanced geothermal systems (EGS) using CO2 as working fluid – A novel approach for generating renewable energy with simultaneous sequestration of carbon. Geothermics, **35**, 351-367

Poujol, M., Robb, L. (1999). New U-Pb zircon ages on gneisses and pegmatite from south of the Murchison greenstone belt, South Africa. South African Journal of Geology, **102**, 93-97

Pruess, K., Azaroual, M. (2006). On the feasibilty of using supercritical CO2 as heat transmission fluid in an Engineered hot dry rock geothermal system. Proceedings: 31st workshop on Geothermal Reservoir Engineering, Stanford Univeristy

Pruess, K. (2007). Enhanced Geothermal Systems (EGS) comparing water with CO_2 as heat transmission fluids. Lawrence Berkeley National Laboratory, Berkeley, CA 94720, USA

Pruess, K. (2007). On the production behaviour of enhanced geothermal systems with CO2 as working fluid. Submitted to Energy Convention and Magmatism

Reid, W.V., Goldemberg, J. (1998). Developing countries are combating climate change: Actions developing countries that slow grother in carbon emissions. Energy Policy, **26**, 233-237

Richardson, S.H., Pöml, P.F., Shirey, S.B., Harris, J.W. (2009). Age and origin of peridotitic diamonds from Venetia, Limpopo Belt, Kaapvaal-Zimbabwe craton. Lithos, **112S**, 785-792

Ridley, J. On the origins and tectonic significance of the charnockite suite of the Archaean Limpopo Belt, Northern Marginal Zone, Zimbabwe. Precambrian Research, **55**, 1-4

Rigby, M., Mouri, H., Brandl, G. (2008). A review of the pressure-temperature-time evolution of the Limpopo Belt: Constraints for a tectonic model. Journal of African Earth Sciences, **50**, 120-132

Rose, P., Mella, M., McCullough, J. (2006). A comparison of hydraulic stimulation experiments at the Soultz, France and Coso, California Engineered Geothermal Systems. Proceedings: 31st Workshop on Geothermal Reservoir Engineering, Stanford University

Rose, P., Xu, T., Kovac, K., Mella, M., Pruess, K. (2007). Chemical stimulation in near-wellbore geothermal formations: Silica dissolution in the presence of calcit at high temperatre and high pH. Proceedings: 32nd Workshop on Geothermal Reservoir Engineering, Stanford university, SGP-TR-183

Sanjuan, B., Pinault, J., Rose, P., Gerard, A., Brach, M., Braibant, G., Crouzet, C., Foucher, J., Gautier, A., Touzelet, S. (2006). Tracer testing of the geothermal heat exchanger at Soult-sous-Forêts (France) between 2000 and 2005. Geothermics, **35**, 622-653

Sanyal, S.K., Morrow, J.W., Butler, S.J., Tait, A.R. (2007). Cost of electricity from enhanced geothermal systems. Proceedings: 32nd workshop on geothermal reservior engineering Stanford University

Sanyal, S. (2009). Cost of elctric power from Enhanced Geothermal Systems-its sensitivity and optimisation. Geothermal Reservoir Congress Transactions, **33**, 245-250

SARS. (2011). Tax proposals Budget 2011, pp16-17

Sauret, E and Rowlands, A. Candidate radial-inflow turbines and high-density working fluids for geothermal power systems. Energy, **36**, 4460-4467

Schaller, M., Steiner, O., Studer, I., Holzer, L., Herwegh, M., Kramers, J.D. (1999). Exhumation of Limpopo Central Zone granulites and dextral continental-scale transcurrent movement at 2.0 Ga along the Palala Shear Zone, Northern Province, South Africa. Precambrian Research, **96**, 263-288

Schellschmidt, R., Sanner, B., Pester, S., Schulz, R. (2010). Geothermal energy use in Germany. Proceedings: World Geothermal Congress 2010, Bali, Indonesia

Schill, E., Geiermann, J., Kümmritz, J. (2010). 2D Magnetotellurics and gravity at the geothermal site at Soultz-sous-Forêts. Proceedings: World Geothermal Congress 2010, Bali, Indonesia

Schilling, J.G. (1973). Afar mantle plume: rare earth evidence. Nature, **242**, 2-5

Schmitz, M., Bowring, S. (2003). Ultrahigh-temperature metamorphism in the lower crust during Neoarchean Ventersdorp rifting and magmatism, Kaapvaal Craton, southern Africa. GSA Bulletin, **115**, 533-548

Schmitz, M., Bowring, S. (2004). Lower crustal granulite formation during Mesoproterozoic Namaqua-Natal collisional orogenesis, southern Africa. South African Journal of Geology, **107**, 261-284

Schon, S. (2011). Hydraulic fracturing not responsible for methane migration. Proceedings of the National Academy of Science of the United States of America, **108**, E664

Schroeder, R., Swenson, D., Shinohara, N., Okabe, T., Tagasugi, S., Hayashi, K. (1998). Strategies for the Hijiori long term flow test. Proceedings: 23rd Workshop on Geothermal Reservoir Engineering, Stanford University

Sclater, J.G and Francheteau, J. (1970). The implications of terrestrial heat flow observations on current tectonic and geochemical models of the crust and upper mantle of the Earth. Geophysic Journal, **20**, 509-542

Shin, K., Ito, H., Oikawa, Y. (2000). Stress state at the Ogachi site. Proceedings: World Geothermal Congress 2000, Kyushu-Tohoku, Japan

Short, W., Packey, D.J., Holt, T. (1995). A manual for the economic evaluation of energy efficiency and renewable energy technologies. National Renewable Energy Laborator. NREL/TP-462-5173

Silver, P., Fouch, M., Geo, S., Schmitz, M., Kaapvaal Seismic Group. (2004). Seismic anisotropy, mantle fabric, and the magmatic evolution of the Precambrian southern Africa. South African Journal of Geology, **107**, 45-58

Simiyu, S.M. (2008). Status of geothermal exploration in Kenya and future plans for its development. Geothermal Training Programme: 30th Anniversay Workshop, August 26-27, Reykjavik, Iceland

Somerville, M., Wyborn, D., Chopra, P., Rahman, S., Estrella, D., van der Muelen, T. (1994). Hot dry rock feasibility study. Energy Research and Development Corporation, Report 94/243, Canberra, ACT, Australia, pp 133

South African Government Gazette. (1998). The National Environmental Management Act, 1998: http://www.info.gov.za/view/DownloadFileAction?id=70641. Last accessed: May 2012

Statistics South Africa. (2001). STATS SA: Census 2001. Primary tables, census 1996 and 2001 compared. Report number 03-02-11

Statistics South Africa. (2012). Census 2011 in brief. Report number 03-01-41

Swenson, D., Schroeder, R., Shinohara, N, Okabe, T. (1999). Analyses of the Hijiori long term circulation test. Proceedings: 24th Workshop on Geothermal Reservoir Engineering, Stanford University, Stanford, SGP-TR-162

Tekere, M., Lotter, A., Olivier, J., Jonker, N., Venter, S. (2011). Metagenomic analysis of bacterial diversity of Siloam hot water spring, Limpopo, South Africa. African Journal of Biotechnology, **10**, 18005-18012

Tenman, N., Yamaguchi, T., Tenzuki, K., Karasawa., H (2000). A study of the pressure-flow response of the Hijiori reservoir at the Hijiori HDR test site. Proceedings: World Geothermal Congress 2000, Kyushu-Tohoku, Japan

Tenman, N., Yamaguchi, T., Oikawa, Y., Zyvoloski, G. (2001). Comparison of the deep and the shallow reservoirs at the Hijiori HDR test site using FEHM code. Proceedings: 26th Workshop on Geothermal Reservoir Engineering, Stanford University

Tenma, N., Yamaguchi, T., Zyvoloski, G. (2008). The Hijiori Hot Dry Rock test site, Japan: Evaluation and optimisation of heat extraction from a two-layered reservoir. Geothermics, **37**, 19-52

Tenzer, H. (2001). Development of hot dry rock technology. GHC Bulletin, December 2001

Tester, J.W. and Albright, J.N. (1979). Hot Dry Rock Energy Extraction Field Test: 75 Days of operation of a prototype reservoir at Fenton Hill, Segment 2 of phase 1, Informal Report No. LA-7771-MS, Los Alamos Scientific Laboratory, Los Alamos, New Mexico

Teza, D., Baumgartner, J., Lerch, C., Gandy, T., Hettkamp, T., Penzkofer, P., Schindler, M., Wahl, G. (2011). Developing and circulating a fault system in the crystalline rock for geother power generation in Insheim, Germany. American Geophysical Union, Fall Meeting 2011, abstract S44B-03

Thomas, R.J., Agenbacht, A.L.D., Cornell, D.H., Moore, J.M. (1994). The Kibaran of southern Africa: Tectonic evolution and metallogeny. Ore Geology Reviews, **9**, 131-160

Ting, D. (2011). Geothermal Energy: Renewable energy and the environment. International Journal of Environmental Studies, **68**, 229-234

Tisdell, C. (2002). Globilisation, development and povery in the Pacific Islands: The situation of the least developed nations. International journal of Social Economics, **29**, 902-922

Tol, R., Klein, R., Nicholls, J. (2008). Towards successful adaption to sea-level rise along Europe's cost. Journal of Coastal Research, **24**, 432-442

Tshibalo, A.E., Olivier, J., Venter, J. (2008). South Africa geothermal country update (2006-2009), Proceedings: World Geothermal Congress 2010, Bali, Indonesia

Ueda, A., Kato, K., Ohsumi, T., Yajima, T., Ito, H., Kaieda, H., Metcalfe, R., Takase, H. (2005). Experimental studies of CO2-rock interactions at elevated temperatures under hydrothermal conditions. Geochemical Journal, **39**, 417-425

United Nations Framework Convention on Climate Change. (2003). White Paper on Renewable Energy, 2003: http://unfccc.int/files/meetings/seminar/ application/ pdf/sem_sup1_south_africa.pdf. Last accessed: May 2012

United Nations Framework Convention on Climate Change. (2007). Report of the Conference of the Parties on its thirteenth session, held in Bali from 3 to 15 December 2007. Available from: http://unfccc.int/resource/docs/2007/ cop13/eng/06a01.pdf£page=3. Last accessed: May 2012

U.S. Nuclear Regulatory Commision. (2011). Technical evaluation report on the content of the U.S. Department of Energy's Yucca Mountain reposotory license application. Preclosure volume: repository safety before permanent closure. NUREG-2108. Available from: www.nrc.gov/reading-rm/doc-collections/nureg/staff/sr2108. Last accessed: May 2012

Valley, B., Dezayes, C., Genter, A. (2007). Multi-scale fracturing in the Soultz-sous-Forêts basement from borehole images analyses. EHDRA Scientifc Conference 2007

van Reenen, D.D., Roering, C., Ashwal, L.D., de Wit, M.J. (1992). Regional geological setting of the Limpopo Belt. Precambrian Research, **55**, 1-5

Vogt, C., Kosack, C., Marquart, G. (2012). Stochastic inversion of the tracer experiment of the enhanced geothermal system demonistarion reservoir in Soultz-sous-Forêts-Revealing pathways and estimating permeability distribution. Geothermics, **42**, 1-12

Walton, F.B., Ross, J.P.M, Juhnke, D.G. (1985). The effects of simultaneous heat and mass transport on radionuclide migration. Material Research Society Proceedings, **50**, 663 doi:10.1557/PROC-50-663

Wan, Y., Xu, T., Pruess, K. (2011). Impact of fluid-rock interactions on Enhanced Geothermal Systems woth CO_2 as heat transmission fluid. Proceedings: 36th Workshop on Geothermal Reservoir Engineering, Stanford University, SGP-TR-191

Warrick, R., Oerlemans, J. (1990). Climate change – the IPCC scientific assessment. Cambridge University Press, ISBN: 978-0521407205, 257-281

Weiss (1929). Journal of Chemical Society of South Africa, **39**, 149-166

Weight, W., Sonderegger, J. (2000). Manuel of applied field hydrogeology. McGraw-Hill, ISBN 0-07-069639-X

Wesson, R., Nicholson, C. (1987). Earthquake hazard associated with deep well injection. Prepared by the US Geological Survey. Open-file Report 87-331

West, F.G. (1974). Dry Hot Rock project. New Mexico Geological Society Guidebook, 25th field conference, Ghost Ranch (Central-Northern NM), 1974. Commisioned under the US Atmoic Energy Commision

Wheeler, D. (2008). Crossroads at Mmamabula: Will the World Bank choose the clean energy path? Center for Global Development Working Paper No. 140. Available at SSRN: http://ssrn.com/abstract=1099949. Last accessed: May 2012

Wheildon, J., Francis, M.F., Thomas-Betts, A. (1977). Seminar of Geothermal Energy, Brussels. EUR 5920, **1**, 175-188

Wingate, M.T. (1998). A palaeomagnetic test of the Kaapvaal-Pilbara (Vaalbara) connection at 2.78 Ga. South African Journal of Geology, **101**, 257-274

Xie, H., Hofmann, A., Hegner, E., Wilson, A., Wan, Y., Dunyi Liu, D. (2012). Zircon SHRIMP dating confirms a Palaeoarchean supracrustal terrain in the southeastern Kaapvaal Craton, southern Africa. Gondwana Research, **21**, 818-828

Yamaguchi, S., Akibayashi, S., Rokugawa, S., Fujinaga, Y., Tenma, N., Sato, Y. (2000). The numerical modelling study of the Hijiori HDR test site. Proceedings: World Geothermal Congress 2000, Kyushu-Tohoku, Japan, pp 3975-3980

Yanagisawa, N., Matsunaga, I., Sugita, H. (2007). Estimation of mineral transport in HDR circulation test. Proceedings: 32nd Workshop on Geothermal Reservoir Engineering, Stanford Univeristy, SGP-TR-183

Yanagisawa, N. (2010). Ca and CO2 transportation and scaling in HDR systems. Proceedings: World Geothermal Congress, 2010

Zeh, A., Gerdes, A., Klemd, R., Barton, J.M. (2007). Archaean to Proterozoic crustal evolution in the Central Zone of the Limpopo Belt (South Africa-Botswana): Constraints from combined U-Pb and Lu-H isotope analyses of zircon. Journal of Petrology, **48**, 1605-1639

Zeh, A., Gerdes, A., Klemd, R., Barton, J.M. (2008). U-Pb and Lu-Hf isotope record of detrital zircon grains from the Limpopo Belt- Evidence for crustal recycling at the Hadean to early-Archean transition. Geochimica et Cosmochimica Acta, **72**, 5304-5329

Zeh, A., Gerdes, A., Millonig, L. (2011). Hafnium isotope record of the Ancient Gneiss Complex, Swaziland, southern Africa: evidence for Archean crust-mantle formation and crust reworking between 3.66 and 2.73 Ga. Journal of the Geological Society of London, **168**, 953-964

Appendices

A.1 LCOE Variables

Table 3: Variables used within the LCOE model, blue denotes those that are calculated within the model and black are input parameters

LCOE	
LCOE ($/MWh)	**132,49**
LCOE ($c/KWh)	**13,25**

SCENARIO	
Capital Cost per KW (Incl installation)	$39 984,61
Nameplate Plant Size (KW)	72 268
Total Capital Cost	$2 889 590 132,05
Life of Asset (years)	30
Construction Time (months)	36
O&M Costs per MWh	$25,00
Utilization Factor	100%
Annual Degradation	0,50%
Reoccurring Capital Costs	$0,00
Years between Reoccurring Capital Costs	0
Tax Rate	40%
Annual Inflation	6,00%
RETFIT (NERSA)	$25,00
PTC	$0,00
Selling Price per MWh	$0
Other Incentives	0
Interest Rate	6%
Yearly Payment	$25 896 084

GEOLOGY AND ENGINEERING	
Geothermal 1 (°C/km)	50
Thickness 1 (km)	2
Geotherm 2 (°C/km)	25
Thickness 2 (km)	4
Expected basal temperature (°C)	169,75
Thermal Drawdown (%)	0,15%
Well Depth (km)	4
Heat Rate	7,196
Input Water Temperature (°C)	55
Flow Rate (kg/s)	50
Flow Rate (m^3/h)	180
Recovery Factor	15%
Expected Energy (KWh)	24 089,18
Expected Energy for 3 wells (KWh)	72 268
Average Volume of Aquifers (m^3)	248 918 838,927
Average Depth of Fractured Zone (m)	171,166
Average Volume stored in Fracture Zone (m^3)	59 811 468,910
Ave Exploitation Volume (m^3)	8 100 323,004
Average Discharge (m^3)	2 395 866,979
Average Recharge (m^3)	15 141 318,266
Average Recharge Drought (m^3)	11 032 151,528
Number of Geothermal Wells	3
Geothermal Water Loss (%)	0,5%

A.2 Capital Cost

Table 4: Derivation of the total capital costs used within the LCOE model with oil-industry drilling rig costs considered with the appropriate inflation index. Construction costs are related to South African standards with data from the construction of the Medupi power station, similarly in the Limpopo Province; derived from the African Development Bank.

CAPITAL COSTS	
36 months	8 651 356 630,16
Grand Total	8 668 770 396,16
For 3 wells (Mil USD)	**2 889 590 132,05**

DRILLING (Augustine)				
Depth	**USD (2003)**	**CPI**	**USD (2012)**	**USD (2012)**
557	0,227	6,20%	0,353666	353 666,00
964	0,267	6,20%	0,415986	415 986,00
1329	0,3	6,20%	0,4674	467 400,00
1912	0,543	6,20%	0,845994	845 994,00
2613	1,01	6,20%	1,57358	1 573 580,00
3380	2,033	6,20%	3,167414	3 167 414,00
4092	2,949	6,20%	4,594542	4 594 542,00
4868	5,168	6,20%	8,051744	8 051 744,00
5648	11,177	6,20%	17,413766	17 413 766,00

RSA BUILD SCENARIO (AFD, 2009)					
Component	**UA**	**rate**	**2009**	**CPI**	**2012**
civil works	1,23	1,5533	1,910559	6,20%	2,265922974
housing	0,52	1,5533	0,807716	6,20%	0,957951176
turbines	1,93	1,5533	2,997869	6,20%	3,555472634
boilers	0,00	1,5533	0	6,20%	0
electrical	0,40	1,5533	0,62132	6,20%	0,73688552
control instruments	0,20	1,5533	0,31066	6,20%	0,36844276
low pressure services	0,12	1,5533	0,186396	6,20%	0,221065656
transmission	1,00	1,5533	1,5533	6,20%	1,8422138
owner cost	0,86	1,5533	1,335838	6,20%	1,584303868
Total			9,723658		11,53225839
Grand Total (USD)					**11 532 258 388**

A.3 Modelled Calculations

Table 5: Table listing the total costs expected for the development of the full-scale EGS plant, including the annual payments related to all anticipated costs. The LCOE model does not incorporate possible tariffs and revenues incurred from privately development

Capital Costs	0	1	2	3	4	5	6	7	8	9
Drilling and Fracturing	$4 360 000,00	$-	$-	$-	$-	$-	$-	$-	$-	$-
Construction	$2 889 590 132,05	$-	$-	$-	$-	$-	$-	$-	$-	$-
Subtotal	$2 893 950 132,05	$-	$-	$-	$-	$-	$-	$-	$-	$-
Interest Rate	6%	6%	6%	6%	6%	6%	6%	6%	6%	6%
Interest	$173 637 007,92	$161 665 022,38	$150 411 355,98	$139 832 909,55	$129 889 169,91	$120 542 054,65	$111 755 766,31	$103 496 655,27	$95 733 090,89	$88 435 340,37
Yearly Payment	$25 896 084,41	$25 896 084,41	$25 896 084,41	$25 896 084,41	$25 896 084,41	$25 896 084,41	$25 896 084,41	$25 896 084,41	$25 896 084,41	$25 896 084,41
Debt Paid	$199 533 092,33	$187 561 106,79	$176 307 440,39	$165 728 993,96	$155 785 254,33	$146 438 139,07	$137 651 850,72	$129 392 739,68	$121 629 175,30	$114 331 424,78
Debt Remaining	$2 694 417 039,72	$2 506 855 932,92	$2 330 548 492,54	$2 164 819 498,57	$2 009 034 244,25	$1 862 596 105,18	$1 724 944 254,46	$1 595 551 514,78	$1 473 922 339,48	$1 359 590 914,70
Yearly Payment	**$25 896 084,41**									

Possible Income	0	1	2	3	4	5	6	7	8	9
Present Value of Energy Produced	0	0	704215,1225	742 735,69	783 363,33	826 213,31	871 407,17	919 073,15	969 346,45	1 022 369,70
Selling Price per MWh	$-	$-	$-	$-	$-	$-	$-	$-	$-	$-
Raw Income	$-	$-	$-	$-	$-	$-	$-	$-	$-	$-
Inflation	6,00%	6,00%	6,00%	6,00%	6,00%	6,00%	6,00%	6,00%	6,00%	6,00%
Primary Income	$-	$-	$-	$-	$-	$-	$-	$-	$-	$-
Tax Rate	40%	40%	40%	40%	40%	40%	40%	40%	40%	40%
Final Income	$-	$-	$-	$-	$-	$-	$-	$-	$-	$-

2 154 831 2 272 700 2 397 017 2 528 134 2 666 423 2 812 276 2 966 108 3 128 354 3 299 475 3 479 956

10	11	12	13	14	15	16	17	18	19	20	21
$-	$-	$-	$-	$-	$-	$-	$-	$-	$-	$-	$-
$-	$-	$-	$-	$-	$-	$-	$-	$-	$-	$-	$-
$-	$-	$-	$-	$-	$-	$-	$-	$-	$-	$-	$-
6%	6%	6%	6%	6%	6%	6%	6%	6%	6%	6%	6%
$81 575 454,88	$75 127 162,52	$69 065 767,71	$63 368 056,58	$58 012 208,12	$52 977 710,57	$48 245 282,87	$43 796 800,83	$39 615 227,72	$35 684 548,99	$31 989 710,99	$28 516 563,26
$25 896 084,41	$25 896 084,41	$25 896 084,41	$25 896 084,41	$25 896 084,41	$25 896 084,41	$25 896 084,41	$25 896 084,41	$25 896 084,41	$25 896 084,41	$25 896 084,41	$25 896 084,41
$107 471 539,29	$101 023 246,94	$94 961 852,12	$89 264 140,99	$83 908 292,53	$78 873 794,98	$74 141 367,28	$69 692 885,25	$65 511 312,13	$61 580 633,40	$57 885 795,40	$54 412 647,67
$1 252 119 375,41	$1 151 096 128,47	$1 056 134 276,35	$966 870 135,36	$882 961 842,83	$804 088 047,85	$729 946 680,57	$660 253 795,32	$594 742 483,19	$533 161 849,79	$475 276 054,39	$420 863 406,72

10	11	12	13	14	15	16	17	18	19	20	21
1 078 293,32	1 137 275,97	1 199 484,96	1 265 096,79	1 334 297,58	1 407 283,66	1 484 262,08	1 565 451,21	1 651 081,39	1 741 395,55	1 836 649,88	1 937 114,63
$-	$-	$-	$-	$-	$-	$-	$-	$-	$-	$-	$-
$-	$-	$-	$-	$-	$-	$-	$-	$-	$-	$-	$-
6,00%	6,00%	6,00%	6,00%	6,00%	6,00%	6,00%	6,00%	6,00%	6,00%	6,00%	6,00%
$-	$-	$-	$-	$-	$-	$-	$-	$-	$-	$-	$-
40%	40%	40%	40%	40%	40%	40%	40%	40%	40%	40%	40%
$-	$-	$-	$-	$-	$-	$-	$-	$-	$-	$-	$-

22	23	24	25	26	27	28	29	30	31	32
$-	$-	$-	$-	$-	$-	$-	$-	$-	$-	$-
$-	$-	$-	$-	$-	$-	$-	$-	$-	$-	$-
$-	$-	$-	$-	$-	$-	$-	$-	$-	$-	$-
6%	6%	6%	6%	6%	6%	6%	6%	6%	6%	6%
$25 251 804,40	$22 182 931,07	$19 298 190,14	$16 586 533,67	$14 037 576,59	$11 641 556,93	$9 389 298,45	$7 272 175,48	$5 282 079,88	$3 411 390,02	$1 652 941,56
$25 896 084,41	$25 896 084,41	$25 896 084,41	$25 896 084,41	$25 896 084,41	$25 896 084,41	$25 896 084,41	$25 896 084,41	$25 896 084,41	$25 896 084,41	$25 896 084,41
$51 147 888,81	$48 079 015,49	$45 194 274,56	$42 482 618,08	$39 933 661,00	$37 537 641,34	$35 285 382,86	$33 168 259,89	$31 178 164,29	$29 307 474,44	$27 549 025,97
$369 715 517,90	$321 636 502,42	$276 442 227,86	$233 959 609,78	$194 025 948,78	$156 488 307,44	$121 202 924,58	$88 034 664,70	$56 856 500,40	$27 549 025,97	$0,00

22	23	24	25	26	27	28	29	30	31	32
2 043 074,80	2 154 830,99	2 272 700,25	2 397 016,95	2 528 133,78	2 666 422,70	2 812 276,02	2 966 107,52	3 128 353,60	3 299 474,54	3 479 955,80
$-	$-	$-	$-	$-	$-	$-	$-	$-	$-	$-
$-	$-	$-	$-	$-	$-	$-	$-	$-	$-	$-
6,00%	6,00%	6,00%	6,00%	6,00%	6,00%	6,00%	6,00%	6,00%	6,00%	6,00%
$-	$-	$-	$-	$-	$-	$-	$-	$-	$-	$-
40%	40%	40%	40%	40%	40%	40%	40%	40%	40%	40%
$-	$-	$-	$-	$-	$-	$-	$-	$-	$-	$-

Table 6: Representation of the geological factors used within calculating the expected basal reservoir temperature and the overall heat loss over the lifetime of the plant, in addition considers the hydrogeological parameters associated with the surrounding area toward the development of the groundwater sustainability profile of the plant.

Geological Characteristics	1	2	3	4	5	6	7	8	9
Primary Geotherm (°C/km)	50	50	50	50	50	50	50	50	50
Primary Thickness (km)	2	2	2	2	2	2	2	2	2
Secondary Geotherm (°C/km)	25	25	25	25	25	25	25	25	25
Secondary Thickness (km)	4	4	4	4	4	4	4	4	4
Average Geotherm (°C/km)	50	50	50	50	50	50	50	50	50
Estimated Base Temperature (°C)	200	200	200	200	200	200	200	200	200
Thermal Drawdown (%)	0,15%	0,15%	0,15%	0,15%	0,15%	0,15%	0,15%	0,15%	0,15%
Net Temperature Loss (°C)	199,7	199,40045	199,1013493	198,8026973	198,5044933	198,2067365	197,9094264	197,6125623	197,3161434

Hydrogeology Characteristics	1	2	3	4	5	6	7	8	9
Water Flow Rate (m^3/h)	180	180	180	180	180	180	180	180	180
Total Water Flow Rate (m^3/h)	540	540	540	540	540	540	540	540	540
Water Influx Required m^3 in a year	-4 730 400	-4 730 400	-4 730 400	-4 730 400	-4 730 400	-4 730 400	-4 730 400	-4 730 400	-4 730 400
Water Available in Fracture Zones (m^3)	59 811 469	59 811 469	59 811 469	59 811 469	59 811 469	59 811 469	59 811 469	59 811 469	59 811 469
Geothermal Loss Rate (%)	0,5%	0,5%	0,5%	0,5%	0,5%	0,5%	0,5%	0,5%	0,5%
Resulting Water Available (m^3)	59 512 412	59 214 850	58 918 775	58 624 181	58 331 060	58 039 405	57 749 208	57 460 462	57 173 160
Natural Discharge (m^3)	-2 395 867	-2 395 867	-2 395 867	-2 395 867	-2 395 867	-2 395 867	-2 395 867	-2 395 867	-2 395 867
Natural Recharge (m^3)	15 141 318	15 141 318	15 141 318	15 141 318	15 141 318	15 141 318	15 141 318	15 141 318	15 141 318
Average Exploitation Discharge (m^3)	-8 100 323	-8 100 323	-8 100 323	-8 100 323	-8 100 323	-8 100 323	-8 100 323	-8 100 323	-8 100 323
Net Water Supply (m^3)	119 238 609	118 941 047	118 644 972	118 350 379	118 057 258	117 765 602	117 475 405	117 186 659	116 899 357

10	11	12	13	14	15	16	17	18	19	20	21
50	50	50	50	50	50	50	50	50	50	50	50
2	2	2	2	2	2	2	2	2	2	2	2
25	25	25	25	25	25	25	25	25	25	25	25
4	4	4	4	4	4	4	4	4	4	4	4
50	50	50	50	50	50	50	50	50	50	50	50
200	200	200	200	200	200	200	200	200	200	200	200
0,15%	0,15%	0,15%	0,15%	0,15%	0,15%	0,15%	0,15%	0,15%	0,15%	0,15%	0,15%
197,0201692	196,724639	196,429552	196,1349077	195,8407053	195,5469443	195,2536238	194,9607434	194,6683023	194,3762998	194,0847354	193,7936083

10	11	12	13	14	15	16	17	18	19	20	21
180	180	180	180	180	180	180	180	180	180	180	180
540	540	540	540	540	540	540	540	540	540	540	540
-4 730 400	-4 730 400	-4 730 400	-4 730 400	-4 730 400	-4 730 400	-4 730 400	-4 730 400	-4 730 400	-4 730 400	-4 730 400	-4 730 400
59 811 469	59 811 469	59 811 469	59 811 469	59 811 469	59 811 469	59 811 469	59 811 469	59 811 469	59 811 469	59 811 469	59 811 469
0,5%	0,5%	0,5%	0,5%	0,5%	0,5%	0,5%	0,5%	0,5%	0,5%	0,5%	0,5%
56 887 294	56 602 858	56 319 843	56 038 244	55 758 053	55 479 263	55 201 866	54 925 857	54 651 228	54 377 971	54 106 082	53 835 551
-2 395 867	-2 395 867	-2 395 867	-2 395 867	-2 395 867	-2 395 867	-2 395 867	-2 395 867	-2 395 867	-2 395 867	-2 395 867	-2 395 867
15 141 318	15 141 318	15 141 318	15 141 318	15 141 318	15 141 318	15 141 318	15 141 318	15 141 318	15 141 318	15 141 318	15 141 318
-8 100 323	-8 100 323	-8 100 323	-8 100 323	-8 100 323	-8 100 323	-8 100 323	-8 100 323	-8 100 323	-8 100 323	-8 100 323	-8 100 323
116 613 491	116 329 055	116 046 040	115 764 441	115 484 250	115 205 460	114 928 063	114 652 054	114 377 425	114 104 169	113 832 279	113 561 748

22	23	24	25	26	27	28	29	30	31	32
50	50	50	50	50	50	50	50	50	50	50
2	2	2	2	2	2	2	2	2	2	2
25	25	25	25	25	25	25	25	25	25	25
4	4	4	4	4	4	4	4	4	4	4
50	50	50	50	50	50	50	50	50	50	50
200	200	200	200	200	200	200	200	200	200	200
0,15%	0,15%	0,15%	0,15%	0,15%	0,15%	0,15%	0,15%	0,15%	0,15%	0,15%
193,5029179	193,2126635	192,9228445	192,6334602	192,34451	192,0559933	191,7679093	191,4802574	191,193037	190,9062475	190,6198881

22	23	24	25	26	27	28	29	30	31	32
180	180	180	180	180	180	180	180	180	180	180
540	540	540	540	540	540	540	540	540	540	540
-4 730 400	-4 730 400	-4 730 400	-4 730 400	-4 730 400	-4 730 400	-4 730 400	-4 730 400	-4 730 400	-4 730 400	-4 730 400
59 811 469	59 811 469	59 811 469	59 811 469	59 811 469	59 811 469	59 811 469	59 811 469	59 811 469	59 811 469	59 811 469
0,5%	0,5%	0,5%	0,5%	0,5%	0,5%	0,5%	0,5%	0,5%	0,5%	0,5%
53 566 373	53 298 542	53 032 049	52 766 889	52 503 054	52 240 539	51 979 336	51 719 440	51 460 842	51 203 538	50 947 520
-2 395 867	-2 395 867	-2 395 867	-2 395 867	-2 395 867	-2 395 867	-2 395 867	-2 395 867	-2 395 867	-2 395 867	-2 395 867
15 141 318	15 141 318	15 141 318	15 141 318	15 141 318	15 141 318	15 141 318	15 141 318	15 141 318	15 141 318	15 141 318
-8 100 323	-8 100 323	-8 100 323	-8 100 323	-8 100 323	-8 100 323	-8 100 323	-8 100 323	-8 100 323	-8 100 323	-8 100 323
113 292 571	113 024 739	112 758 246	112 493 086	112 229 251	111 966 736	111 705 533	111 445 637	111 187 040	110 929 735	110 673 718

Table 7: Based on the expected basal reservoir temperature derived within the geological calculations, the engineering section calculates an estimation of the expected overall energy capacity gain from the system. The calculation is based on the heat-energy equation and furthermore adopts an overall thermal loss rate expected over the lifetime of the plant.

Power Generation Estimation	1	2	3	4	5	6	7	8	9
Net Temperature Loss (°C)	199,70	199,40	199,10	198,80	198,50	198,21	197,91	197,61	197,32
Recovery Factor	15%	15%	15%	15%	15%	15%	15%	15%	15%
Final Recovery Temperature (°C)	169,75	169,49	169,24	168,98	168,73	168,48	168,22	167,97	167,72
Temperature at injection (°C)	55	55	55	55	55	55	55	55	55
Heat (J)	24 088 991,58	24 035 538,45	23 982 165,50	23 928 872,62	23 875 659,67	23 822 526,55	23 769 473,12	23 716 499,27	23 663 604,88
Energy (KWh)	24 089,18	24 035,73	23 982,36	23 929,06	23 875,85	23 822,72	23 769,66	23 716,69	23 663,79
Energy (MWh)	24,09	24,04	23,98	23,93	23,88	23,82	23,77	23,72	23,66
Nameplate Size	**72 267,55**								

10	11	12	13	14	15	16	17	18	19	20	21
197,02	196,72	196,43	196,13	195,84	195,55	195,25	194,96	194,67	194,38	194,08	193,79
15%	15%	15%	15%	15%	15%	15%	15%	15%	15%	15%	15%
167,47	167,22	166,97	166,71	166,46	166,21	165,97	165,72	165,47	165,22	164,97	164,72
55	55	55	55	55	55	55	55	55	55	55	55
23 610 789,84	23 558 054,02	23 505 397,30	23 452 819,57	23 400 320,70	23 347 900,58	23 295 559,09	23 243 296,12	23 191 111,53	23 139 005,23	23 086 977,08	23 035 026,98
23 610,98	23 558,24	23 505,59	23 453,01	23 400,51	23 348,09	23 295,75	23 243,48	23 191,30	23 139,19	23 087,16	23 035,21
23,61	23,56	23,51	23,45	23,40	23,35	23,30	23,24	23,19	23,14	23,09	23,04

22	23	24	25	26	27	28	29	30	31	32
193,50	193,21	192,92	192,63	192,34	192,06	191,77	191,48	191,19	190,91	190,62
15%	15%	15%	15%	15%	15%	15%	15%	15%	15%	15%
164,48	164,23	163,98	163,74	163,49	163,25	163,00	162,76	162,51	162,27	162,03
55	55	55	55	55	55	55	55	55	55	55
22 983 154,80	22 931 360,43	22 879 643,76	22 828 004,65	22 776 443,01	22 724 958,71	22 673 551,63	22 622 221,66	22 570 968,70	22 519 792,60	22 468 693,28
22 983,34	22 931,54	22 879,83	22 828,19	22 776,63	22 725,14	22 673,73	22 622,40	22 571,15	22 519,97	22 468,87
22,98	22,93	22,88	22,83	22,78	22,73	22,67	22,62	22,57	22,52	22,47

Table 8: Outline of the modelled LCOE calculations in this study; over the 30-year lifetime and structured considering all associated costs and variables weighed against the total expected energy production. This equates to the total cost of the LCOE model, relative to the underlying geological and engineering calculations. The table continues laterally, separated into three sections.

Case Assumptions	**0**	**1**	**2**	**3**	**4**	**5**	**6**	**7**	**8**	**9**	**10**
Annual Inflation	6,00%	6,00%	6,00%	6,00%	6,00%	6,00%	6,00%	6,00%	6,00%	6,00%	6,00%
O&M Cost per MWh	$25,00	$26,50	$28,09	$29,78	$31,56	$33,46	$35,46	$37,59	$39,85	$42,24	$44,77
Carbon cost (revenue) per MWh	$25,00	$25,00	$25,00	$25,00	$25,00	$25,00	$25,00	$25,00	$25,00	$25,00	$25,00
RETFIT increase %	5,00%	5,00%	5,00%	5,00%	5,00%	5,00%	5,00%	5,00%	5,00%	5,00%	5,00%
RETFIT	$25,00	$26,25	$27,56	$28,94	$30,39	$31,91	$33,50	$35,18	$36,94	$38,78	$40,72
Incentives, other	$-	$-	$-	$-	$-	$-	$-	$-	$-	$-	$-

Cash Flows	**-**	**1**	**2**	**3**	**4**	**5**	**6**	**7**	**8**	**9**	**10**
AT O&M costs	$-	$-	$10 563 226,84	$11 141 035,35	$11 750 449,98	$12 393 199,59	$13 071 107,61	$13 786 097,20	$14 540 196,71	$15 335 545,47	$16 174 399,81
Carbon Tax	$-	$-	$(17 274 767,99)	$(18 047 813,86)	$(18 855 453,53)	$(19 699 235,07)	$(20 580 775,84)	$(21 501 765,56)	$(22 463 969,57)	$(23 469 232,21)	$(24 519 480,35)
Tax benefits:											
Depreciation Effect	$-	$-	$-	$231 167 210,56	$369 867 536,90	$221 920 522,14	$133 152 313,28	$133 152 313,28	$66 576 156,64	$-	$-
PTC	$-	$-	$-	$-	$-	$-	$-	$-	$-	$-	$-
Construction Costs	$963 196 710,68	$963 196 710,68	$963 196 710,68	$-	$-	$-	$-	$-	$-	$-	$-
Terminal Value	$-	$-	$-	$-	$-	$-	$-	$-	$-	$-	$-
AT Cash Flow to Enterprise	$963 196 710,68	$963 196 710,68	$956 485 169,53	$224 260 432,05	$362 762 533,35	$214 614 486,66	$125 642 645,05	$125 436 644,92	$58 652 383,79	$(8 133 686,74)	$(8 345 080,54)
Discount Factor	1,00	0,94	0,89	0,84	0,79	0,75	0,70	0,67	0,63	0,59	0,56
Present Value of Cash Flow	$963 196 710,68	$908 676 142,15	$851 268 395,81	$188 293 383,17	$287 341 903,93	$160 372 429,17	$88 573 106,96	$83 422 533,01	$36 799 231,20	$(4 814 316,68)	$(4 659 849,39)
Final Income	$-	$-	$-	$-	$-	$-	$-	$-	$-	$-	$-
Net Present Value of Cash Flow	**$3 513 675 056,89**										

Plant Production	**-**	**1**	**2**	**3**	**4**	**5**	**6**	**7**	**8**	**9**	**10**
Capacity (KW)	0,00	72 267,55	72 267,55	72 267,55	72 267,55	72 267,55	72 267,55	72 267,55	72 267,55	72 267,55	72 267,55
Utilization/Capacity Factor (%)	100,0%	99,5%	99,0%	98,5%	98,0%	97,5%	97,0%	96,6%	96,1%	95,6%	95,1%
Annual Degradation	0,50%	0,50%	0,50%	0,50%	0,50%	0,50%	0,50%	0,50%	0,50%	0,50%	0,50%
Production (KW)	0	71 906	71 547	71 189	70 833	70 479	70 126	69 776	69 427	69 080	68 734
Construction Factor	24	12	0	0	0	0	0	0	0	0	0
Downtime Percentage	200%	100%	0%	0%	0%	0%	0%	0%	0%	0%	0%
Annual Production (MWh)	0	629 898	626 749	623 615	620 497	617 395	614 308	611 236	608 180	605 139	602 113
Total Annual Production (MWh)	0,00	0,00	626 748,95	623 615,21	620 497,13	617 394,65	614 307,67	611 236,13	608 179,95	605 139,05	602 113,36
Discount Factor	1	1,06	1,12	1,19	1,26	1,34	1,42	1,50	1,59	1,69	1,79
Present Value of Energy Produced	0	0	704 215	742 736	783 363	826 213	871 407	919 073	969 346	1 022 370	1 078 293

11	12	13	14	15	16	17	18	19	20	21	22
6,00%	6,00%	6,00%	6,00%	6,00%	6,00%	6,00%	6,00%	6,00%	6,00%	6,00%	6,00%
$47,46	$50,30	$53,32	$56,52	$59,91	$63,51	$67,32	$71,36	$75,64	$80,18	$84,99	$90,09
$25,00	$25,00	$25,00	$25,00	$25,00	$25,00	$25,00	$25,00	$25,00	$25,00	$25,00	$25,00
5,00%	5,00%	5,00%	5,00%	5,00%	5,00%	5,00%	5,00%	5,00%	5,00%	5,00%	5,00%
$42,76	$44,90	$47,14	$49,50	$51,97	$54,57	$57,30	$60,17	$63,17	$66,33	$69,65	$73,13
$-	$-	$-	$-	$-	$-	$-	$-	$-	$-	$-	$-

11	12	13	14	15	16	17	18	19	20	21	22
$17 059 139,48	$17 992 274,41	$18 976 451,82	$20 014 463,74	$21 109 254,90	$22 263 931,14	$23 481 768,18	$24 766 220,90	$26 120 933,18	$27 549 748,23	$29 056 719,45	$30 646 122,01
$(25 616 727,10)	$(26 763 075,63)	$(27 960 723,27)	$(29 211 965,63)	$(30 519 201,10)	$(31 884 935,35)	$(33 311 786,20)	$(34 802 488,63)	$(36 359 900,00)	$(37 987 005,53)	$(39 686 924,02)	$(41 462 913,87)
$-	$-	$-	$-	$-	$-	$-	$-	$-	$-	$-	$-
$-	$-	$-	$-	$-	$-	$-	$-	$-	$-	$-	$-
$-	$-	$-	$-	$-	$-	$-	$-	$-	$-	$-	$-
$-	$-	$-	$-	$-	$-	$-	$-	$-	$-	$-	$-
$(8 557 587,62)	$(8 770 801,22)	$(8 984 271,45)	$(9 197 501,90)	$(9 409 946,20)	$(9 621 004,20)	$(9 830 018,02)	$(10 036 267,74)	$(10 238 966,82)	$(10 437 257,30)	$(10 630 204,57)	$(10 816 791,87)
0,53	0,50	0,47	0,44	0,42	0,39	0,37	0,35	0,33	0,31	0,29	0,28
$(4 508 030,40)	$(4 358 819,50)	$(4 212 177,04)	$(4 068 063,96)	$(3 926 441,77)	$(3 787 272,55)	$(3 650 518,93)	$(3 516 144,09)	$(3 384 111,75)	$(3 254 386,16)	$(3 126 932,11)	$(3 001 714,88)
$-	$-	$-	$-	$-	$-	$-	$-	$-	$-	$-	$-

11	12	13	14	15	16	17	18	19	20	21	22
72 267,55	72 267,55	72 267,55	72 267,55	72 267,55	72 267,55	72 267,55	72 267,55	72 267,55	72 267,55	72 267,55	72 267,55
94,6%	94,2%	93,7%	93,2%	92,8%	92,3%	91,8%	91,4%	90,9%	90,5%	90,0%	89,6%
0,50%	0,50%	0,50%	0,50%	0,50%	0,50%	0,50%	0,50%	0,50%	0,50%	0,50%	0,50%
68 391	68 049	67 709	67 370	67 033	66 698	66 364	66 033	65 702	65 374	65 047	64 722
0	0	0	0	0	0	0	0	0	0	0	0
0%	0%	0%	0%	0%	0%	0%	0%	0%	0%	0%	0%
599 103	596 107	593 127	590 161	587 210	584 274	581 353	578 446	575 554	572 676	569 813	566 964
599 102,79	596 107,28	593 126,74	590 161,11	587 210,30	584 274,25	581 352,88	578 446,11	575 553,88	572 676,11	569 812,73	566 963,67
1,90	2,01	2,13	2,26	2,40	2,54	2,69	2,85	3,03	3,21	3,40	3,60
1 137 276	1 199 485	1 265 097	1 334 298	1 407 284	1 484 262	1 565 451	1 651 081	1 741 396	1 836 650	1 937 115	2 043 075

23	24	25	26	27	28	29	30	31	32
6,00%	6,00%	6,00%	6,00%	6,00%	6,00%	6,00%	6,00%	6,00%	6,00%
$95,49	$101,22	$107,30	$113,73	$120,56	$127,79	$135,46	$143,59	$152,20	$161,33
$25,00	$25,00	$25,00	$25,00	$25,00	$25,00	$25,00	$25,00	$25,00	$25,00
5,00%	5,00%	5,00%	5,00%	5,00%	5,00%	5,00%	5,00%	5,00%	5,00%
$76,79	$80,63	$84,66	$88,89	$93,34	$98,00	$102,90	$108,05	$113,45	$119,12
$-	$-	$-	$-	$-	$-	$-	$-	$-	$-

23	24	25	26	27	28	29	30	31	32
$32 322 464,88	$34 090 503,71	$35 955 254,26	$37 922 006,67	$39 996 340,44	$42 184 140,26	$44 491 612,73	$46 925 303,95	$49 492 118,07	$52 199 336,93
$(43 318 379,27)	$(45 256 876,74)	$(47 282 121,98)	$(49 397 996,93)	$(51 608 557,30)	$(53 918 040,24)	$(56 330 872,54)	$(58 851 679,08)	$(61 485 291,72)	$(64 236 758,53)
$-	$-	$-	$-	$-	$-	$-	$-	$-	$-
$-	$-	$-	$-	$-	$-	$-	$-	$-	$-
$-	$-	$-	$-	$-	$-	$-	$-	$-	$-
$-	$-	$-	$-	$-	$-	$-	$-	$-	$-
$(10 995 914,39)	$(11 166 373,03)	$(11 326 867,71)	$(11 475 990,26)	$(11 612 216,86)	$(11 733 899,98)	$(11 839 259,81)	$(11 926 375,14)	$(11 993 173,65)	$(12 037 421,60)
0,26	0,25	0,23	0,22	0,21	0,20	0,18	0,17	0,16	0,15
$(2 878 700,27)	$(2 757 854,60)	$(2 639 144,66)	$(2 522 537,75)	$(2 408 001,62)	$(2 295 504,53)	$(2 185 015,18)	$(2 076 502,74)	$(1 969 936,82)	$(1 865 287,51)
$-	$-	$-	$-	$-	$-	$-	$-	$-	$-

23	24	25	26	27	28	29	30	31	32
72 267,55	72 267,55	72 267,55	72 267,55	72 267,55	72 267,55	72 267,55	72 267,55	72 267,55	72 267,55
89,1%	88,7%	88,2%	87,8%	87,3%	86,9%	86,5%	86,0%	85,6%	85,2%
0,50%	0,50%	0,50%	0,50%	0,50%	0,50%	0,50%	0,50%	0,50%	0,50%
64 398	64 076	63 756	63 437	63 120	62 804	62 490	62 178	61 867	61 558
0	0	0	0	0	0	0	0	0	0
0%	0%	0%	0%	0%	0%	0%	0%	0%	0%
564 129	561 308	558 502	555 709	552 931	550 166	547 415	544 678	541 955	539 245
564 128,85	561 308,21	558 501,67	555 709,16	552 930,61	550 165,96	547 415,13	544 678,05	541 954,66	539 244,89
3,82	4,05	4,29	4,55	4,82	5,11	5,42	5,74	6,09	6,45